Investigation of divalent metal ion detection using 17E DNAzyme Biosensor

by
Woohyun Jennifer Moon

A thesis
presented to the University of Waterloo
in fulfilment of the
thesis requirement for the degree of
Master of Science
in
Chemistry (Nanotechnology)

Waterloo, Ontario, Canada, 2021

Authour’s Declaration

I hereby declare that I am the sole author of this thesis. This is a true copy of the thesis, including any required final revisions, as accepted by my examiners.

I understand that my thesis may be made electronically available to the public.

Statement of Contribution

This thesis was written by Woohyun Jennifer Moon under the supervision of Dr. Juewen Liu.

Chapter 1 is written as an introduction to the original research projects described in Chapter 2, 3, and 4. Selected figures from the published reviews listed below are reproduced with the permission from the publishers. The thesis chapter 1 itself is not written for publication.

- Moon, W. J., Huang, P.-J. J., and Liu, J. (2020) DNA-Enabled Heavy Metal Detection in Water, Encyclopedia of Analytical Chemistry, pp 1-22.
- Moon, W. J., and Liu, J. (2020) Interfacing Catalytic DNA with Nanomaterials, *Advanced Materials Interfaces 7*, 2001017.
- Moon, W. J., Yang, Y., and Liu, J. (2021) Zn^{2+}-Dependent DNAzymes: From Solution Chemistry to Analytical, Materials and Therapeutic Applications, *ChemBioChem 22*, 779-789.

Dr. Juewen Liu is the primary investigator for the published reviews. Manuscripts were prepared by Woohyun Jennifer Moon with the co-authours Dr. Po-Jung Jimmy Huang and Dr. Yongjie Yang for the respective manuscripts.

Chapter 2 includes the work under review for publication at the time of thesis submission. The manuscript was submitted to the *Biochemistry* journal. All the discussed experiments were performed by Woohyun Jennifer Moon. The manuscript was written by Woohyun Jennifer Moon and Dr. Juewen Liu. Dr. Po-Jung Jimmy Huang provided the isolated and purified stereoisomers

for the phosphorothioate substitution study and provided many meaningful helps with the experimental designs.

- Moon, W. J., Huang, P-J. J., Liu, J. (2021) Probing Metal-dependent Phosphate Binding for the Catalysis of the 17E DNAzyme, *Biochemistry*, under review for publication.

Chapter 3 work has been published and is reproduced in the thesis with the permission from the publisher. All the discussed experiments were designed and performed by Woohyun Jennifer Moon. The manuscript was written under the supervision of Dr. Juewen Liu.

- Moon, W. J., and Liu, J. (2020) Replacing Mg^{2+} by Fe^{2+} for RNA-Cleaving DNAzymes, *ChemBioChem 21*, 401-407.

Chapter 4 work manuscript preparation is in progress and has not been submitted nor published yet. The discussed experiments were performed by Woohyun Jennifer Moon.

Abstract

DNAzymes are in vitro selected oligonucleotides that can catalyze reactions, such as RNA cleavage. Most DNAzymes require metal ions as cofactors. Unlike ribozymes, which have been found in nature, all known DNAzymes are artificially selected from a pool of random nucleotide sequences by narrowing down specific sequences that exhibit the desired activities. Since the first reported selection, the field of research has exploded to examine its fundamental properties and potential applicability as a biosensor and therapeutic agent. 17E is one of the most extensively examined RNA-cleaving DNAzymes to date. The catalytic activity is observed to be the highest in the presence of Pb^{2+} as a cofactor. As a result, many studies have focused their attention on Pb^{2+}. However, it exhibits varying degrees of catalytic activities in the presence of various divalent metals. The mechanism of which different metal ions assist with the RNA-cleaving reaction is still in debate. Further understanding of the DNAzyme activities in the presence of different metal ions, in a buffered environment as well as in complex samples, can provide valuable information for designing systems that utilize DNAzymes.

Throughout the studies in this thesis, various aspects of the divalent metal ions and their interaction with the 17E DNAzyme are probed. Briefly, the phosphorothioate substitution at the pro-R_p position of the non-bridging oxygen significantly decreased cleavage activity while the pro-S_p position was unaffected for less thiophilic metals, such as Mg^{2+}, Mn^{2+}, and Co^{2+}. This indicates that the pro-R_p position at the cleavage site plays an important role. However, thiophilic metals, such as Cd^{2+}, did not show significantly different activity between the R_p and S_p isomers. Water ligand exchange rates were also found to be correlated to the observed cleavage rates, which may suggest an inner-sphere coordination mechanism. Inhibition by the free phosphate was also

quantified and found to correlate to the rate constants of each metal ion, which indirectly indicates that the metal-phosphate affinity correlates to the cleavage activity. Comparing to the available mechanism data for Pb^{2+} with 8-17 DNAzymes, it can be suggested that other divalent metal ions work via a different mechanism than Pb^{2+}. While Pb^{2+} cleaves the RNA cleavage site by a general acid/base mechanism, other divalent metals are suggested to act as Lewis acids.

Screening of different transition metals found that Fe^{2+} exhibits high activity with 17E and the metal was studied in more depth. While Fe^{3+} shows no activity, maintaining the oxidation state of Fe^{2+} in an inert atmosphere or the presence of reducing agents could cleave the substrate with the DNAzyme. Studies with ribozymes reported that Fe^{2+} could replace Mg^{2+} and this observation provides insights about the role of Fe^{2+} in the early earth. Comparison with different DNAzymes that are active with Mg^{2+} found that Fe^{2+} can also replace Mg^{2+} for DNAzymes as well. The Fe^{2+} increased the reaction rates compared to Mg^{2+} by 21-fold for 17E, 25-fold for 8-17, and 1-fold for E5. pH higher than 7.2 was found to degrade the DNA in the presence of high Fe^{2+} concentration. The use of reducing agents, such as ascorbate, or N_2 environment could reduce oxidation to Fe^{3+} which does not exhibit any cleavage reaction activities.

For detecting metal ions in more complex samples, metal-protein binding interaction may be affecting the overall observed DNAzyme activity by decreasing the effective metal concentrations. Examining the model protein of bovine serum albumin (BSA) and its interaction with different metal ions, the decreased DNAzyme activities were correlated to the BSA-metal binding. Fluorescence polarization assay results indicated minimal binding of the BSA with the 17E DNAzyme, but longer NaH1 DNAzyme was observed to bind with the protein. These observations identify the need to consider protein-metal interaction when designing intracellular DNAzyme biosensors for metal quantification.

Throughout this thesis, aspects concerning the divalent metal ion detection using the 17E DNAzyme as a biosensor are carefully examined to further our fundamental understanding. Mainly, the mechanism of metal-phosphate interaction is probed. Fe^{2+} behaviour with the 17E DNAzymes was also examined for the first time. Understanding the metal-dependent activities and the interaction with proteins in complex samples can guide improved biosensor designs for future applications.

Acknowledgment

I sincerely thank my supervisor, Dr. Juewen Liu, for the learning opportunity, helpful discussions, constructive feedback for scientific communication, and valuable thinking skills as a scientist. I also thank Dr. Guy Guillemette and Dr. Scott Smith for serving as the committee members. Special thanks to all the colleagues in the lab, especially Jimmy Huang for exciting discussions about chemistry.

The research work has been funded by the Global Water Futures project of the Canada First Research Excellence Fund (CFREF) and supported by the Department of Chemistry, University of Waterloo.

Thanks to my dear Mom, Dad, Andrew, Chris, colleagues, and friends for their love and support throughout my graduate school adventure. Their encouragement helped me out of my comfort zone to continue to grow and learn.

Dedication

Dedicated to my Mother, Kyunghyun Song.

Table of Contents

List of Figures

List of Tables

List of Abbreviations

%cleavage	Cleavage activity %
$\%cleavage_{MOPS}$	Cleavage activity % in MOPS buffer
$\%cleavage_{PBS}$	Cleavage activity % in PBS buffer
$\%cleavage_{PO}$	Cleavage activity % with PO-Sub
$\%cleavage_{PS}$	Cleavage activity % with PS-Sub
$\%P_0$	Initial cleavage activity %
$\%P_\infty$	cleavage activity % at the end of the reaction
A	Adenine
aM	α-macroglobulin
APS	Ammonium persulfate
AuNP	Gold nanoparticles
BHQ	Blackhole Quencher
B_{max}	Maximum saturation %cleavage
BSA	Bovine Serum Albumin
C	Cytosine
CD	Circular Dichroism
CTAB	Cetyltrimethylammonium bromide
DNA	Deoxyribonucleic acid
DNAzyme	Deoxyribozyme
dPAGE	Denaturing Polyacrylamide Gel Electrophoresis
EDTA	Ethylenediaminetetraacetic acid
FAM	Carboxyfluoresceine
FBS	Fetal Bovine Serum
FRET	Förster Resonance Energy Transfer
G	Guanine
Hb	Hemoglobin
HPLC	High-Performance Liquid Chromatography
$\boldsymbol{I_{cleaved}}$	Gel Fluorescence Intensity of the cleaved band
$\boldsymbol{I_{degraded}}$	Gel Fluorescence Intensity of the degraded band
$I_{parellel}$	The intensity of parallel polarized light
$I_{perpendicular}$	The intensity of perpendicular polarized light
$\boldsymbol{I_{sum}}$	Sum of $\boldsymbol{I_{cleaved} + I_{uncleaved}}$
$\boldsymbol{I_{total}}$	Sum of $\boldsymbol{I_{cleaved} + I_{uncleaved} + I_{degraded}}$
$\boldsymbol{I_{uncleaved}}$	Gel Fluorescence Intensity of the uncleaved band
K_d	Dissociation Constant
k_{obs}	Rate Constant
LOD	Limit of Detection
MES	2-(N-morpholino)ethanesulfonic acid
miRNA	micro-RNA
MOPS	3-(N-morpholino)propanesulfonic acid
N_{50}	50-nucleotide length random region
PBS	Phosphate Buffer Saline
PCR	Polymerase Chain Reaction

PG	Protecting Group
PO-Sub or PO	A substrate with non-bridging oxygen
PS-Sub or PS	A substrate with non-bridging oxygen switched with sulfur
PS-R_p	PS substrate with a sulfur atom in the R_p position
PS-S_p	PS substrate with a sulfur atom in the S_p position
rA	riboadenine
RNA	Ribonucleic acid
SERS	Surface-enhanced Raman spectroscopy
siRNA	Small interfering RNA
ssDNA	Single strand DNA
T	Thymine
TBE	Tris-Borate EDTA
TEMED	Tetramethylethylenediamine
T_m	Melting Temperature
U	Uracil
UV	Ultraviolet

Chapter 1 Introduction to DNAzyme for biosensor applications

Introduction

DNAzymes (deoxyribozymes) are in vitro selected sequences of deoxyribonucleic acid (DNA) that can catalyze chemical and biological transformations. For most of the DNAzymes studied to date, metal cofactors are required for their reactions. Some DNAzymes have excellent specificity for certain metal ions, allowing their applications as biosensors. Interests in using these DNAzymes for metal ion detection are increasing due to the advantages of stability, selectivity, adaptability, and low cost. Because of these benefits, various designs of biosensors have been studied in research laboratories. An ideal design should also be resistant to matrix effect from more complex samples such as environmental or biological samples. Efforts to resolve some of the remaining challenges are a very important research direction. Studies in this thesis work attempt to probe and contribute to such fundamental understanding, especially the DNAzyme-metal ion interaction and the effect of the proteins on the biosensor sensitivity.

DNA and its stabilization by metal ions

The structure of nucleotides is composed of three main components: the deoxyribose or ribose, phosphate group, and the nucleobases **(Figure 1.1A**). The phosphodiester linkage between C5 and C3 positions of deoxyribose with a phosphate group forms the phosphate backbone of the DNA chain. In physiological pH, the phosphate groups are deprotonated, and the overall charge of the molecule is negative. The C1 position of the deoxyribose is bonded with four types of charge-neutral nucleobases (**Figure 1.1B**). Hydrogen bonding between the nitrogen and oxygen atoms of these nucleobases stabilizes the complementary strands of nucleic acids. The typical Watson-Crick base pairing occurs in between the cytosine (C) and guanine (G), as well as adenine

(A) and thymine (T) for DNA or uracil (U) for RNA (**Figure 1.1D**). Although less common, Hoogsteen and wobble base pairing can also be observed. The presence or the absence of hydroxyl group at C2 position of the carbohydrate makes the difference between the deoxyribose or the ribose, which identifies the nucleotide to be either DNA or RNA (ribonucleic acid), respectively. When DNA and RNA are compared, DNA is often categorized to be more stable. This is because the 2′-OH of RNA makes it easier to hydrolyze and break the phosphodiester bonds in the physiological pH range.[1]

DNA can be stabilized with metal ions either via the phosphate backbone or the nucleobases. Because the phosphate backbone of the DNA is negatively charged, metal cations can bind with DNA via electrostatic interactions. In addition, the nitrogen and oxygen atoms of the nucleobases can behave as ligands to coordinate with the metal ions. The coordination mechanism may be different depending on the different metal.[2] Common coordination sites of the nucleobases are highlighted in **Figure 1.1B**. The metal ion coordination stabilizes the DNA structure, which enables folding and subsequent catalysis.

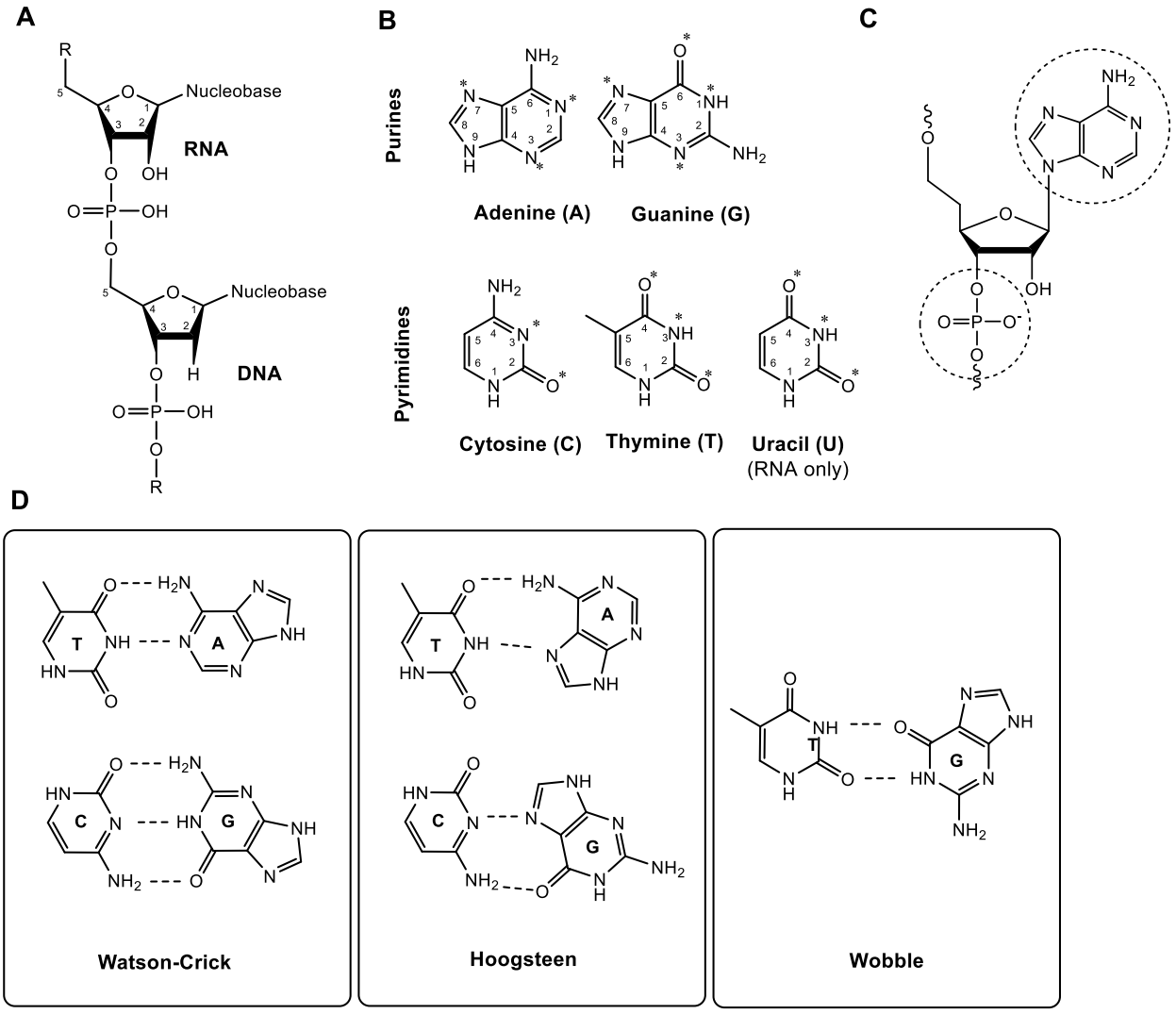

Figure 1.1 A) Structure of RNA and DNA, **B)** structures of the nucleobases, **C)** possible binding sites of different metal ions, and **D)** base pairing via hydrogen bonding. Figure adapted from Moon, W. J., and Liu, J.[3]

S block metal ions, such as Na^{+} and Mg^{2+}, mainly interact with the phosphate backbone of the DNA and screens the charge repulsion with a duplex DNA. This increases the melting temperature (T_m), which indicates the duplex stability. Comparatively, strong interaction with the nucleobases often decreases the T_m by weakening the base-pairing hydrogen bonding. Heavy metals, such as Hg^{2+} and Ag^{+}, have been found to mainly interact with the nucleobases. For

example, Hg^{2+} binds in between T-T mismatch at the deprotonated N3 position[4-6] and Ag^{+} binds in between C-C mismatch at the N3 position in duplex DNA.[7] Lastly, other divalent transition metals and trivalent lanthanides can interact with both the phosphate backbone and the nucleobases. This leads to the breaking of DNA duplex and non-specifically folding the single-stranded DNA at high metal concentrations (**Figure 1.1C**).[8]

Metal-binding to the DNA can be utilized to promote folding and catalysis for the detection of metal ions. Understanding the interaction with different metals can give insights into creative and rational biosensor designs. For example, the G-quadruplex structure that mimics the peroxidase activity can be folded into its structure from a G-rich ssDNA in the presence of K^{+}.[9, 10] The conformation of the G-quadruplex changes in the presence of Pb^{2+} and the catalytic activity is inhibited. Also, simply a strong affinity between the adenine base to gold can be utilized to design an electrochemical probe for Au^{3+} detection.[11, 12] By studies that probed the fundamental interaction of the metal ions and the DNA, unique methods for the metal ion biosensors could be designed. Therefore, it is important to deepen the knowledge about the metal ion's role in the presence of DNA of interest, such as the DNAzymes to be discussed in the upcoming sections.

In vitro selection of DNAzymes

In 1994, Breaker and Joyce reported a powerful technique called the in vitro selection.[13] The process narrows down specific sequences of DNA from a large random pool of library that has the targeted activity of interest. By repeating the incubation, separation, and amplification process with the target metal ion, a specific sequence of the DNA with the highest targeted activity can be obtained (**Figure 1.2**). For example, a pool of random sequence DNA library with a single riboadenine (rA) as the cleavage site is designed with a binding arm region and a 50-nucleotide

length random sequence region (N_{50}). By incubating with a metal ion of interest, the sequences that perform the RNA cleaving reaction and those that are not reactive are separated by denaturing polyacrylamide (dPAGE) gels. The purified fraction then undergoes two polymerase chain reaction (PCR) cycles to amplify the sequences. The amplified sequences are subjected to the target metal ion again. Upon repeating the process multiple times,

The binding arm is purposely designed to have a similar T_m to dehybridize the binding arms at a similar temperature. However, once the N_{50} region sequence has been identified, the binding arm can usually be altered for downstream applications. The purpose of the two PCR cycles are 1) to extend the sequence and 2) to add the rA base and fluorophore label again. In PCR 1, Primer 1 (P1) and Primer 2 (P2) are used to anneal and extend the complementary sequence. As the PCR process continues, P1 will also extend the amplified strand from P2, which will be used in the second cycle of PCR. In PCR 2, The extended product from PCR 1 will further be amplified with Primer 3 (P3) that has a spacer region, and Primer 4 (P4) that has a fluorophore and rA. The final product of PCR 2 will have a long complementary sequence with the spacer and a fluorophore-labeled product. To distinguish the two strands, P3 purposely has the spacer region to increase the molecular weight. This way, the two strands are separated on dPAGE. This completes a single round of *in-vitro* selection. The purified fluorophore-labeled library goes through more rounds of the *in-vitro* selection cycle until the cleavage activity is high. Then the narrow pool of DNA can be sequenced and further characterized to determine a specific DNA sequence with RNA cleaving activity. The process can be adapted for other types of DNAzymes, such as ligation DNAzymes as well.

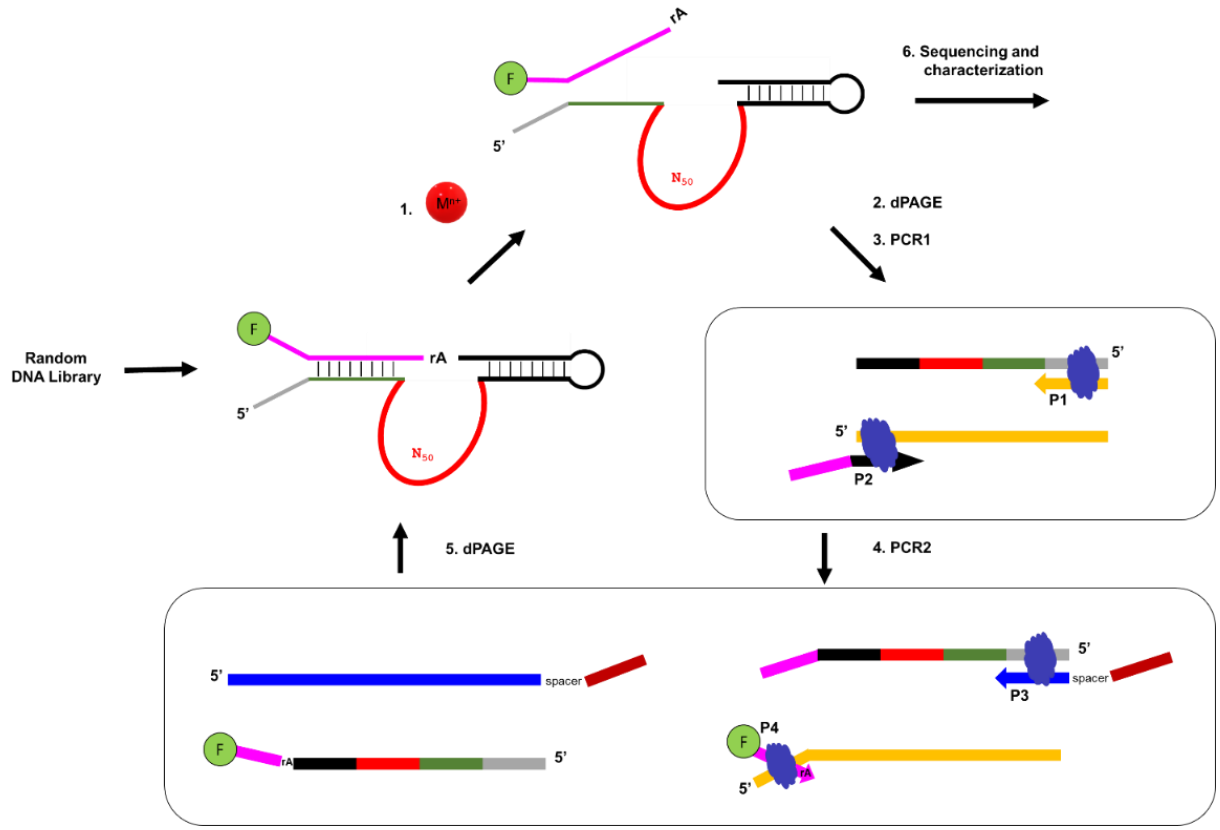

Figure 1.2 General scheme of in vitro selection process for metal-dependent RNA-cleaving DNAzymes. Fluorophore-labeled strand containing a single riboadenine (rA) and 50 random sequence regions (N_{50}) incubated with the target metal ion undergoes rounds of separation, purification, and amplification by polymerase chain reaction (PCR) to narrow down specific sequences that are highly active. The figure is adapted from Zhou, W., *et al.* 2017.[14]

RNA-cleaving DNAzymes and the role of metal ions

Many DNAzymes have been in vitro selected and reported to catalyze various reactions.[14-19] The in vitro selection of the first reported DNAzyme was demonstrated with an RNA-cleaving reaction in the presence of the metal cofactors. More catalytic reactions by DNAzymes studied include ligation, phosphorylation, and capping of RNA and DNA, [20-23] as well as peroxidation, [24-26] porphyrin metalation, [27-29] and organic transformations[18, 30] of non-nucleic acid substrates. The RNA-cleaving reaction is the most extensively studied type of reaction by DNAzymes. **Figure 1.3A-F** illustrates the secondary structures of some example DNAzymes for the RNA-cleaving

reaction. Although some of the DNAzymes were selected with all-RNA substrates, many further studies replaced the substrate with a single-RNA containing chimeric DNA oligomer due to the stability issue of RNA. Usually, rA is used as the single-RNA cleavage site.

The general mechanism of RNA-cleaving reaction is shown in **Figure 1.3G**. The cleavage site RNA contains a 2′-OH group that serves as a nucleophile that can attack the adjacent phosphate. A general base can help deprotonate the 2′-OH to make it a better nucleophile. The transition state is a penta-coordinated species that can be stabilized by the metal cations to neutralize the negative charges. The 5′-oxygen as a leaving group will eventually cleave the substrate to complete the reaction.

DNAzyme GR5 (**Figure 1.3A**) requires Pb^{2+} to cleave the single RNA linkage in the substrate strand.[31, 32] Under optimized conditions, high cleavage rates can be achieved (>10 min^{-1}).[33] However, using the DNAzyme only dependent on Pb^{2+} is not useful for various intracellular therapeutic applications because Pb^{2+} is usually not present in living cells. The selection of the DNAzyme 8-17 (**Figure 1.3E**) appeared to have solved this problem because it has high activity with Pb^{2+}, but also various other divalent metals commonly present in cells such as Mg^{2+} and Zn^{2+}. The DNAzyme named 10-23 (**Figure 1.3B**) has also been one of the most popular sequences to be used for intracellular detection or gene therapy application studies.[34, 35] In addition, Na^{+}-specific DNAzymes were also reported to eliminate the need for the divalent metal ions for RNA-cleaving reactions. An aptamer motif for Na^{+} has been found to be responsible for the specificity.[36-39] These DNAzymes are called the NaA43t (**Figure 1.3C**), NaH1 (**Figure 1.3D**), and Ce13d.[40-42]

One of the most characterized and studied is the class of 8-17 DNAzymes. The 8-17 DNAzymes can cleave the single-RNA cleavage site in the presence of various divalent metal ions. The 8-17 class of DNAzymes are interesting because even though different in vitro selection

conditions were used in a few different research laboratories, extremely similar sequences were obtained.[34, 43, 44] The 8-17 and Mg5 were selected using the Mg^{2+}, but 17E sequence was obtained using Zn^{2+} as the cofactor.[45] The secondary structures of the 8-17 and 17E DNAzymes are shown in **Figure 1.3 E-F**. This class of DNAzymes was found to have the highest activity with Pb^{2+} but are also highly active with various divalent metal ions.

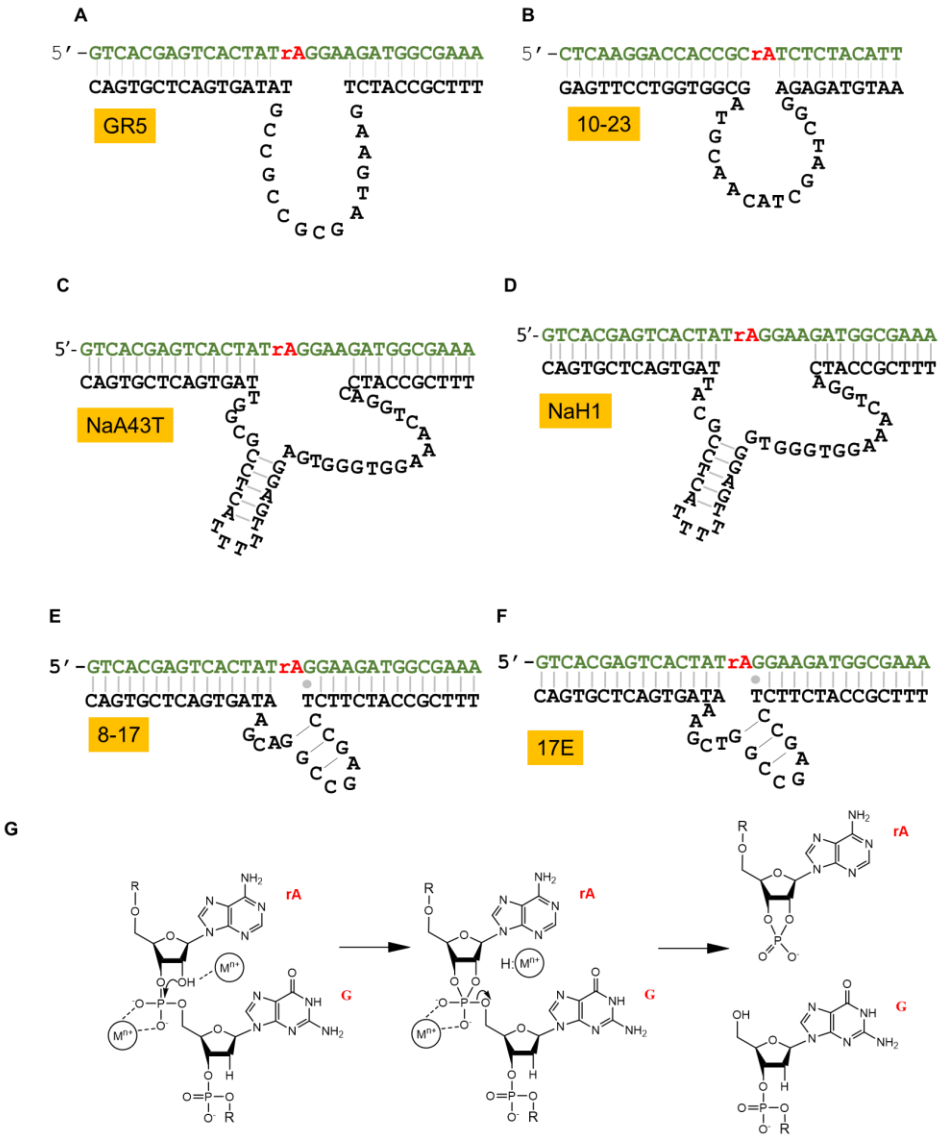

Figure 1.3. The secondary structures of various DNAzymes: **A)** GR5 DNAzyme is active only with Pb^{2+}, **B)** 10-23 is often used in therapeutic studies, **C)** NaA43T (a truncated version of NaA43) is specifically active with Na^{+}, **D)** NaH1 is another similar DNAzyme specifically active with Na^{+}, **E)** 8-17 DNAzyme is active with many divalent metal ions and the most active with Pb^{2+}, **F)** 17E is another similar DNAzyme separately selected that behaves similar to the 8-17, and **G)** the general mechanism of RNA cleaving reaction.[46]

The activity of the 17E DNAzyme in the presence of metal ions

17E DNAzyme cleaves the single RNA-substrate in the presence of various divalent metal ions. 17E was in vitro selected by Li, J. *et al* and reported in 2000.[44] The authours used Zn^{2+} as the target metal ion, but Pb^{2+} exhibited the highest cleavage activity (**Figure 1.4**).[45] Comparison of activities in pH 6 and 7 showed that pH 7 required only 100 µM of the divalent metals (Ba^{2+}, Sr^{2+}, Mg^{2+}, Ca^{2+}, Ni^{2+}, Cd^{2+}, Co^{2+}, Mn^{2+}, and Zn^{2+}) to achieve similar or higher cleavage rates as 10 mM, indicating higher pH to be more optimal for the reaction.[44] Indeed, pH dependence study using the 200 µM Pb^{2+} as the metal cofactors also exhibited a linear response to the log k_{obs}, which indicates a single deprotonation as the rate-limiting step.[45]

Hammerhead ribozymes are often compared to 17E or 8-17 because it is also active with divalent metal ions.[47, 48] However, in vitro selected DNAzyme compared to the naturally found ribozymes show a difference with the monovalent metal ion activity. While the hammerhead ribozyme exhibits ~10-fold less activity with 4M Li^{+} compared to 10 mM Mg^{2+}, 8-17 DNAzyme shows ~1000-fold less activity with the same metal ion concentrations.[48] Also, $Co(NH_3)_6^{3+}$, which is often utilized as an indicator for outer-sphere metal coordination for activity, does not induce detectable cleavage activity with the 8-17 DNAzyme while hammerhead ribozyme exhibits activity. This information hints at the inner-sphere coordination mechanism, although this observation alone does not support the hypothesis.

Recently, it was proposed that Fe^{2+} behaves similarly to Mg^{2+} in terms of interacting with nucleic acids. Considering that the early earth might be rich in Fe^{2+} due to its reducing environment, abundant Fe^{2+} is suggested to have played diverse roles in RNA structures and catalytic functions. Quantum mechanical calculation and modeling calculations show that the RNA-Mg^{2+} clamp is similarly oriented to that of the RNA-Fe^{2+} clamp in L1 Ribozyme Ligase (**Figure 1.5A-C**). The comparison of the two metal ion activities with the L1 Ribozyme Ligase and Hammerhead Ribozyme shows that Fe^{2+} can replace Mg^{2+} with 25- and 3-fold higher activity, respectively (**Figure 1.5D-E).** This reported observation suggests that Fe^{2+} could replace Mg^{2+}-binding sites of nucleic acid-based structures, such as 17E DNAzymes that are active with Mg^{2+}.

Structurally, the most extensively studied metal ion of Pb^{2+} showed a difference in terms of global folding compared to other monovalent and divalent metals screened by Mazumdar, D. *et al* (2009), such as Li^+, Na^+, NH_4^+, Mg^{2+}, Cd^{2+}, Zn^{2+}, and Pb^{2+}.[48] The K_d of folding of different metals were examined by Förster Resonance Energy Transfer (FRET), as well as Circular Dichroism (CD). Both results suggested that the metal-dependent folding and the resulting formation of Z-DNA structure are correlated to the cleavage activity. However, Pb^{2+} was found to be an exception because it did not induce any global folding nor Z-DNA formation. As a result, Pb^{2+} is hypothesized to function via a completely different mechanism. It is important to note that the different metal-dependent DNAzyme activity rates observed with the 17E DNAzyme are closely related to the structural and chemical interaction of the metal ions at the cleavage site.

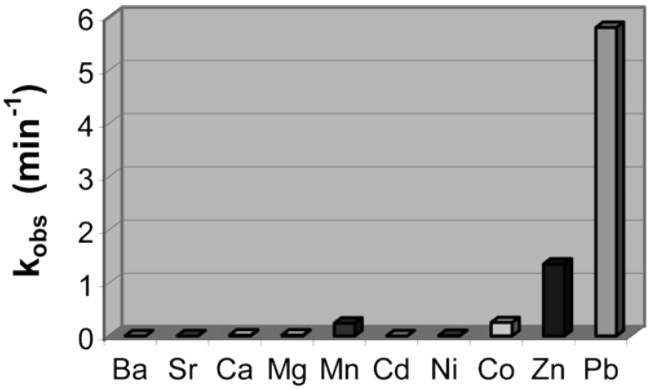

Figure 1.4. Comparison of the 10 mM of different divalent metal ions and 100 µM Pb^{2+} in pH6. Reproduced with the permission from Brown, A, *et al*, Biochemistry 2003.[45]

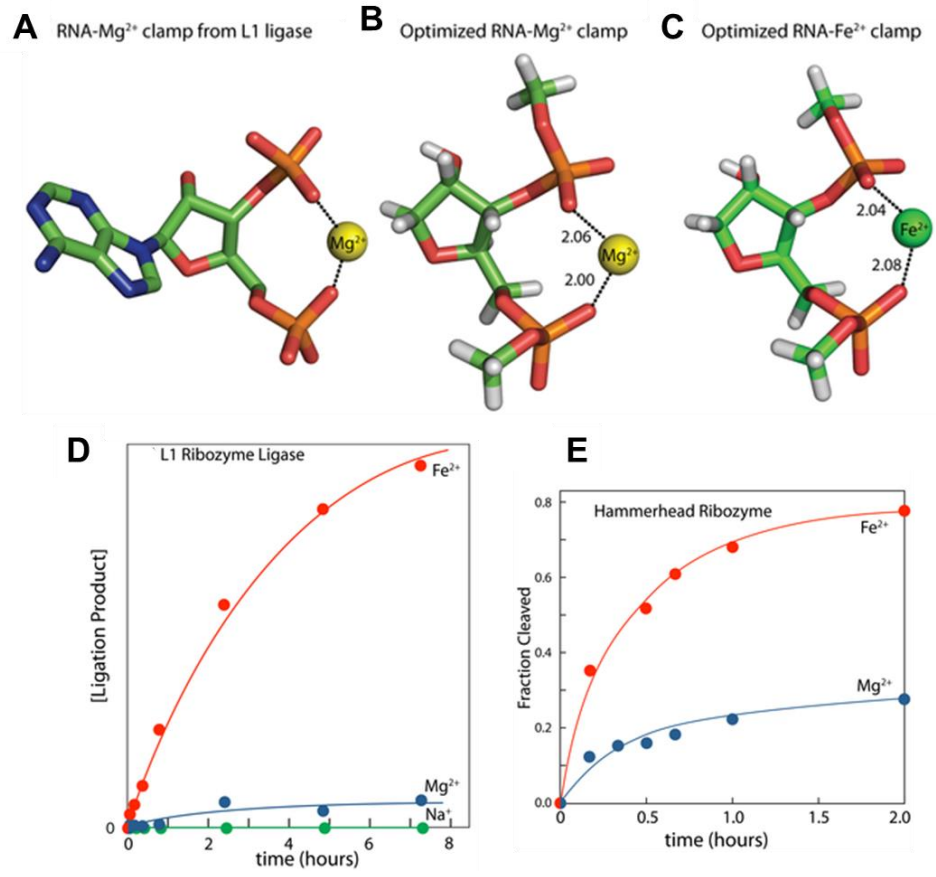

Figure 1.5. Conformation of the RNA-Mg^{2+} and RNA-Fe^{2+} clamp. **A)** RNA-Mg^{2+} clamp from the L1 ribozyme ligase, **B)** theoretically calculated RNA-Mg^{2+} clamp, and **C)** theoretically calculated RNA-Fe^{2+} clamp. DNAzyme reaction kinetic profiles of **D)** L1 ribozyme ligase and **E)**

hammerhead ribozyme, in the presence of Fe^{2+} and Mg^{2+}. Reproduced with a permission from Athavale, S., *et al*, PLoS One 2012.[49]

Mechanistic understanding of the 17E DNAzyme

In addition to the structural orientation of the metal ions to the cleavage site RNA, chemical interaction is also important. The positively charged metal ions can stabilize the negative charge of the DNA. There are a few plausible strategies, as outlined by Breaker and co-workers as follows (**Figure 1.6**).[47, 50] 1) in-line nucleophilic attack (α), 2) the negative charge of the non-bridging oxygen of the phosphodiester linkage are neutralized with the positively charged metal ions (β), 3) deprotonation of the 2′-OH by the metal hydroxide promotes nucleophilic attack of the phosphate (γ), and 4) negative charge on the 5′-oxygen is neutralized by the metal ion to stabilize the leaving group (δ). The metal-dependent activation should be correlated to the affinities to the oxygen (non-bridging and/or bridging oxygen) or the likelihood of 2′-OH deprotonation.

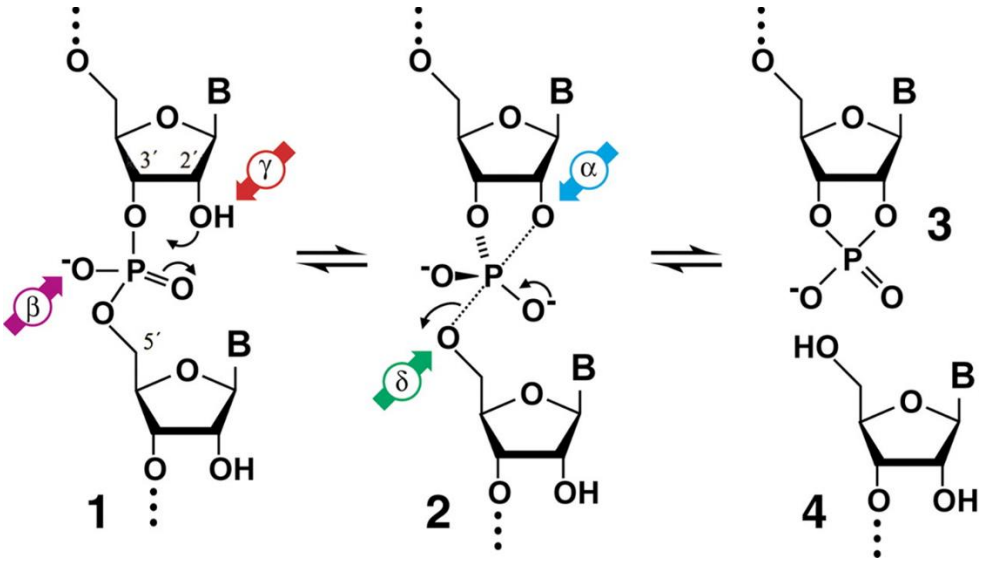

Figure 1.6. Possible strategies for RNA-cleavage by metal ions. α strategy: in-line nucleophilic attack, β strategy: the negative charge of the non-bridging oxygen of the phosphodiester linkage are neutralized with the positively charged metal ions, γ strategy: deprotonation of the 2′-OH by

the metal hydroxide promotes nucleophilic attack of the phosphate, and δ strategy: negative charge on the 5′-oxygen is neutralized by the metal ion to stabilize the leaving group. Reproduced with a permission from Emilsson, G., *et al*, RNA 2003.[50]

For the mechanistic understanding of the 17E DNAzyme with unique properties, many biochemical assays have been carried out to survey the role of various metal cofactors.[44, 45, 47, 48, 51-53]. The furthest progress has been made with Pb^{2+} since it was the mainly focused metal ion cofactor for 17E due to its high activity. In 2017, Liu *et al.* have solved the crystal structure of the 8-17 DNAzyme with Pb^{2+} as a cofactor.[54] It was found that the Pb^{2+} is bound in a pocket of the folded DNAzyme and its metal hydrate stabilizes the 5′-oxygen while specific guanine from the DNAzyme sequence acts as a base to deprotonate the 2′-OH of the RNA for a nucleophilic attack. Therefore, Pb^{2+} interacts via a mixture of γ and δ strategies.

The stories for the different divalent metal ions are still an on-going challenge. The single binding site that appears to bind with different divalent metal ions is understood to be unspecific because it shows activities regardless of the metal ion size, hardness, and coordination preferences. A correlation between the low pK_a of the metal hydrates with the high activities observed was often discussed,[47, 55] but the argument poses many further questions about the validity of such claim because metal ions with lower pK_a are stronger acids that would not deprotonate the 2′-OH easily.

Adding to the various hints, such as no activity of $Co(NH_3)_6^{3+}$ with 8-17 or that the other divalent metal-dependent folding is different than that of the Pb^{2+}, the nature of interaction with the non-bridging phosphate oxygen should provide more mechanical information. By substituting the phosphate with a phosphorothioate which contains a sulfur atom in the place of the non-bridging oxygen, hard or soft metal ions can exhibit different measurable activities. Because

oxygen is a hard ligand and sulfur is a soft ligand, the phosphorothioate substitution inhibits the cleavage activity with the hard metal ion cofactors but is 'rescued' by the soft metals. This is called a 'thio effect.' In addition, stereoisomers R_p and S_p can distinguish which non-bridging position is important for interaction with the metal. This strategy can provide strong evidence for inner-sphere coordination mechanism with the metal, which can ultimately provide valuable information to effectively utilize 17E as a general biosensor for metal ion detection.

DNAzyme-based biosensors in biological fluids

Biological fluids contain varying levels of metal ions for their regular functions. An example range of metal ion concentration is listed in

Table 1.1.[56] Some metal ions are also not commonly found in regular condition but only observed in the event of toxic exposures, such as Pb^{2+} poisoning. While developing biosensors for these metal ions in biological fluids, blood serum is often used as a model because it is the most representative that is like the intracellular environment or the cytosol without the fibrinogen, the structural protein for the cells. The blood serum proteins are composed of about 60 – 80 mg/ml of total serum protein, 50 – 60 % of which are the albumins and 40% are globulins.[57]

Table 1.1 Intracellular metal composition and their concentration range in different compartments.[56]

Metal	Concentration range	
Na^{+}	Extracellular	~ 135 – 147 mM
	Cytosol	~ 10 – 20 mM
	Nucleus	~ 10 – 15 mM
Mg^{2+}	Extracellular	~ 0.5 – 1 mM
	Cytosol	~ 4 – 5 mM
	Nucleus	~ 17 – 20 mM
Mn^{2+}	Extracellular	~ 10 – 50 nM
	Cytosol	< fM
	Nucleus	< fM
Fe^{2+}	Extracellular	~ 15 – 20 μM
	Cytosol	~ uM
	Nucleus	~ ?
Zn^{2+}	Extracellular	10 – 20 μM
	Cytosol	~ 180 nM
	Nucleus	~ ?

RNA-cleaving DNAzymes have a great potential to be developed as a biosensor. In vitro selection technique can ensure selectivity of the target-dependent catalytic reaction. Although the DNAzyme activities can commonly be analyzed using the gel electrophoresis technique, simpler operation and higher sensitivity can be achieved using the appropriate detection methods. For example, colourimetric detection using the colour-changing property of the AuNP (gold

nanoparticle) aggregation via the substrate and DNAzyme hybridization that can be reversed in the presence of metal ions can achieve the limit of detection (LOD) of 100 nM Pb^{2+} (**Figure 1.7A**).[58] Coupling the DNAzymes with nanomaterial is also very adaptable by functionalizing the AuNP with other DNAzymes for different metal ion targets,[59, 60] or by using label-free DNA for even lower LOD. Adapting the basic design, improvements could lower the LOD to 0.2 nM Pb^{2+}.[61] Another example developed gold electrode surface-immobilized with the reporter molecule labeled 8-17 DNAzyme for the detection of Pb^{2+} upon the cleavage reaction using the differential pulse voltammetry (LOD 0.3 µM)[62, 63] or the Surface Enhanced Raman Spectroscopy (SERS) (LOD 70 fM).[64, 65]

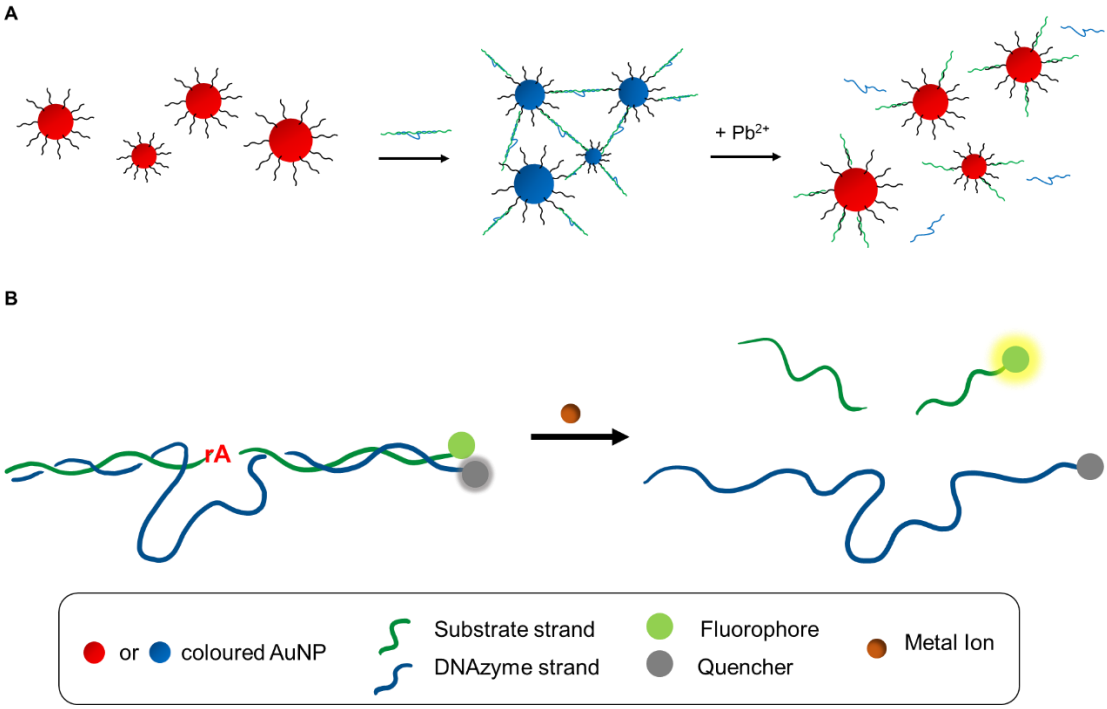

Figure 1.7. A) Aggregation-based colorimetric detection of Pb^{2+}. Aggregation of the AuNP changes colour to blue from red. The DNAzyme-labeled AuNP are interlinked with each other until Pb^{2+} cleaves the substrates, releasing the AuNPs to change colour to red. Illustration adapted from Liu, J. *et al* 2003.[58] **B)** General fluorescence sensor design commonly used for DNAzyme studies.[3]

The most frequently used detection mode is the fluorescence-based method. By labeling the substrate strands with a fluorescent marker, such as carboxyfluorescein (FAM), and the DNAzyme strand with a quencher molecule, such as Black Hole Quencher® dyes (BHQ), the annealed DNAzyme: Substrate complex will have reduced fluorescence signals. Upon the cleavage of the substrate, the shortened substrate DNA is released to increase the detectable fluorescence signal (**Figure 1.7B**).[66] The buffered environment can be optimized further by varying the type and the concentration of the buffer molecule and the stabilizing salt. The binding arm composition and the length can also determine the melting temperature, which is proportional to the stability of the sequence or how easily the cleaved fragment will dehybridize from the DNAzyme binding arm. The combination of these variables can affect the kinetics of the sensor activities and are considered during the binding arm design process.

Using such fluorescence-based DNAzyme biosensor design works well in buffered samples, but spatiotemporal control of the cleavage reaction is one of the challenges of intracellular detection of metal ions because the sensor needs to be delivered into the cells. To solve this issue, Lu and co-workers utilized an attachment of the O-nitrobenzyl group to the 2′ position of the cleavage site ribose to prevent the cleavage reaction until the photocage molecule is detached with 365nm UV light irradiation (**Figure 1.8**).[67] This strategy allowed the control of reaction initiation as well as low non-specific background for cellular imaging applications. Therefore, different nanomaterial or detection methods can achieve creative new ways to simplify operation, lower detection limit, and adapt to the sample of interest.

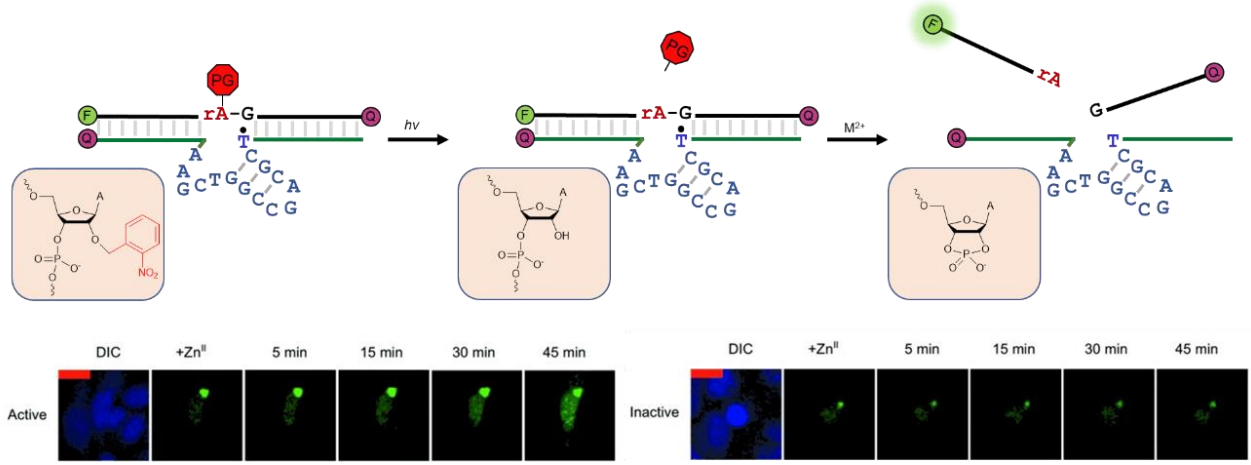

Figure 1.8. The photocaging protecting group at the cleavage site can inhibit the cleavage reaction until removed by UV light irradiation. This strategy allows temporal control until the DNAzyme biosensor is delivered into the cells for intracellular detection and imaging applications.[67, 68] PG indicates protecting group.

Research Problem

DNAzymes have a great potential for a wide range of sensing applications. The development of the DNAzyme biosensors can be divided into four main stages: 1) in vitro selection with the target sequence, 2) characterization of the obtained DNAzyme sequence, 3) preparation of the biosensor application, and 4) characterization of the designed biosensor. Although the success of step 1 may be exciting, a thorough characterization and in-depth understanding of the DNAzyme mechanism is very important. The class of 8-17 DNAzymes, including the 17E used in the studies to be discussed in the following chapters, have been one of the most extensively studied DNAzymes to date. However, the attention has been mainly focused on Pb^{2+} as the target metal ion due to its high RNA-cleaving activity. The mechanistic roles of other divalent metal ions that are also active with 17E remains a challenge still to be further understood.[69] Studies with Pb^{2+} suggest that 8-17 does not induce global folding, but other metal ions such as Zn^{2+} and Mg^{2+} induce global folding that leads to catalysis.[70-73] Different structural rearrangements by the different metal

ions were also observed, which suggest a different mechanistic pathway. To date, the studies that examine the effect of different metal ions are scattered. Therefore, the first part of this work attempts to examine the correlation of the various divalent metal ions with the 17E DNAzyme. This knowledge will provide more insights into the fundamental roles that the divalent metal ions play in promoting RNA-cleaving catalytic reaction.

While systematically screening the different divalent transition metal ions, previously unnoticed high activity of Fe^{2+} with the 17E DNAzyme was observed. Because Fe^{2+} is easily oxidized to Fe^{3+} in the presence of air and an aqueous environment, the metal may not have been examined with the DNAzymes. To explore this observation in greater detail, reports studying the ribozymes were referenced. Williams and coworkers reported that Fe^{2+} and Mg^{2+} had some similarities when it comes to binding to the RNA binding site.[49] Based on this, we hypothesized that the DNAzymes active with Mg^{2+} could also be active with the Fe^{2+}. The second part of this work explores using the Fe^{2+} as a cofactor and compares different DNAzymes' activity with them.

Lastly, the third part of this work attempts to identify one of the remaining challenges for using the DNAzyme as a biosensor with real-world samples, such as the environmental heavy metal detection in water or the intracellular metal ion quantification. **Table 1.2** summarizes some of the metal-dependent DNAzymes and their sensitivities, quantified as LOD, in different samples found to date. Generally, the LOD increases in the complex samples for the DNAzyme biosensors. While the DNAzymes are biocompatible to the biological or environmental samples, the presence of other species in such complex samples can affect the DNAzyme activity in a reverse direction. For example, nucleases are proteins that degrade nucleic acids and can affect the stability of the DNAzyme biosensors for normal function. As an example of many solutions that have been suggested, the extended stability of chemically modified aptamers in serum was reported to reduce

the degradation process.[74] However, not only the protein-DNA interaction but also the protein-metal analyte interaction can also affect accurate quantification of the analyte. Identification of the variables that can affect the sensor sensitivities can provide valuable information for the DNAzyme biosensor designs.

Throughout the three studies presented in this thesis, the general theme of understanding the interaction mechanism of RNA-cleaving DNAzymes 17E and more with various metal ions are probed. The gained knowledge can provide more insights into the future biosensor application designs using the DNAzymes that have great potential as a sensor.

Table 1.2. Different metal-dependent DNAzymes and their sensitivities.

DNAzyme	Active metals	LOD as a sensor	LOD in biological samples	References
17E	Pb^{2+}	10 nM	-	*75*
8-17	Pb^{2+}	7.8 nM	-	*32*
GR5	Pb^{2+}	3.7 nM	-	*32*
Tm7	Tl^{+}	1.5 nM	-	*76*
Ag10c	Ag^{+}	24.9 nM	-	*77*
Ce13d	Ce^{3+}	1.7 nM	-	*78*
Ce13d	Cr^{3+}	70 nM	-	*79*
Ce13d	Cr^{4+}	140 nM	-	*79*
Cd16	Cd^{2+}	1.1 nM	-	*80*
NaA43(T)	Na^{+}	1.35 μM	1.9 mM	*40, 81*
NaH1	Na^{+}	223 μM	676 μM	*82*
Lu12	Nd^{3+}	0.4 nM	-	*83*
39E	UO_2^{2+}	45 pM	-	*84*

Chapter 2 Probing Metal-dependent Phosphate Binding for the Catalysis of the 17E DNAzyme

Introduction

DNAzymes are DNA-based catalysts and were found to have interesting applications as metal sensors, anti-viral agents, and DNA-based switches.[14, 85] Many metal-specific RNA-cleaving DNAzymes have been obtained via a combinatorial method called in vitro selection.[14, 86, 87] They have been used to detect monovalent Na^+ [40, 88, 89] and Ag^+;[77] divalent Pb^{2+},[13] Zn^{2+},[44, 90] Cu^{2+},[91] UO_2^{2+},[84] Cd^{2+},[80] and Hg^{2+};[92] and trivalent lanthanides.[42, 78, 83, 93]

Some of the most extensively studied DNAzymes contain the 8-17 motif.[34, 69, 94] Extensive biochemical assays have been carried out using various metal cofactors,[34, 44, 45, 47, 48] core mutation,[52, 53, 95], and change of the substrate cleavage junction.[96] The same catalytic motifs have been reported in many different selection conditions by multiple research groups. The 8-17 DNAzyme was first selected in the presence of Mg^{2+} with an all-RNA substrate.[34] Then, it was selected in the presence of Mg^{2+} again (called Mg5) with a single RNA linkage,[43] although this was not realized until a careful subsequent analysis.[97] Lu and coworkers obtained a closely related sequence 17E using Zn^{2+}.[44] Li and coworkers performed comprehensive selections and articulated the reason for the recurrence of the 8-17 motif for its small size, high activity, and tolerance to mutation.[98, 99] Cd^{2+} was also used to yield the motif.[100] In addition, a selection in serum was performed and Ca^{2+} was believed to be the main metal cofactor responsible for isolating the 17E.[101] These examples indicated the motif's tolerance to various divalent metal ions.

Different divalent metals have different activities for the 8-17 motif. Pb^{2+} is the most active, followed by the transition metals such as Zn^{2+}, Co^{2+}, and Cd^{2+}, while Mg^{2+} and Ca^{2+} have the lowest activity.[45, 100] The role of Pb^{2+} has been described as a general acid in the crystal structure

of the Pb^{2+}-bound 8-17,[54] where Pb^{2+} bound water was found to act to assist the leaving group. Guanine (G14) served as a general base to help deprotonate the 2′-OH nucleophile.[102] However, sufficient evidence showed that Pb^{2+} might have a distinct mechanism from the rest of divalent metal ions. For example, Pb^{2+} cannot induce a global conformational change of the DNAzyme yet it had much higher activity than Mg^{2+} and Zn^{2+} that can induce a global folding.[70]

Metal ions have multiple important properties, including shifting the pK_a of the metal-bound water, Lewis acidity, and thiophilicity.[14, 87, 103, 104] They may play several mechanistic roles for the RNA cleavage reaction as well.[46] Aside from the general acid role by Pb^{2+}, another commonly cited role of metal ions is to interact with the scissile phosphate by balancing the negative charges built during the transition state. In this work, we probed the interaction between various metals with the scissile phosphate. We believe most metals function by coordinating to the phosphate via a Lewis acid catalysis, while Pb^{2+} has a different mechanism of general acid catalysis.

Materials and Methods

Chemicals. DNAzyme (17E) and FAM-labelled substrates were purchased from Integrated DNA Technologies and were purified by denaturing polyacrylamide gel electrophoresis (dPAGE). 17E sequence was 5′-TTTCGCCATCTTCTCCGAGCCGGTCGAAATAGTGACTCGTGAC-3′ and the substrate sequence was 5′ – GTCACGAGTCACTAT rA GGAAGATGGCGAAA-FAM -3′. The phosphorothioate substituted substrate strand was named PS. The two HPLC isolated isomers of the PS were named R_p and S_p. The two phosphorothioate substrate isomers were separated and purified by HPLC by the previously reported method.[80] Sodium chloride, 10x Tris Buffer EDTA (TBE), urea, ammonium persulfate (APS), tetramethylethylenediamine (TEMED), 3-(N-morpholino) propanesulfonic acid (MOPS), and 2-(N-morpholino)ethanesulfonic acid (MES)

were purchased from Bio Basic Inc. Gel loading dyes for gel electrophoresis were purchased from New England Biolabs. Magnesium chloride, calcium chloride, and cesium chloride were from Amresco. Iron (II) chloride and iron (III) chloride were from Alpha Aesar. Monobasic sodium phosphate, dibasic sodium phosphate, rubidium chloride, cobalt chloride, nickel chloride, copper chloride, zinc chloride, cadmium chloride, and lead nitrate, silver chloride, lanthanum chloride, cerium chloride, europium chloride, ytterbium chloride, and mercury chloride were from Sigma Aldrich. A BioRad ChemiDoc MP Imaging System was used for gel imaging.

Activity assays. To test the cleavage activities of the 17E and the substrates, incubated FAM-labelled substrates were analyzed by dPAGE. Reactions with the substrates PO, as well as PS, PS-R_p, and PS-S_p, were used throughout this study. As an example of the typical activity assay, 17E DNAzyme and PO substrate experimental condition is described here.

The molar ratio of 1.5:1 of DNAzyme to FAM-labelled substrate was used to ensure that all substrates are formed into complex when preparing the DNAzyme complex. The final FAM-labelled substrate concentration was 5 μM. Typically, 14 μL of the complex was annealed fresh on the day of the experiment for a set of 12 samples. For example, 1.0 μL of 100 μM 17E DNAzyme and 1.4 μL of 50 μM PO substrates were diluted into 11.5 μL of annealing buffer (50 mM MES pH 6, 25 mM NaCl). The mixture was incubated at 95°C for 1 min, then at 4°C for 30 min to anneal the DNAzyme and the substrate strands together. Then, 1 μL of the DNAzyme complex was diluted into 4 μL of the reaction buffer (50 mM MOPS pH 7.5, 25 mM NaCl).

To start the incubation with the metal, 2 μL of concentrated metal stock solution was added to obtain the desired final concentration. All the reported metal concentrations are the final concentration at this stage before the reaction is quenched with urea. To the 7 μL reaction solution,

7 μL of quenching dye (1x purple loading dye, 8 M urea) was added after an incubation period (10 min, unless otherwise indicated) to quench the reaction and prepare for gel electrophoresis. 15% dPAGE gel (14 mL 15% dPAGE solution, 64 μL 10% APS, 10 μL TEMED) was used to run the samples for 80 min at 200 V. The obtained gels were fluorescence imaged with Bio-Rad ChemiDoc MP Imaging System.

Activity in phosphate buffer. All the conditions for the tests in phosphate buffer were the same as normal activity assay protocols, except that the reaction buffers were switched to phosphate buffer saline (PBS) which is 50 mM phosphate pH 7.5, 25 mM NaCl for the preliminary study. For the detailed inhibition study, 1 μL of the annealed DNAzyme complex was diluted into 4 μL of the inhibition reaction buffer (50mM MOPS buffer pH7.5, 25 mM NaCl, and varying concentrations of phosphate).

Data analysis. Gel micrographs were analyzed using the Image Lab software to define the areas of the lanes and bands. The fluorescence intensities of each band were used to calculate the % cleavage of the DNAzyme cleavage reaction from the user-identified uncleaved and cleaved bands. Throughout this paper, the cleavage activity will be notated as % cleavage for 17E: PO cleavage reaction in MOPS buffer as default, with the description of experimental conditions if necessary. For various comparisons, % cleavage_{PO} and % cleavage_{PS} will describe the cleavage of PO substrate and PS substrates, respectively. % cleavage_{MOPS} and % cleavage_{PBS} will describe the cleavage of PO substrate in MOPS or PBS buffer conditions, respectively. The degree of inhibition will be denoted as Δ cleavage which is quantified by the difference between the % cleavage_{MOPS} and the % cleavage_{PBS}. The kinetics curve data were fitted into the binding model equation

(Eqation 2.1) to obtain the observed rate constant, b or k_{obs}.[45] The slower rate constants for only a few of the metals with R_p substrate stereoisomer were estimated from the slopes of the linear 24 h kinetic profiles. Single metal-binding model equation (Equation 2.2) was also used to fit the metal concentration dependence plots at a fixed reaction time of 10 minutes, where b is the apparent dissociation constant K_d.

$$y = y_0 + a(1 - e^{-bt}) \qquad \textbf{\textit{Eqn. 2.1}}$$

$$y = \frac{a[M]}{(b+[M])} \qquad \textbf{\textit{Eqn. 2.2}}$$

Results and Discussion

The 17E DNAzyme is active with most divalent metals but not mono or trivalent metals.

The secondary structure of the 17E DNAzyme complex is illustrated in **Figure 2.1A**. Its substrate strand contains a single RNA linkage rA that serves as the cleavage site. The 17E DNAzyme is active with many divalent metal ions. To monitor its cleavage activity, we used a FAM-labeled substrate strand and denaturing polyacrylamide gel electrophoresis (dPAGE). A representative gel micrograph is shown in **Figure 2.1B**, where 10 μM of various divalent metals yielded different fractions of cleavage after 10 min.

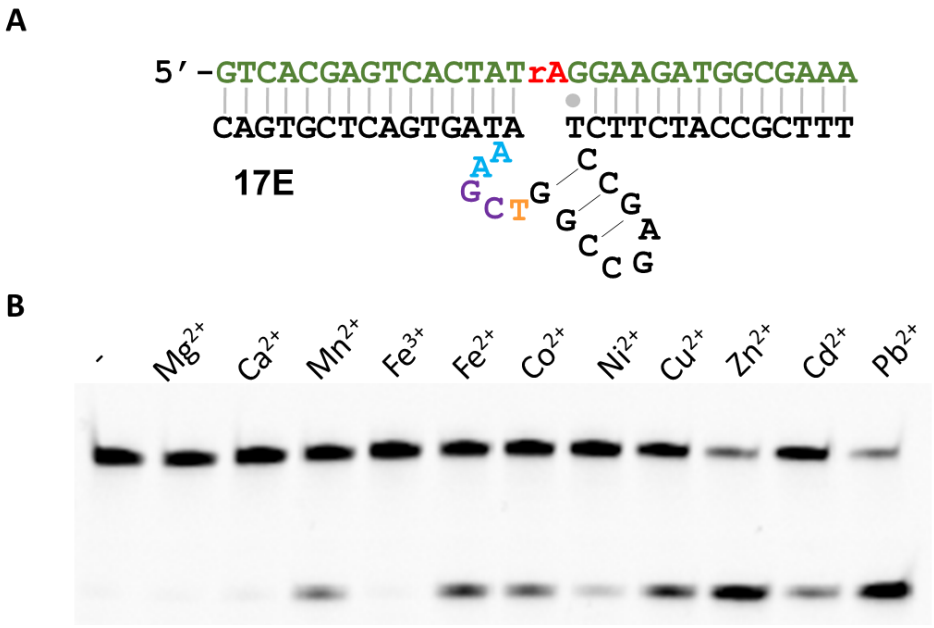

Figure 2.1. A) The secondary structure of the 17E DNAzyme complex and **B)** A representative gel micrograph showing a cleavage assay in the presence of various divalent metal ions (10 μM each) after 10 min of incubation at pH 7.5.

To have a full understanding of the effect of metal ions, the cleavage yields in the presence of various monovalent (**Figure 2.2A**), divalent (**Figure 2.2B**), and trivalent (**Figure 2.2C**) metal ions at 10 μM, 100 μM, and 1 mM were measured after 10 min. Among the tested, neither the monovalent nor the trivalent metals showed any cleavage activity. The low activities with group 1A metals were previously reported.[48] All the tested divalent metals showed various levels of cleavage, and the divalent charge may be critical for 17E activation.

A careful examination of the activity trends in **Figure 2.2B** revealed a few interesting observations. Divalent metals with a higher concentration generally produced a higher cleavage yield, except for Cu^{2+} at 100 μM and 1 mM; and Pb^{2+} at 1 mM. Their inhibition was likely caused by the strong interactions between Cu^{2+} or Pb^{2+} and the DNA bases to disrupt the active DNAzyme structure and result in misfolding of the DNA.[8, 105] Out of the metals tested, Pb^{2+} had the highest

activity while group 2A metals (Mg^{2+} and Ca^{2+}) had the lowest activity at the same metal concentrations.[44, 45, 100] When the first-row transition metals (from Mn^{2+} to Zn^{2+}) were examined, Ni^{2+} had the lowest activity (**Figure 2.2B**). This trend remained true for higher concentrations except for Cu^{2+} as mentioned above. For the three group 2B metals, the activity dropped to zero with Hg^{2+}.

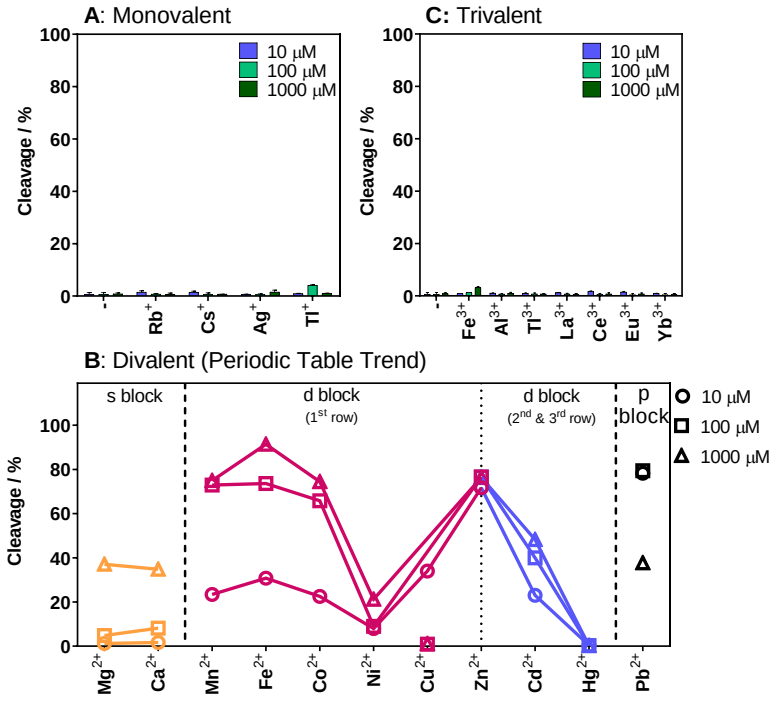

Figure 2.2. Quantified cleavage yields of the 17E DNAzyme in the presence of various concentrations of **A)** monovalent, **B)** divalent, and **C)** trivalent metal ions after 10 min reaction in 50 mM MOPS buffer at pH 7.5.

The 17E has been most thoroughly studied with Pb^{2+} for its highest activity,[45, 53, 102, 106] and with Mg^{2+} for potential biomedical applications.[70, 107, 108] The different activities of the metal ions were discussed previously. Studies showed a linear relationship with the cleavage activity and pK_a of metal-bound water.[109-111] The metal hydroxides may deprotonate the 2′-OH to facilitate the

nucleophilic attack on the scissile phosphate. The lower pK_a of Pb^{2+} and the high pK_a of the group 2A metals (i.e. Mg^{2+} and Ca^{2+}) were often cited to correlate the activity. However, this argument was questioned by Pontius et al.[111, 112] Since metals with a lower pK_a are stronger acids, it would be less likely for such acidic metals to deprotonate the 2′-OH (pK_a ~12).[1] From the activity comparison in **Figure 2.2B**, even with the similar pK_a of Co^{2+} (9.65) and Ni^{2+} (9.86),[113] they had quite different activities. Indeed when the rates of metal ions were plotted against the pK_a, Ni^{2+} seemed to be an outlier (**Figure 2.3**).[55] In addition, based on the crystal structure[54] and the subsequent biochemical assays,[102] the general base role was performed by guanine instead of a metal ion. Thus, we became interested in probing other possible roles of metal ions in the reaction.

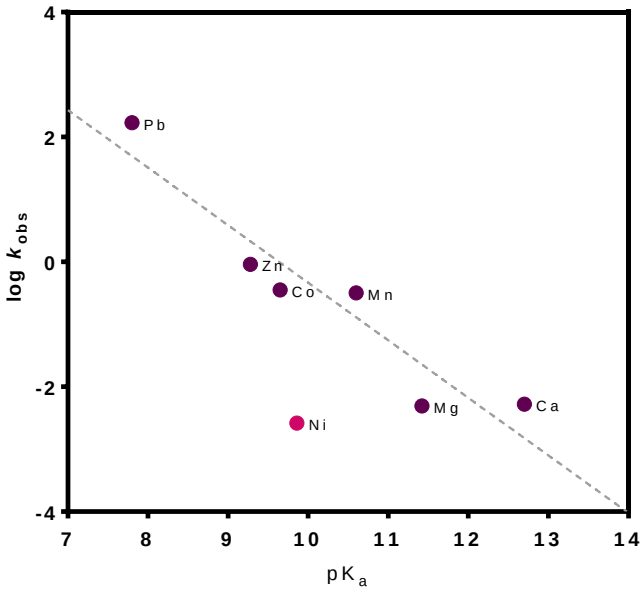

Figure 2.3. Metal activity correlation with the pK_a. The kinetic assays were performed between 1 μM – 1 mM metal ions in 50 mM MOPS buffer pH 7.5, 25 mM NaCl. The calculated k_{obs} were normalized to 100 μM. pK_a values for each metal ions were referenced from Hud, N., et al. [113]

The group 2B metals showed a descending trend down the column (Zn^{2+} > Cd^{2+} > Hg^{2+}), which correlated to the thiophilicity of the metals.[114] In the context of the RNA cleavage reaction,

this may suggest an interaction between metal ions as a Lewis acid and oxygen on the scissile phosphate.

Probing phosphate-binding using phosphorothioate substrate.

To directly probe the interaction between metal ions with the scissile phosphate, the phosphorothioate (PS) substrate was used. Many DNAzymes,[115] such as the 10-23,[116] Ce13d,[117] and Tm7[93] have been carefully studied using PS substrates. The PS substrate used in this experiment was a mixture of two stereoisomers: R_p and S_p (**Figure 2.4A**). Typically, the two isomers are present in an approximately 1:1 ratio (50% each). Depending on the metal-binding preference, varying degrees of inhibition can be observed (called the thio effect).

To examine this effect more carefully with the 17E DNAzyme, a range of concentrations for each of the metal ions with the PO and PS substrates were compared (**Figure 2.4B-I**). By fitting the curves into the one site binding model (Equation 2.1), the cleavage saturation and the K_d (**Table 2.1**) at 10 min reaction were obtained. For most of the metals, the cleavage yield with the PS substrate was lower than half of that of the PO substrate. In particular, Ni^{2+} was strongly affected by the PS modification since its cleavage yields were less than 20% of that of the PO substrate (**Figure 2.4E**). Exceptions were observed with more thiophilic metals such as Zn^{2+}, Cd^{2+}, and Pb^{2+}, where their PS yield reached more than half of the PO. For Pb^{2+}, the same yield was observed for these two types of substrates, which suggested a distinct mechanism for Pb^{2+}.

Table 2.1. Dissociation constants (K_d, μM) of different metal ions with 17E DNAzyme and PO or PS substrates in 50mM MOPS buffer pH 7.5, 25 mM NaCl. The reaction time was 10 min.

	PO in MOPS	PS in MOPS
Mg^{2+}	1158	6852
Ca^{2+}	1236	2658
Mn^{2+}	17.83	61.47
Fe^{2+}	29.7[a]	81.63
Co^{2+}	26.96	140.7
Ni^{2+}	700.3	461.9
Cu^{2+}	25.94	193.8
Zn^{2+}	3.692	2.302
Cd^{2+}	13.52	25.17
Pb^{2+}	0.4187	0.9674

[a] Ref. *118*

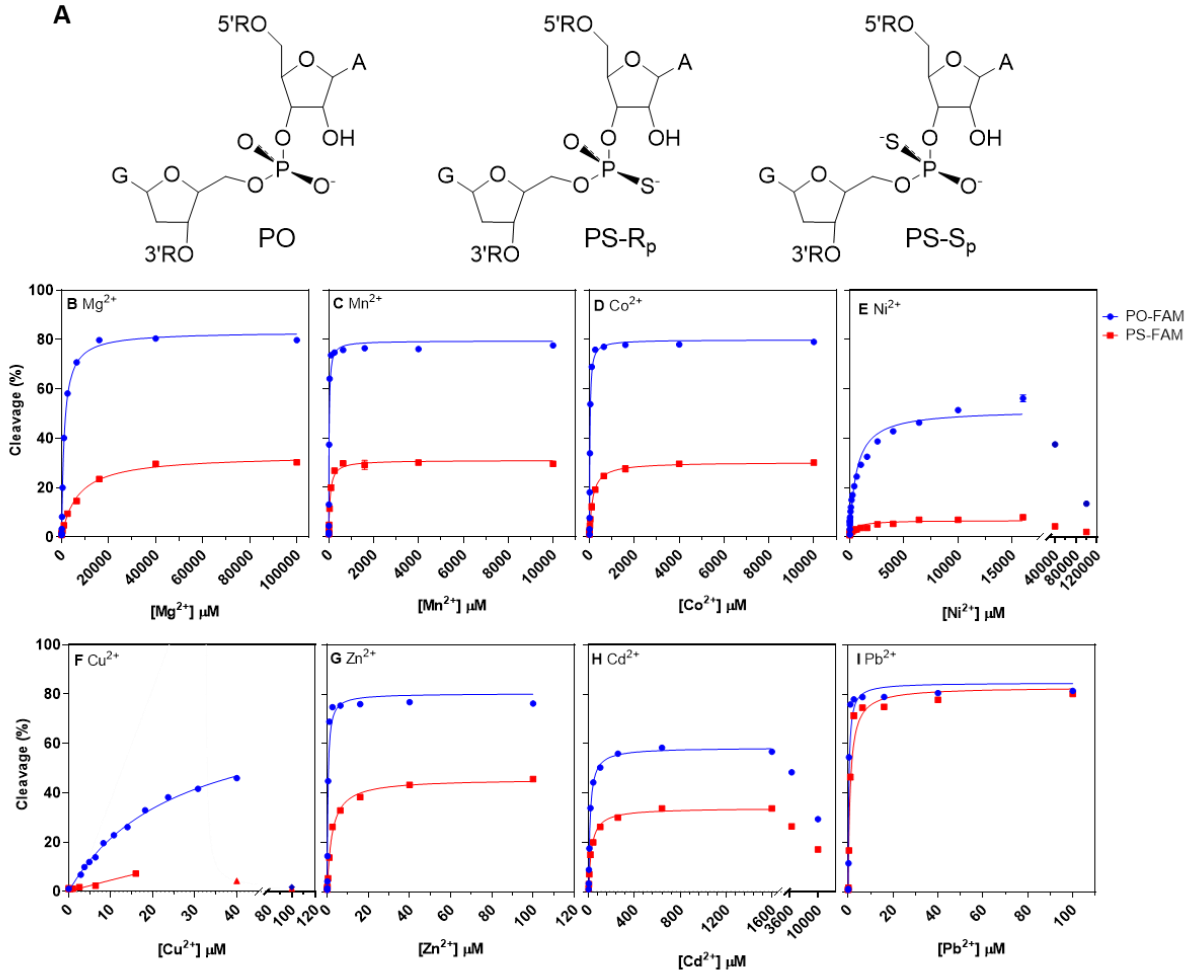

Figure 2.4. **A)** The structure of the cleavage site with normal PO and PS linkages for both R_p and S_p isomers. **(B-I)** Concentration-dependent plots of substrate cleavage using 17E DNAzyme and

different metal cofactors after 10 min reaction. PO-FAM and PS-FAM substrates are compared. These plots were used to obtain the saturation cleavage % (B_{max}) and dissociation constant (K_d) according to the single binding model equation. The obtained K_d are summarized in **Table 2.1**.

The above assay gave us a general understanding of the cleavage of the PS substrate and the metal ion concentration range. To have a more quantitative understanding, the R_p and S_p isomers were prepared by HPLC and individually tested. Metal ions that represent hard, borderline, and soft metals were chosen (10 mM Mg^{2+}; 1 mM Mn^{2+}, Co^{2+}, Ni^{2+}, Zn^{2+}, and Cd^{2+}; 10 μM Cu^{2+}, and 1 μM Pb^{2+}).[119, 120] These metal concentrations were chosen to ensure a high cleavage activity without inhibition effects.

When assayed with 10 mM Mg^{2+} (**Figure 2.6A**), the S_p isomer had a rate of 0.16 min^{-1}. On the other hand, the R_p isomer had a maximum yield of about 10%. This 10 % R_p cleavage can be attributed to the S_p contamination due to the incomplete HPLC separation since this 10% yield was achieved very fast. After that, almost no further cleavage occurred. Therefore, the true rate for the R_p should be estimated from the slower phase. After incubating 10 mM Mg^{2+} with the 17E/R_p for up to 24 h, the rate was estimated to be 7.4×10^{-5} min^{-1} (**Figure 2.5**). Therefore, the S_p/R_p activity ratio was calculated to be 2083 (**Table 2.2**), suggesting that Mg^{2+} interacted with the pro-R_p oxygen.

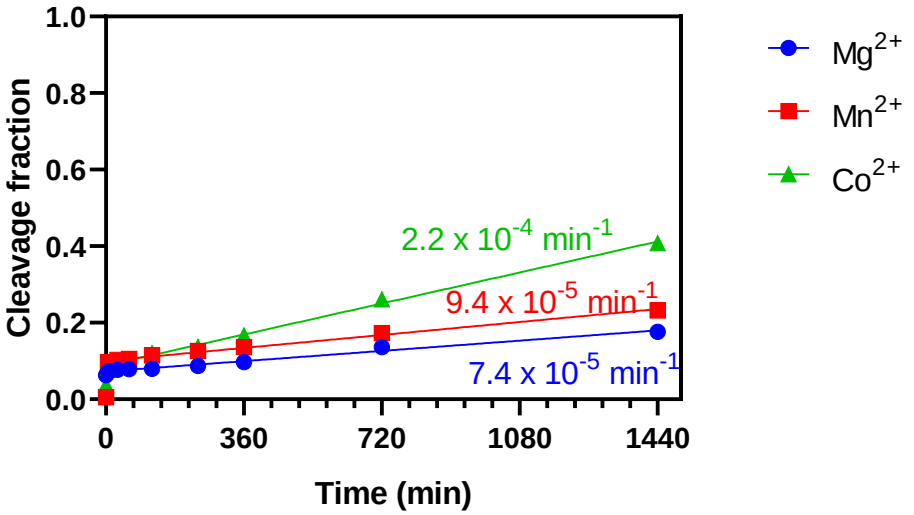

Figure 2.5. Rate constant K_{obs} (min^{-1}) estimation from 24 h kinetic profile of 10 mM Mg^{2+}, 1 mM Mn^{2+}, and 1 mM Co^{2+} with the PS-R_p substrates. The slopes of the linear regression from 5 min to 24 h were calculated as the rates for the slower reaction conditions.

For Mn^{2+} and Co^{2+}, a similar trend was observed (**Figure 2.6B-C**), where the activity was significantly reduced with the R_p substitution, and their S_p/R_p activity ratios were 5345 and 934, respectively (**Table 2.2**). For the PO substrate, these two metals were about 4-fold more active than Mg^{2+} even when their concentration was 10-fold lower. This can be explained by their stronger affinity to the scissile phosphate, yet Mg^{2+}, Mn^{2+}, and Co^{2+} all followed the same metal binding mechanism as probed by the PS substrates.

Similarly, Cu^{2+}, Zn^{2+}, and Cd^{2+} were also examined (**Figure 2.6E-G**). The S_p/R_p ratio was 26 for Zn^{2+} (**Table 2.2**), which was due to the substantial activities with the R_p substrate. The S_p/R_p ratio was only 0.9 for Cu^{2+} and 0.8 for Cd^{2+}, and the two isomers did not differ much in the activity. In other words, these three more thiophilic metals can rescue the activity (e.g. of Mg^{2+}).

The 17E DNAzyme (with the PO substrate) was able to effectively use Cd^{2+} despite that Cd^{2+} is a thiophilic metal. Once replaced by sulfur at the R_p position, the activity decreased only

3-fold compared to the PO substrate. In previous work using Cd^{2+} to do DNAzyme selection, the 8-17 motif was obtained.[100] When we used a PS-modified library and Cd^{2+}, a DNAzyme named Cd16 was obtained, which is only active with the PS substrate (the PO substrate had no activity at all).[80] Therefore, the DNAzyme sequence is critical. Overall, using a hard metal such as Mg^{2+}, Mn^{2+}, or Co^{2+}, 17E showed a very large thio effect. This observation suggests that most divalent metals bind specifically to the pro-R_p oxygen via inner-sphere coordination. Similar behavior has been observed with ribozymes.[121] The fact that 17E can also use thiophilic metal such as Cd^{2+} for catalysis can explain its wide acceptance of divalent metal ions, at least with thiophilicity between Mg^{2+} and Cd^{2+}. Of note, when the thiophilicity is too strong, such as Hg^{2+}, the activity is lost.

For Pb^{2+}, the S_p and R_p isomers' cleavage rates were measured to be 0.42 min^{-1} and 0.080 min^{-1}, respectively (**Figure 2.6H**). The resulting S_p/R_p ratio of Pb^{2+} was just 5, and the PO was only 4-fold faster than the S_p. Therefore, Pb^{2+} is not very sensitive to the thio substitution. Based on the crystal structure, Pb^{2+} does not coordinate via the inner-sphere mechanism with the scissile phosphate,[54] but it rather serves as a general acid to interact with the leaving group. Other spectroscopic studies also indicated a different mode of Pb^{2+} binding compared to other metal ions such as Mg^{2+} and Zn^{2+}.[71] Among the tested metal ions, Pb^{2+} had the lowest concentration of only 10 μM (100-fold lower than the transition metals), yet it still had the highest activity. Such high activity also suggested a different catalytic mechanism. The small thio effect of Pb^{2+} and the small difference between R_p and S_p are consistent with the crystal structure (e.g. no direct inner-sphere Pb^{2+}/phosphate interactions).

As observed in **Figure 2.6D** and **Table 2.2**, PO substrate cleavage activity with Ni^{2+} is much lower than that of Zn^{2+} and Cd^{2+}, although they have a similar thiophilicity. Zn^{2+} has a high thiophilicity (and thus less oxophilicity) than Co^{2+} and Mn^{2+}, but it is more active. So, the activity

of cleaving the PO substrate did not directly correlate with oxophilicity. On the other hand, it seems that the activity of the R_p substrate had some correlation for the metals listed in **Table 2.2**, but still, the low activity with Ni^{2+} cannot be explained. So, some other factors need to be considered. Nevertheless, using the PS substrates, we demonstrated the importance of divalent metal ions interacting with the scissile phosphate and discussed Pb^{2+} as a unique metal using a different mechanism.

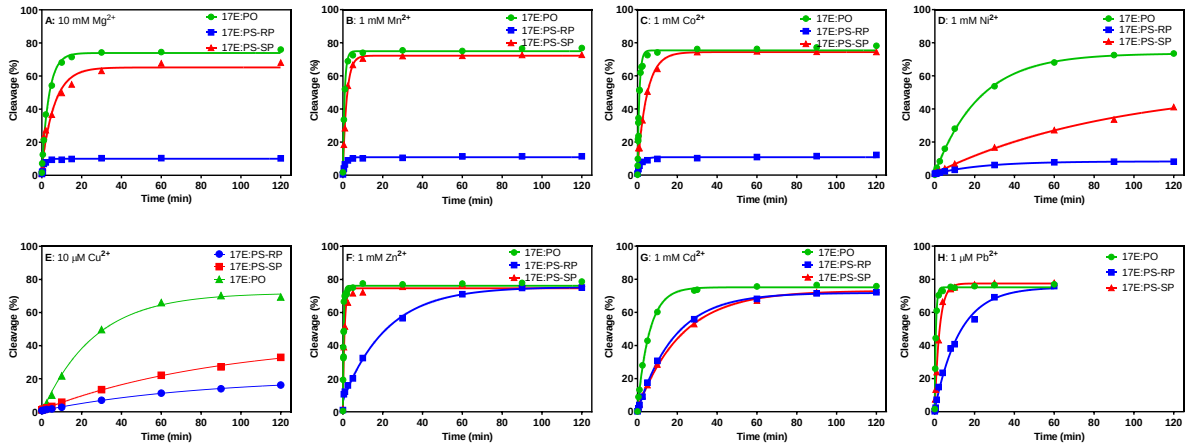

Figure 2.6. PO, R_p, and S_p cleavage kinetics of **A)** 10 mM Mg^{2+}, **B)** 1 mM Mn^{2+}, **C)** 1 mM Co^{2+}, **D)** 1mM Ni^{2+}, **E)** 10 μM Cu^{2+}, **F)** 1 mM Zn^{2+}, **G)** 1 mM Cd^{2+}, and **H)** 1 μM Pb^{2+}.

Table 2.2. Thiophilicity/Oxophilicity,[122] observed rate constants, k_{obs} (min^{-1}), the S_p/R_p ratios, and the PO/R_p ratios of the respective metal ions.

	Mg^{2+}	Mn^{2+}	Co^{2+}	Ni^{2+}	Cu^{2+}	Zn^{2+}	Cd^{2+}	Pb^{2+}
Thiophilicity	0.4	0.6	0.6	0.8	0.8	0.8	0.8	0.9
Oxophilicity	0.6	0.4	0.4	0.2	0.2	0.2	0.2	0.1
k_{obs} **PO**	0.28	1.12	1.08	0.045	0.038	2.45	0.17	1.66
k_{obs} S_p	0.16	0.50	0.21	0.011	0.011	1.19	0.045	0.42
k_{obs} R_p	7.44×10^{-5} *	9.40×10^{-5} *	2.25×10^{-4} *	0.041	0.012	0.045	0.054	0.080
S_p/R_p	2083	5345	934	0.27	0.89	26	0.84	5
PO/R_p	3755	11956	4795	1.1	3.1	54	3	21

Ligand exchange rate

Based on the observed thio effect, the interaction of the metal ions and the pro-R_p oxygen can be assigned to be an inner-sphere coordination mechanism, except for Pb^{2+}. To achieve inner-sphere coordination, a water ligand of metal ions needs to be replaced by the scissile phosphate. We wondered if the cleavage rates for the non-Pb^{2+} metal ions were related to their water ligand exchange rate. Among these first-row transition metal ions, Ni^{2+} is known to have the highest hydration enthalpy and the slowest water ligand exchange rate, which is consistent with our observation of the lowest activity with Ni^{2+}.

To test this hypothesis, the kinetic profile for each metal ion at their respective K_d was obtained. Since the cleavage rate can be expressed as $r = k[M^{2+}]$, $k = r/[M^{2+}]$ is the apparent rate constant mainly related to the activation energy of the rate-limiting step. The literature reported water exchange rates (k_{H2O}) were plotted against the k for each metal ion (**Figure 2.7**). A linear correlation was observed, which supported the hypothesis. Therefore, the step of inner-sphere metal coordination with the pro-R_p oxygen at the scissile phosphate would be the rate-limiting step for these metal ions.

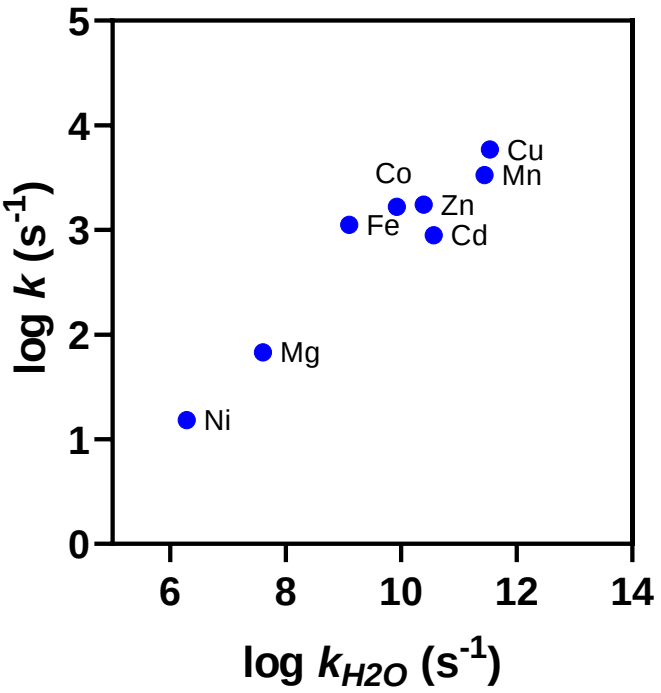

Figure 2.7. Comparison of the experimentally determined cleavage rates and the literature reported theoretical water exchange rates for the respective metals hypothesized to have an inner-sphere coordination mechanism of interaction with the non-bridging oxygen of the phosphate. For ligand exchange rate, the Mg^{2+}, Ni^{2+}, Cu^{2+} data were from ref.[123]; the Mn^{2+}, Fe^{2+}, Co^{2+} data were from ref.[124]; and the Zn^{2+}, Cd^{2+} data were from ref.[125]

Probing phosphate binding by using phosphate buffer as a competitor

To further probe the metal-phosphate interaction, we designed an inhibition study to examine the metal-phosphate binding affinity by intentionally adding the inorganic phosphate. Usually, phosphate buffer was avoided to minimize its potential inhibition effect due to the abundant metal binding.[33] In a preliminary screening, where phosphate buffer saline (PBS) and MOPS buffer were compared, it appeared that the cleavage yield decreased more for the metals with greater activities than those with lower activities (**Figure 2.8**). The highly active Pb^{2+} and Zn^{2+} were more inhibited, but metals such as Mg^{2+} that are less active did not have a significant

difference in PBS. Ca^{2+} formed precipitates with the phosphate, disabling accurate estimation. Further examination of the inhibition effects by the phosphate required changing the phosphate concentration and this could result in changing buffer effect. To eliminate such a problem, addition of varying concentrations of phosphate to the fixed 50 mM MOPS buffer, 25 mM NaCl was used for the subsequent experiments.

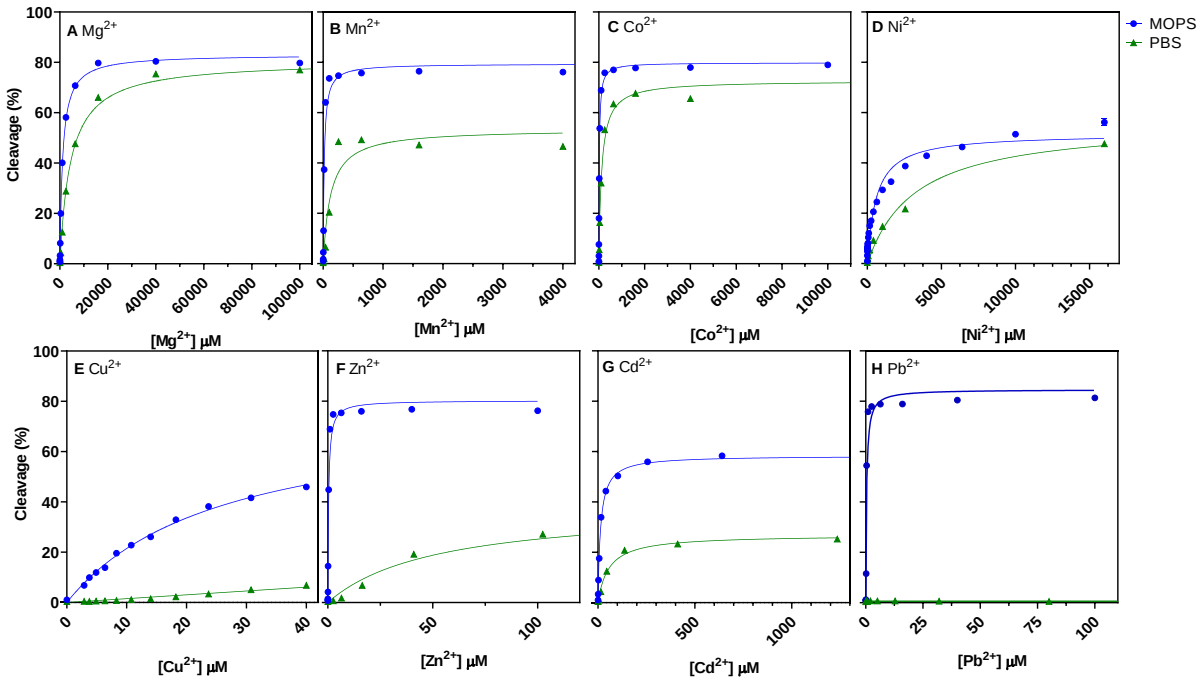

Figure 2.8. Comparison of the concentration-dependent activities with different metal ions in the normal MOPS buffer saline and the PBS buffer with the reaction time of 10 min. These plots were used to obtain the dissociation constant (K_d) according to the single binding model equation. The obtained K_d are summarized in

Table 2.3.

Table 2.3. Dissociation constants (K_d, μM) of different metal ions with 17E DNAzyme in 50mM MOPS buffer pH 7.5, 25 mM NaCl or 50mM PBS buffer pH 7.5, 25 mM NaCl, reaction time was 10 min.

	PO in MOPS	PO in PBS
Mg^{2+}	1158	4485
Ca^{2+}	1236	N/A[a]
Mn^{2+}	17.83	121.3
Fe^{2+}	29.7[b]	N/A
Co^{2+}	26.96	122
Ni^{2+}	700.3	4554
Cu^{2+}	25.94	59.1
Zn^{2+}	3.692	64.25
Cd^{2+}	13.52	55.28
Pb^{2+}	0.4187	N/A[c]

[a] Estimation was ~994 μM, but it is inaccurate due to precipitation. Increasing Ca^{2+} concentration up to 2.5 mM yielded ~20 % cleavage and the DNAzyme were denatured beyond 2.5 mM. All samples had precipitates formed. Ca^{2+} was not included in further studies.

[b] Ref. *118*

[c] Completely inactivated by phosphate until Pb^{2+} concentration reached 50 mM (buffer concentration) and precipitates formed beyond 50 mM. The same observation happened when tested in a lower PBS buffer concentration of 15 mM.

For the inhibition study, the kinetic profiles of each metal ion at two metal concentrations with different phosphate concentrations were examined (**Figure 2.9**). The phosphate concentrations were different for each metal to ensure inhibition was observed. As the phosphate concentration increased, the reaction rate generally slowed down due to the metal ions complexing with the inorganic phosphate instead of binding with the DNAzyme. For some metals such as Cd^{2+} and Pb^{2+}, the cleavage maximum plateau decreased, suggesting irreversible inhibition (e.g. non-competitive). However, the cleavage maximum plateau does not change with the other metals such as Mg^{2+}, Mn^{2+}, Co^{2+}, and Zn^{2+}, suggesting a reversible inhibition (e.g. competitive). The exceptional metal ions were Ni^{2+} and Cu^{2+}.

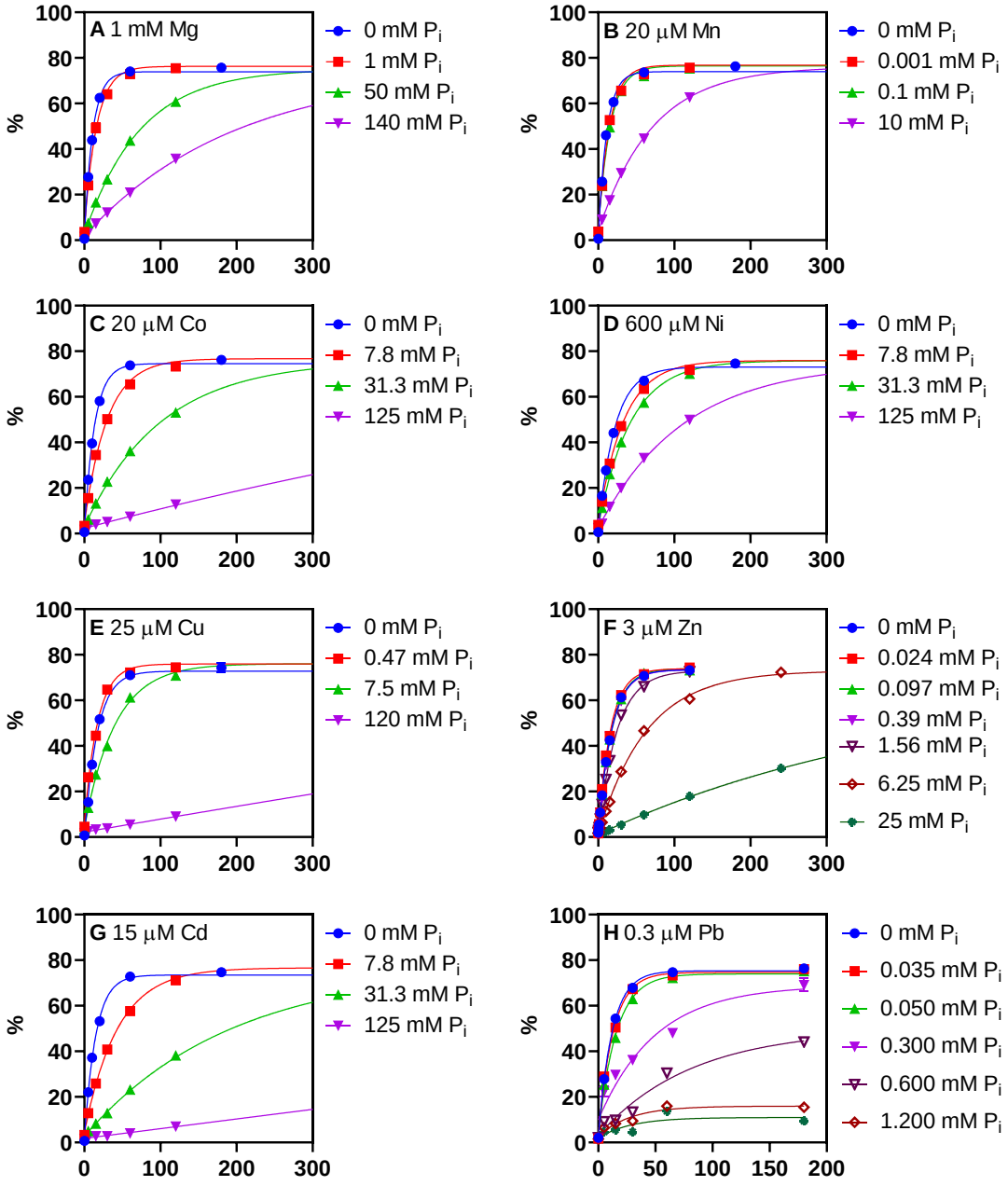
A 1 mM Mg
0 mM Pi
1 mM Pi
50 mM Pi
140 mM Pi
B 20 µM Mn
0 mM Pi
0.001 mM Pi
0.1 mM Pi
10 mM Pi
C 20 µM Co
0 mM Pi
7.8 mM Pi
31.3 mM Pi
125 mM Pi
D 600 µM Ni
0 mM Pi
7.8 mM Pi
31.3 mM Pi
125 mM Pi
E 25 µM Cu
0 mM Pi
0.47 mM Pi
7.5 mM Pi
120 mM Pi
F 3 µM Zn
0 mM Pi
0.024 mM Pi
0.097 mM Pi
0.39 mM Pi
1.56 mM Pi
6.25 mM Pi
25 mM Pi
G 15 µM Cd
0 mM Pi
7.8 mM Pi
31.3 mM Pi
125 mM Pi
H 0.3 µM Pb
0 mM Pi
0.035 mM Pi
0.050 mM Pi
0.300 mM Pi
0.600 mM Pi
1.200 mM Pi
%

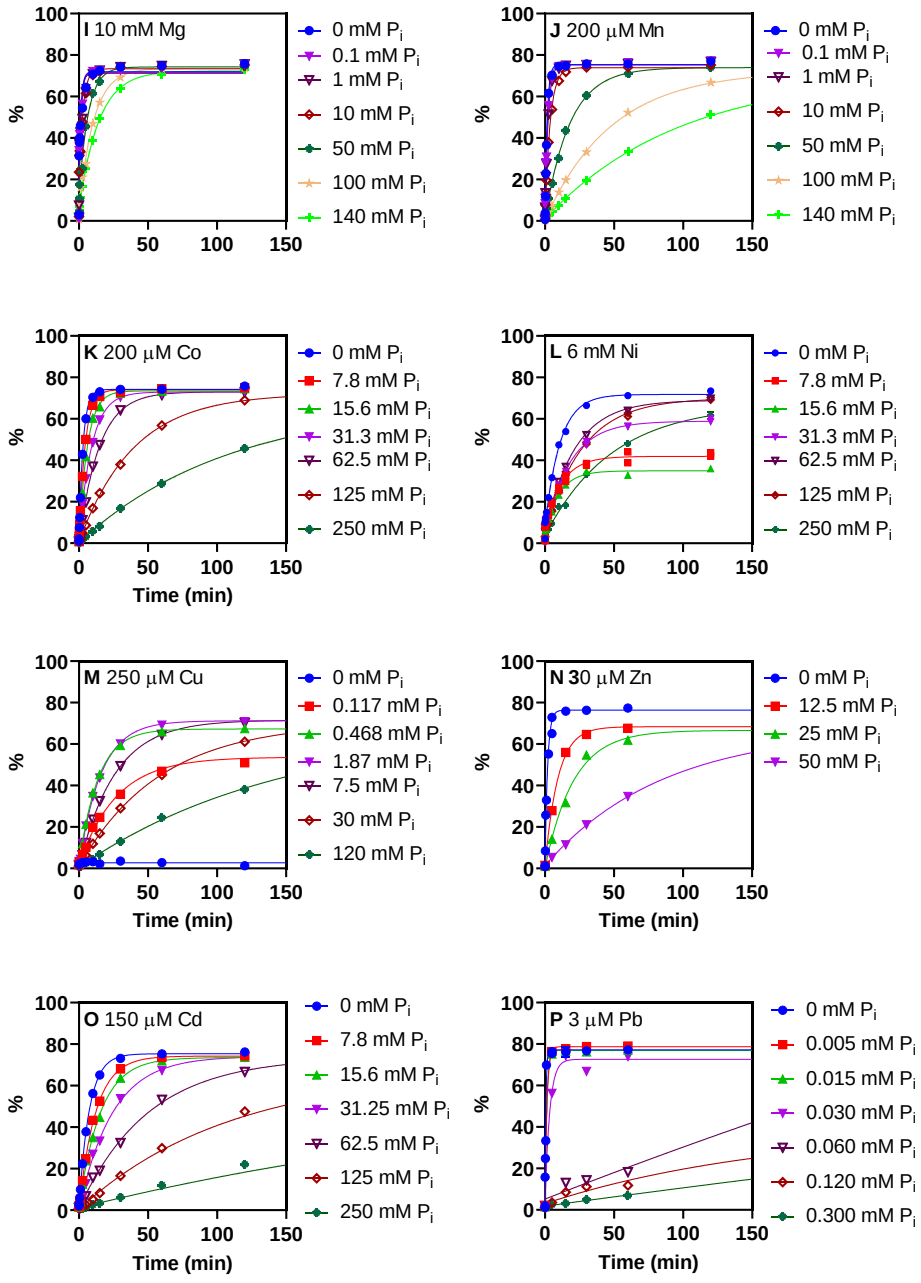

Figure 2.9. Kinetic profiles of metal ions at their K_d **(A-H)** and at $10K_d$ **(I-P)** metal concentrations with different inorganic phosphate concentrations. The obtained k_{obs} are summarized in **Table 2.4.**

Table 2.4. Rate constants (k_{obs}) of different metal ions with 17E DNAzyme and PO substrate in 50 mM MOPS buffer pH 7,5, 25 mM NaCl, and varying inorganic phosphate concentrations.

uM metal	mM phosphate	Rate (min-1)		uM metal	mM phosphate	Rate (min-1)
1 mM Mg	0.00	0.09111		25 µM Cu	0.00	0.05887
	1.00	0.06270			0.47	0.05787
	50.00	0.01369			7.50	0.02464
	140.00	0.00508			120.00	0.00020
10 mM Mg	0.00	0.67580		250 µM Cu	0.00	1.46800
	0.00	0.46320			0.12	0.03686
	0.01	0.57830			0.47	0.07311
	0.10	0.69830			1.87	0.06300
	1.00	0.70320			7.50	0.03846
	10.00	0.34690			30.00	0.01697
	50.00	0.15020			120.00	0.00686
	100.00	0.09415		3 µM Zn	0.00	0.05703
	140.00	0.07038			0.02	0.06137
20 µM Mn	0.00	0.08992			0.10	0.05617
	0.00	0.06777			0.39	0.05622
	0.10	0.06361			1.56	0.04039
	10.00	0.01406			6.25	0.01703
200 µM Mn	0.00	0.66780			25.00	0.00001
	0.00	0.53570		30 µM Zn	0.00	0.52340
	0.01	0.50350			12.50	0.10610
	0.10	0.52930			25.00	0.04852
	1.00	0.44520			50.00	0.01176
	10.00	0.26600		15 µM Cd	0.00	0.06673
	50.00	0.05543			7.81	0.02289
	100.00	0.02070			31.25	0.00523
	140.00	0.01027		150 µM Cd	0.00	0.13370
20 µM Co	0.00	0.07482			7.80	0.08207
	7.81	0.03335			15.60	0.06454
	31.25	0.00991			31.25	0.04098
	125.00	0.00079			62.50	0.02006
200 µM Co	0.00	0.33430			125.00	0.00919
	7.81	0.22360			250.00	0.00262

	15.60	0.16270		0.3 µM Pb	0.00	0.08230
	31.25	0.10980			0.04	0.07763
	62.50	0.06835			0.05	0.06370
	125.00	0.02535			0.30	0.01999
	250.00	0.00917			0.60	0.01222
600 µM Ni	0.00	0.04527			1.20	0.03566
	7.81	0.02986			2.40	0.03502
	31.25	0.02328		3 µM Pb	0.00	1.54000
	125.00	0.00893			0.01	0.69960
6 mM Ni	0.00	0.09165			0.02	0.76300
	7.81	0.08177			0.03	0.29670
	15.60	0.09698			0.06	0.00083
	31.25	0.05456			0.12	0.00605
	62.50	0.04597			0.30	0.00060
	125.00	0.03648				
	250.00	0.02058				

At the 10-fold concentration of K_d of Cu^{2+}, the DNAzyme complex was completely denatured and showed no activity at all. The addition of the phosphate rescued its activity back up before inhibiting the activity again at an even higher phosphate concentration. This interesting observation gives an example of how the metal-phosphate affinity can affect the 17E DNAzyme activity. As for the Ni^{2+}, it appears to exhibit a mixed type of inhibition because lower phosphate concentrations lowered the cleavage maximum plateau, but higher phosphate concentration brought the plateau back up. From this observation, it can be speculated that Ni^{2+} has a slightly different mechanism of phosphate-binding interaction than the rest of the active divalent transition metals. At lower Cu^{2+} and Ni^{2+} concentrations though (e.g. at $1K_d$), these exceptional trends were not observed and normal phosphate inhibition was followed.

From these plots, the inhibition effects of the inorganic phosphate can be quantified using the Dixon plot analysis by plotting the $1/k_{obs}$ with the phosphate inhibitor concentration (**Table 2.4** and **Figure 2.10**). The intersection of the two lines from the two metal concentrations was used to

quantify the inhibition constant, K_i. This K_i is a dissociation constant for the metal-phosphate interaction. When compared with the cleavage rates for each metal ion, this affinity of the metal-phosphate binding was nicely correlated (**Figure 2.11**). This observation from the inhibition study indicates that the slower the ligand exchange rate, the less interaction with the phosphate, which is consistent with the slower cleavage rate.

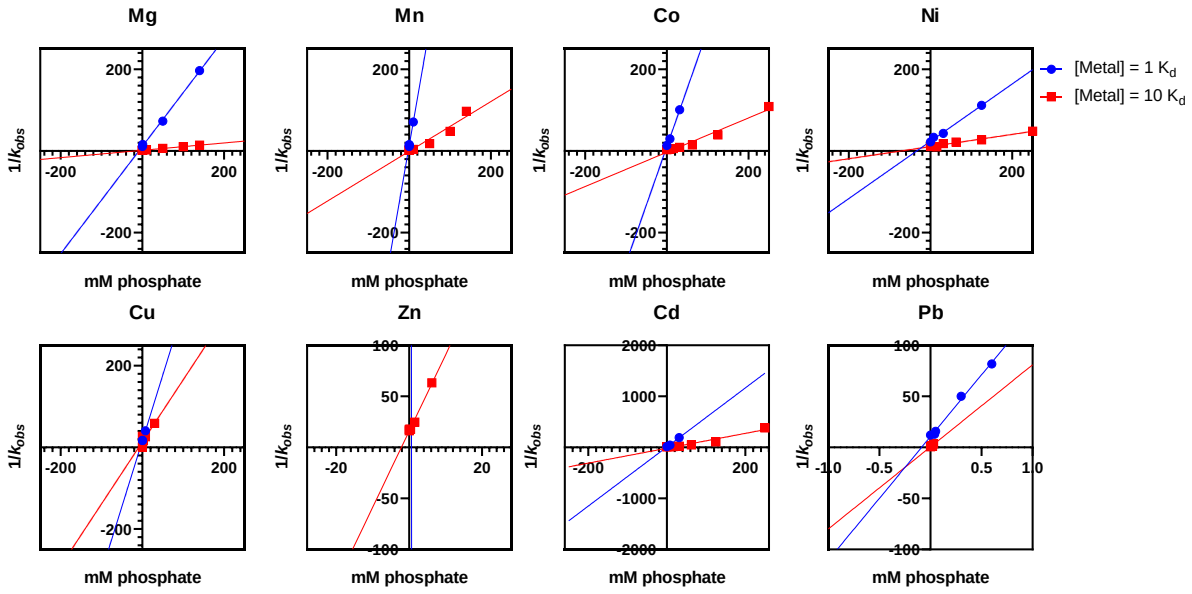

Figure 2.10. Graphical analysis to determine the inhibition constant, K_i, of the phosphate as an inhibitor for the DNAzyme activity with each metal ions.

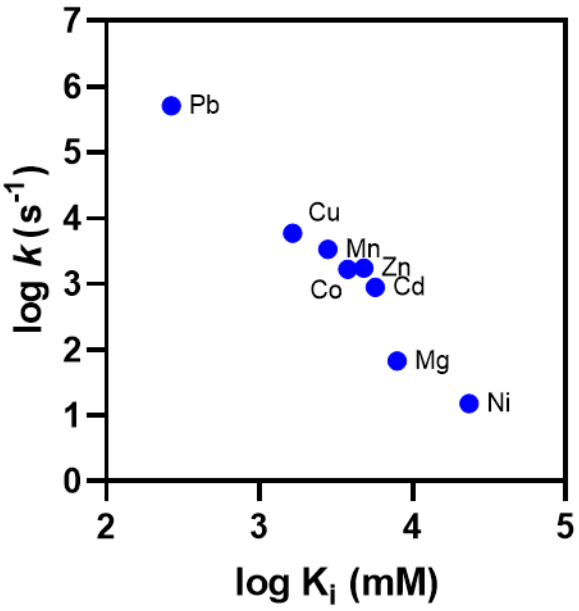

Figure 2.11. The correlation of the phosphate affinity to each metal ions and the cleavage rates of each metal ions. The metals with slower rates exhibit the weakest affinity to the phosphate. This observation also aligns with the observation from **Figure 2.7.**

Two types of mechanisms.

Many studies have examined the mechanism of the RNA cleavage reaction by ribozymes and DNAzymes.[51, 69, 102, 126-128] It is generally accepted that the 2′-OH acts as a nucleophile to attack the scissile phosphate.[50] Recent literature further identified key factors that govern the cleavage reaction with the Pb^{2+}. For example, the X-ray crystal structure of 8-17 DNAzyme with Pb^{2+} suggested an in-line attack mechanism where the conserved guanine residue (highlighted in purple in **Figure 2.1**) acts as a general base and the catalytic water acts as a general acid (**Figure 2.12A**).[54] Modeling studies by York and coworkers also build on the crystal structure study and compares with ribozymes to provide more evidence of guanine residue that behaves as a general base.[128,127] Based on the thousand-fold or more activity difference between Pb^{2+} and other metal ions, previous crystallography and spectroscopic data, and our current PS-substrate data, we believe that there

are two mechanisms for this DNAzyme. The mechanism is general acid catalysis for Pb^{2+} (**Figure 2.12A**), while the mechanism is Lewis acid catalysis for other divalent metal ions (**Figure 2.12B**).

We also cannot rule out that metal ions may play both roles during catalysis. Since no evidence showed that the 17E can bind two divalent metal ions, if both catalysis mechanisms take place at the same time, one is likely to be dominating. The fact that the 17E DNAzyme can accept both mechanisms may explain the wide-ranged metal tolerance of it.

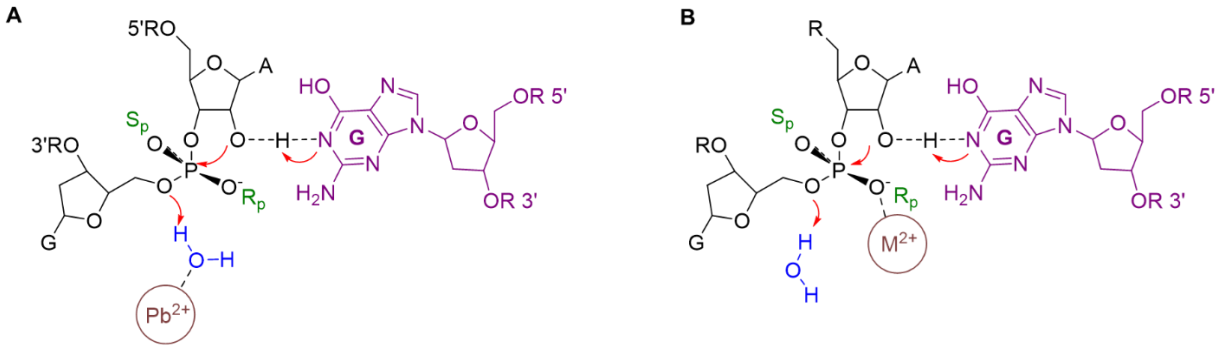

Figure 2.12. Proposed mechanism of RNA cleavage with A) Pb^{2+} and B) other divalent metal ions. Conserved guanine residue (purple) behaves as a general base for the deprotonation of 2′-OH. Hydrated Pb^{2+} behaves as a general acid to protonate the leaving group oxygen. However, other divalent metals may be directly coordinated to the Pro-R_p oxygen to stabilize the phosphate for the nucleophilic attack by 2′-OH and the substrate cleavage may be governed by the binding affinity of the metal to the non-bridging phosphate oxygen.

Summary

The 17E DNAzyme is unique in terms of its general activity with a wide range of divalent metal ions, but a unified understanding of the roles of different metal ions and the activity trends has not yet been established. In this study, we aimed to test the hypothesis of inner-sphere metal-phosphate interactions being the determining factor. Phosphorothioate substitution and activity assays with its isomers confirmed that the non-bridging oxygens in the pro-R_p position are

important for the inner-sphere divalent metal binding. The comparison of cleavage rate constants and the rate of water ligand exchange on metal ions also rationalized the slowest activity of Ni^{2+}, which further supported the inner-sphere interactions. As a piece of indirect evidence, the phosphate inhibition assay also supported the binding of metal ions to the scissile phosphate. For the experiments presented in this work, we tried to separate our discussion for Pb^{2+} from the rest of the divalent metal ions. In the end, we proposed two types of mechanisms: general acid catalysis for Pb^{2+} and Lewis acid for other divalent metals.

Chapter 3 Replacing Mg^{2+} by Fe^{2+} for RNA-cleaving DNAzymes

Introduction

Metal ions play a critical role in RNA cleavage reactions.[46, 87, 104, 129] Being positively charged, metal ions can stabilize various secondary and tertiary structures in nucleic acids. In addition, they may act as Lewis acid or general acid/base catalysts to assist RNA cleavage. Mg^{2+} is the cofactor in many naturally found ribozymes that catalyze reactions in living cells.[130, 131] Thus, Mg^{2+} has been one of the most popular metals for *in vitro* selection of ribozymes.[132] In 2012, Williams and coworkers proposed that Fe^{2+} and Mg^{2+} are similar in a few aspects, such as size, charge, and the theoretical conformation of the RNA-metal binding site.[49] Both Fe^{2+} and Mg^{2+} ions displayed the hexacoordinate geometry and the metal-oxygen distances were determined to be around 2 Å in the RNA-metal binding site. They also compared these two metals in the hammerhead ribozyme and found that its activity can be significantly enhanced with Fe^{2+} substitution of Mg^{2+} in an oxygen-free environment.

One of the motivations to study Fe^{2+}-dependent activities is the anoxic atmosphere of the early earth when soluble Fe^{2+} was believed to be abundant.[133] It is hypothesized that due to the acidic and reducing environment under a hydrogen-rich atmosphere, most of the iron was in the soluble Fe^{2+} state. The RNA world hypothesis considers ribozymes as the dominant catalysts for biological reactions. Many other researchers have also examined ribozymes' interaction with Fe^{2+}. For example, Ditzler and coworkers performed parallel selections using either Mg^{2+} or Fe^{2+}.[134] They found that Mg^{2+} can replace Fe^{2+} at neutral pH but not at low pH. Fe^{2+} was also able to substitute for Mg^{2+} in DNA polymerases, RNA polymerases, DNA ligases,[135] and in protein translation.[136]

DNAzymes are the DNA counterpart of ribozymes.[31, 137, 138] So far, no natural DNAzymes have been discovered but many were isolated using *in vitro* selection. Since DNAzymes have been extensively selected for metal sensing, aside from Mg^{2+},[31, 139, 140] a diverse range of metal ions are used to help DNAzyme catalysis,[86, 129, 141, 142] such as monovalent Na^{+},[37, 40, 143-146] and Ag^{+},[147] divalent Ca^{2+},[148] Pb^{2+},[31] UO_2^{2+},[149] Cd^{2+},[80] Cu^{2+},[150] and trivalent lanthanides.[42, 151] Whether Mg^{2+} and Fe^{2+} behave similarly in DNAzymes have yet to be answered. Further understanding of this topic would help the development of DNAzyme-based sensors for metal ions in aqueous systems. In addition, we may gain further insights into DNA/metal interactions.

The 17E DNAzyme is an extensively studied model enzyme,[52, 71, 96, 139, 152-155] and it is active in the presence of many divalent metal ions. For this reason, together with its small size and tolerance to mutations,[99, 153] 17E has recurred in many *in vitro* selections from different labs under different selection conditions.[98, 101, 139, 156, 157] The highest activity is achieved with Pb^{2+}, followed by Zn^{2+}, Cd^{2+}, Mn^{2+}, and Co^{2+}, while a high metal concentration is needed for Mg^{2+} and Ca^{2+}. The study on Fe^{2+} has not been systematically explored.[158] In this work, we used the 17E as a model system to understand Fe^{2+} activity in DNAzyme reactions. In addition, a few other DNAzymes were tested, and those active with Mg^{2+} were also found to be active with Fe^{2+}. Since we noticed the effect of Fe^{2+} oxidation during the work, investigation on this front was also performed.

Materials and Methods

Chemicals. $FeCl_2 \cdot 4H_2O$ and $FeCl_3 \cdot 6H_2O$ were purchased from Alpha Aesar. $MgCl_2$, sodium ascorbate, and L-glutathione were purchased from Sigma Aldrich. Tyrosine was purchased from Biobasic Inc. Citric acid trisodium salt dehydrate was purchased from Amresco. The DNA sequences were purchased from Integrated DNA Technologies and Eurofin Genomics (**Table 3.1**).

The glove bag was purchased from VWR International. Sodium Chloride, 10× Tris borate EDTA (TBE), urea, ammonium persulfate (APS), tetramethylethylenediamine (TEMED), 3-(N-morpholino)propanesulfonic acid (MOPS), and 2-(N-morpholino)ethanesulfonic acid (MES) were purchased from Bio Basic Inc. The gel loading dye was from Biolab. BioRad ChemiDoc MP Imaging System was used for analysis.

Table 3.1. DNA sequences, modifications, and the supplier (IDT: Integrated DNA Technologies; Eurofin: Eurofin Genomics). FAM: carboxyfluorescein.

Name	Supplier	Sequence
Sub-FAM	IDT	5′ – GTCACGAGTCACTATrAGGAAGATGGCGAAA /36-FAM/ -3′
17E	IDT	5′-TTTCGCCATCTTCTCCGAGCCGGTCGAAATAGTGACTCGTGAC-3′
GR5	Eurofin	5′ TTT CGCCATCTGAAGTAGCGCCGCCGTATAGTGACTCGTGAC -3′
8-17	Eurofin	5′-TTTCGCCATCTTCTCCGAGCCGGACGAATAGTGACTCGTGAC-3′
E5	IDT	5′- TTTCGCCATCTTCAGCGATTAACGGAAC GTTACACCCATGTTAGTGACTCGTGAC -3′
Ce13d	IDT	5′-TTTCGCCATAGGTCAAAGGTGGGTGCGAGTTTTT ACTCGTTATAGTGACTGGTGAC -3′
39E	Eurofin	5′- TTTCGCCATCTTCAGTTCGGAAACGAAC CTTCAGACATAGTGACTCGTGAC-3′

Activity assays in air. The substrate/DNAzyme complex was prepared freshly each day. In a typical assay, FAM-labelled substrate concentration (5 μM) and the 17E DNAzyme (7.5 μM) were annealed in 50 mM MES, pH 6, 25 mM NaCl (Buffer A) by heating at 95 °C for 1 min followed by cooling to 4 °C for 30 min. The annealed complex concentration is described in terms of substrate concentration. Different concentrations of metal solutions were prepared in Milli-Q water. The reaction buffer was 50 mM MOPS pH7.5, 25 mM NaCl (Buffer B). For a typical reaction, 4 μL of reaction buffer was mixed with 1 μL of 5 μM DNAzyme complex before adding 2 μL of metal solution (e.g. Fe^{2+}) to initiate the reaction for the desired incubation time. The total reaction volume was 7 μL. To quench the reaction, 7 μL of quenching solution (1× gel loading dye and 8

M urea) was added to the reaction mixture. Then, 7 μL of the quenched reaction solution was loaded into 15% denaturing polyacrylamide gel (dPAGE) to perform electrophoresis for 80 min at 200 V. The obtained gels were fluorescence imaged with BioRad ChemiDoc MP Imaging System and analyzed. Different DNAzyme sequences required different buffers. The respective annealing buffer and reaction buffer were Buffer A and B for 17E and GR5; Buffer B and B for 8-17 and E5; and Buffer A and A for Ce13d and 39E, respectively. All of the measurements were replicated at least 2 times and the error bars on plots are standard deviations.

Activity assays in N_2 environment. The DNAzyme complex preparation and the reaction conditions were the same as that in the air. However, all steps were performed in an N_2 filled glove bag, except for the complex annealing process. 10 mL aliquots of Milli-Q water and the reaction buffer were degassed by bubbling N_2 for at least 10-15 min before transferring into the glove bag immediately. The glove bag, which is an isolated system of a large plastic bag with an inward glove, can be tightly sealed to cycle through twice with N_2 gas fill and vacuum to eliminate remaining air. The N_2 and vacuum were adjusted to have a constant in and outflow for the duration of the experiment. The $FeCl_2$ salts were dissolved with the degassed Milli-Q water in the N_2-filled chamber and diluted to eliminate any contact with the ambient air as much as possible. Once the cleavage reaction was quenched, the glove bag was opened to load the samples for gel electrophoresis.

Activity assays in the presence of antioxidants. The DNAzyme complex preparation and the reaction conditions were the same as that in the air, except for the metal and the antioxidant stock concentrations. The antioxidants tested were 2 mM or 10 mM final concentrations of ascorbate,

tyrosine, glutathione, and citrate. For a typical reaction, 4 µL of reaction buffer was mixed with 1 µL of antioxidant before mixing with the 1 µL of DNAzyme. This mixture was incubated for 5-10 min before 1 µL of metal solution (ex. Fe^{2+}) was added. The total reaction volume was still 7 µL. It is important to mix ascorbate with the buffer first before exposing the iron solution to the buffer. **Figure 3.1** illustrates the evidence of oxidation of Fe^{2+} into Fe^{3+} when the metal solution was mixed with the MOPS buffer first.

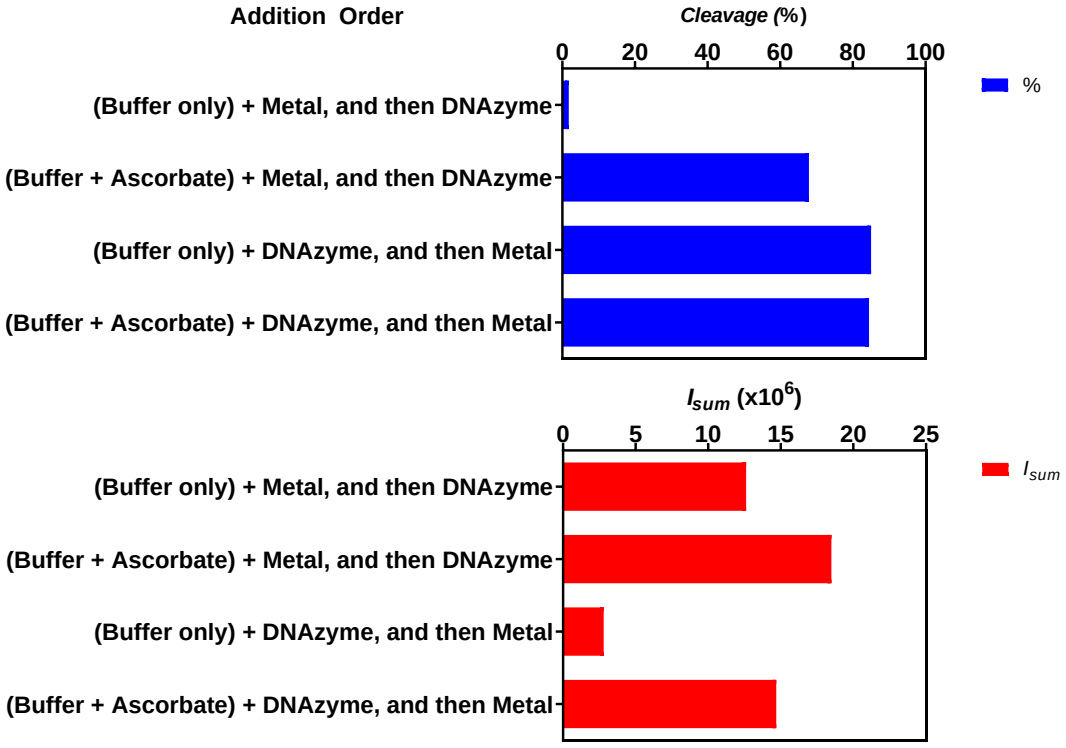

Figure 3.1. Effect of order of addition of reagents. The order of addition is as written in the labels on the left. The addition order test indicated that mixing ascorbate first with the buffer was critical to maintain the activity, as well as decrease non-specific degradation. When ascorbate was added before Fe^{2+}, it had a better protection effect. 1 mM Fe^{2+} with 17E incubated for 10 min yields ~80-90% cleavage yield.

Data analysis. The gel micrographs were analyzed with Image Lab software (v. 6.0.0, 2017 Bio-Rad Laboratories Inc.) to define the lanes and band area for calculation. Once the user defines the area for the location of the bands, the software is programmed to calculate the % of the uncleaved and the cleaved bands with the fluorescence intensities from the FAM-labelled substrate. The activity % used in all of the following analyses was the "band %" function of the cleaved bands (cleaved band/total band), where the total intensity in only the defined band area is considered 100% of the intensity. Therefore, if the reaction products produce any extra bands with different molecular weight fragments due to non-specific cleavage, the calculated "band %" can be biased because it only includes the remaining intensities observed in the defined band area. Metal concentration dependence and kinetic behavior were analyzed using this method. Note that saturated cleavage yield often did not go to 100%, and the maximal cleavage yield was used as saturated yield.

To quantify any non-specific cleavage into different molecular size fragments, the sum of the two bands intensity (I_{sum}) was used. Since equal amounts of FAM-labelled substrates were used throughout all the experimental samples, it worked well to illustrate the degradation. A decrease in the value I_{sum}, as defined in the equations 1 and 2, indicates higher degradation in the sample.

$$I_{\text{total}} = I_{uncleaved} + I_{cleaved} + I_{degraded} \qquad \textbf{Eqn. 3.1}$$

$$I_{sum} = I_{uncleaved} + I_{cleaved} \qquad \textbf{Eqn. 3.2}$$

At the fixed incubation time (ex. 10 min), the metal concentration [M] dependence plot data were fitted to the single metal-binding model of Equation 3,[152] where b is the apparent dissociation constant K_d.

$$y = \frac{a[M]}{(b+[M])} \qquad \textbf{Eqn. 3.3}$$

At the fixed concentration (ex. 1 mM Fe^{2+}), the kinetic data were fitted to the binding model of Equation 3.4, where *b* is the rate constant, k_{obs}.

$$y = y_0 + a(1 - e^{-bt}) \qquad \textbf{\textit{Eqn. 3.4}}$$

Results and Discussion

The 17E DNAzyme is highly active with Fe^{2+}.

The secondary structures of the DNAzymes in this study are shown in **Figure 3.2**. Their substrate strand sequences were all the same, containing constant DNA binding arms and a single RNA linkage (rA for ribo-adenine) that served as the cleavage site, as well as a carboxyfluorescein (FAM) fluorophore label for gel electrophoresis analysis. Only a single RNA at the cleavage site on the substrate was used because DNA is less susceptible to hydrolysis than RNA, and such a chimeric substrate is more stable and cost-effective.[129, 159] In addition, most of the DNAzymes were selected with such as RNA/DNA chimeric substrate, and these DNAzymes were often inactive with the full-RNA substrate.[31] The effect of Fe^{2+} was examined with the 17E DNAzyme first (**Figure 3.2A**) since 17E is active with many divalent metal ions. The experiments were carried out in a nitrogen environment and used freshly prepared Fe^{2+} to minimize the oxidation of Fe^{2+} to Fe^{3+}. Increasing Fe^{2+} concentration gradually increased the cleavage yield and the activity was saturated with 0.25 mM Fe^{2+} (**Figure 3.3**). The apparent dissociation constant (K_d) was calculated using a single metal-binding model (**Equation 3.3**) to be 29.7±2.3 μM Fe^{2+}.

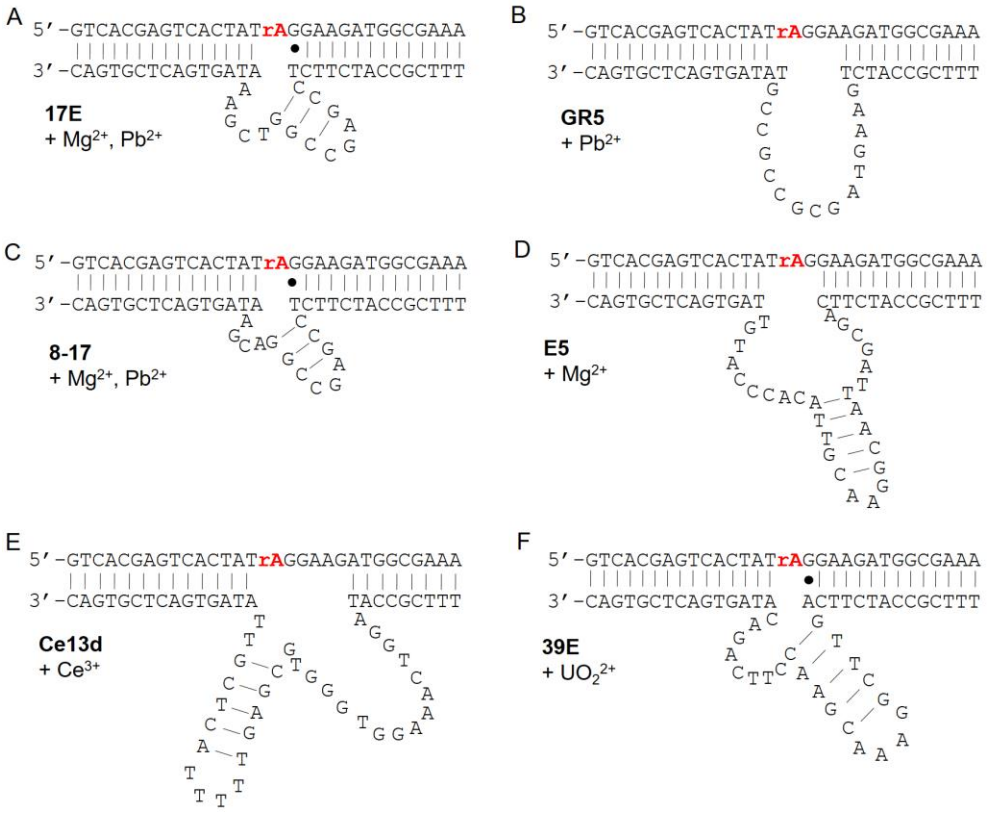

Figure 3.2. The secondary structures of the DNAzymes studied in this work: **A)** 17E; **B)** GR5; **C)** 8-17; **D)** E5; **E)** Ce13d; and **F)** 39E. Most of these DNAzymes are selective for metal ions other than Mg^{2+} or Fe^{2+}. The metal ions used as positive controls respective to each DNAzyme are indicated.

Upon confirming the activity of 17E in the presence of Fe^{2+}, we measured its cleavage kinetics and compared it with some other metals, such as Mg^{2+}, Mn^{2+}, and Co^{2+} (**Figure 3.3**). Since 17E is active with divalent metal ions to different degrees, these metal ions were chosen as examples of divalent species with relatively low and high activities. From the kinetic curve, k_{obs} were obtained by fitting the curves to a first-order reaction (**Figure 3.4**). The kinetics curve saturates around 75-80% activity instead of reaching 100% possibly due to incomplete hybridization, and misfolding of DNAzymes, which is quite common for such reactions. The k_{obs} of the 1 mM metals were calculated to be 0.053±0.002 (Mg^{2+}), 1.19±0.09 (Mn^{2+}), 0.87±0.07 (Co^{2+}),

and 1.12±0.11 (Fe^{2+}) min^{-1}. This indicates that 17E activity with Fe^{2+} compared to Mg^{2+} is 21-fold higher. This difference is comparable with the previous studies on the L1 ribozyme ligase.[49] In their study, the substitution of Mg^{2+} with Fe^{2+} enhanced the activity by 25-fold. However, the difference was only 3-fold for the hammerhead ribozyme. Based on this observation, the replacement of Mg^{2+} with Fe^{2+} seems to increase the DNAzyme activity in general.

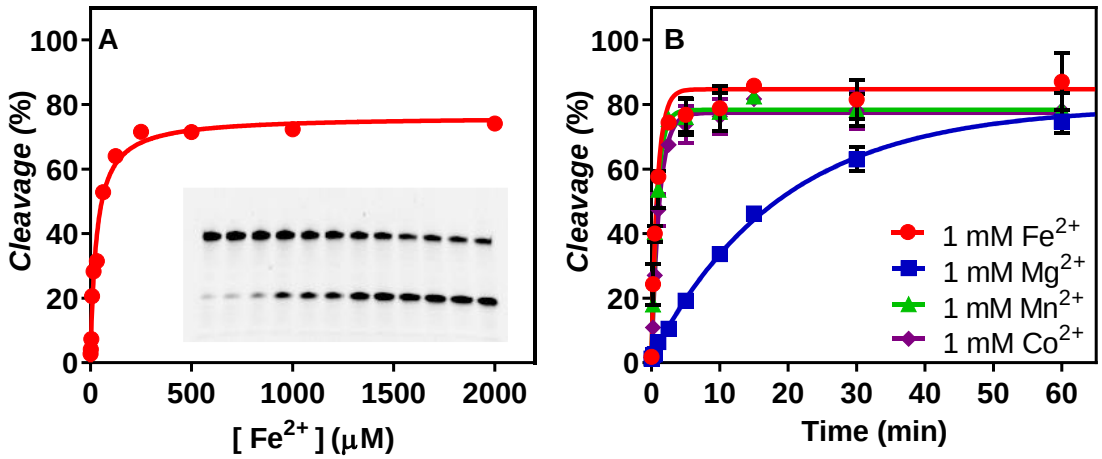

Figure 3.3. A) Substrate cleavage percentage by the 17E DNAzyme using up to 2 mM Fe^{2+} in 50 mM MOPS, pH 7.5, 25 mM NaCl for 10 min reaction time. Inset: a representative gel micrograph with different Fe^{2+} concentrations up to 2 mM. **B)** Comparison of kinetic characteristics of the 17E DNAzyme with 1 mM Fe^{2+}, Mg^{2+}, Mn^{2+}, or Co^{2+}. These experiments were conducted in an N_2 environment. Error bars are standard deviations from n = 2 - 6 measurements and some errors are not visible on the plot due to small values.

Fe^{2+} with other DNAzymes.

After 17E, a total of 6 RNA-cleaving DNAzymes were studied to systematically examine their activities with Fe^{2+} (**Figure 3.2**), including the Mg^{2+}-dependent (8-17,[139] and E5),[140] Ce^{3+}-dependent (Ce13d),[42] UO_2^{2+}-dependent (39E) DNAzymes,[149] as well as another Pb^{2+}-dependent (GR5) DNAzyme.[31] These DNAzymes all shared the same DNA substrate sequence. For each

DNAzyme, positive control was included by reacting with their respective active metal under an optimal buffer condition. Since each DNAzyme was selected under different buffer conditions, the optimal reaction buffer and metal conditions were also different in this study. In addition, each DNAzyme was tested with 10 mM and 0.1 mM Mg^{2+}, and 0.1 mM Fe^{2+} to test their activities with these two metals.

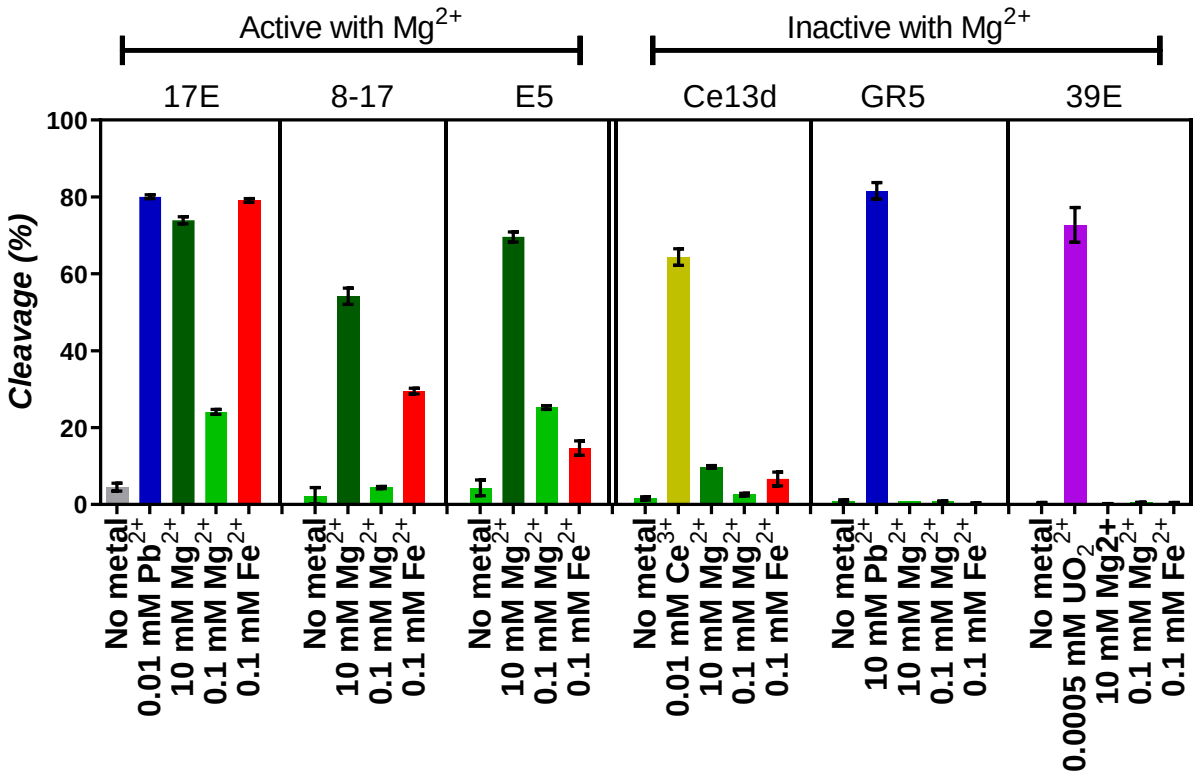

Figure 3.4. RNA-Cleaving activity for different DNAzyme sequences with no metal (- control), respective positive control metal concentration (+ control), and 100 μM Fe^{2+} incubated for 1 h. More detailed experimental conditions such as buffers can be found in the experimental section, as different buffers were used for different DNAzymes. Error bars are standard deviations from *n* = 3 – 5; some error bars invisible due to small values.

Although often referred to as a Pb^{2+}-dependent DNAzyme, 17E is active with many divalent metals, including a high concentration of Mg^{2+}, as shown by the 10 mM Mg^{2+} control in

Figure 3.4. In this figure, it is clear that 0.1 mM Fe^{2+} is much more active than the same concentration of 0.1 mM Mg^{2+} with the 17E. In addition to 17E, the other two Mg^{2+}-dependent DNAzymes, 8-17 and E5, also showed some cleavage activity with Fe^{2+}. Ce13d had only ~10% cleavage after 1 h with 10 mM Mg^{2+}, and we observed even less (~6%) cleavage with 0.1 mM Fe^{2+}. The other Pb^{2+}-dependent DNAzyme, GR5, did not cleave with Mg^{2+} at all, and it also had no activity with Fe^{2+}. Similarly, 39E was inactive with Mg^{2+}, and it had almost no cleavage activity in the presence of Fe^{2+}. Overall, for the six tested DNAzymes, if a DNAzyme is active with Mg^{2+}, it is also active with Fe^{2+}. On the other hand, if a DNAzyme is inactive with Mg^{2+}, it is also inactive with Fe^{2+}.

This study can also provide insights regarding the similarity between Mg^{2+} and Fe^{2+}. In addition to the previously reported Fe^{2+} interactions with ribozymes,[49] we can further provide observations of similar behaviors of Fe^{2+} and Mg^{2+} in DNAzyme systems. 1 mM Fe^{2+} behaved similarly or even exceeded the activities of 1 mM Mg^{2+} (**Figure 3.5**). The Fe^{2+} reaction rates were 21-fold faster than with Mg^{2+} for 17E; 25-fold for 8-17; and 1-fold for E5.

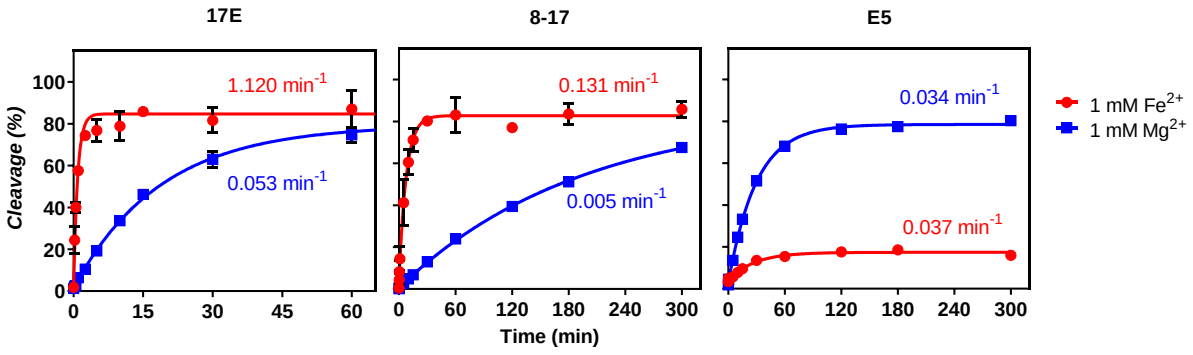

Figure 3.5. k_{obs} and kinetic profile comparison of 1 mM Fe^{2+} and 1 mM Mg^{2+} with different DNAzymes: **A)** 17E, **B)** 8-17, and **C)** E5. The Fe^{2+} samples were handled in N_2 environment. Mg^{2+} in N_2 environment was indifferent than in air condition for 17E (not shown), so data from Mg^{2+}

samples in air was used for this plot. Note that error bars are too small to be visible for E5. Error bars are standard deviations from $n = 2 – 6$; some error bars invisible due to small values.

The sequences of 8-17 and 17E are very similar, where they differ only by two bases in the bulging loop sequence. With both DNAzymes, Fe^{2+} assisted in RNA cleavage much faster than Mg^{2+}. On the other hand, E5 has a completely different sequence than the other two DNAzymes. With E5, 1 mM Fe^{2+} behaved almost equally to 1 mM Mg^{2+}. However, at a lower concentration of 100 μM Fe^{2+}, activity saturation increased to ~45% instead of ~20% with E5, unlike the 17E and 8-17 (**Figure 3.6**). This may indicate that E5 has a different optimal condition than those of 17E and 8-17 with Fe^{2+}. Upon extrapolating the rate to the same metal concentration, the rate of Fe^{2+} becomes slightly faster than Mg^{2+}. In general, the replacement of Mg^{2+} with Fe^{2+} increased the activity, but not to the same degree for different DNAzymes. Similar observations were also made for ribozymes, where the relative activity difference with Mg^{2+} and Fe^{2+} can be quite different.

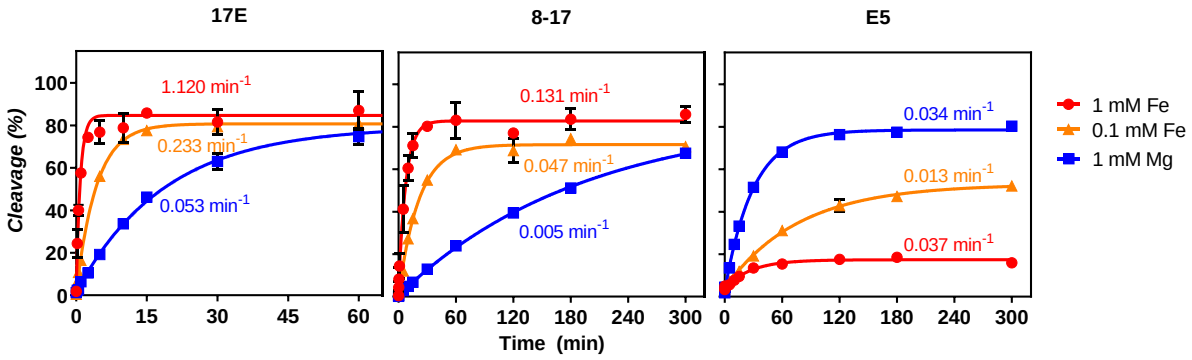

Figure 3.6. k_{obs} and kinetic profile comparison of 1 mM Fe^{2+}, 100 μM Fe^{2+}, and 1 mM Mg^{2+} with different DNAzymes. The Fe^{2+} samples were handled in N_2 environment.

Effect of pH and air.

The activity of the 17E DNAzyme is known to be pH-dependent with faster reaction rates at higher pH.[152] Its cleavage reaction with Fe^{2+} was no exception (**Figure 3.7B**). With 1 mM Fe^{2+}

at pH 7.6, we observed over 80% cleavage in 10 min. In higher pH and high Fe^{2+} concentration, low molecular weight fragments appeared in the gel micrograph below the expected cleaved product band (**Figure 3.7A**). Note that this experiment was conducted in the air atmosphere. This suggested a degradation process of the DNA possibly by reactive oxygen species (ROS), easily formed by the oxidation of Fe^{2+} by the Fenton reaction.[160-164] In the presence of oxygen and basic pH, the ROS are produced faster. Therefore, it is logical to hypothesize that the degradation process by ROS was causing the low molecular weight fragments.

To quantify this degradation reaction, we measured the sum of the two remaining band intensities ($\boldsymbol{I_{uncleaved} + I_{cleaved} = I_{sum}}$) of the uncleaved and the cleaved substrates. A decrease in this $\boldsymbol{I_{sum}}$ indicates higher non-specific cleavage or degradation by the ROS. For example, **Figure 3.7C** illustrates significant degradation in the presence of 1 mM Fe^{2+} as pH increased above 7.2. The same observation can be made visually on the gel micrographs (**Figure 3.7A**). We also systematically compared the reaction in air and in N_2, confirming the role of oxygen in the degradation process (**Figure 3.10** in a later section). Therefore, it is critical to run Fe^{2+} related reactions in an oxygen-free environment.

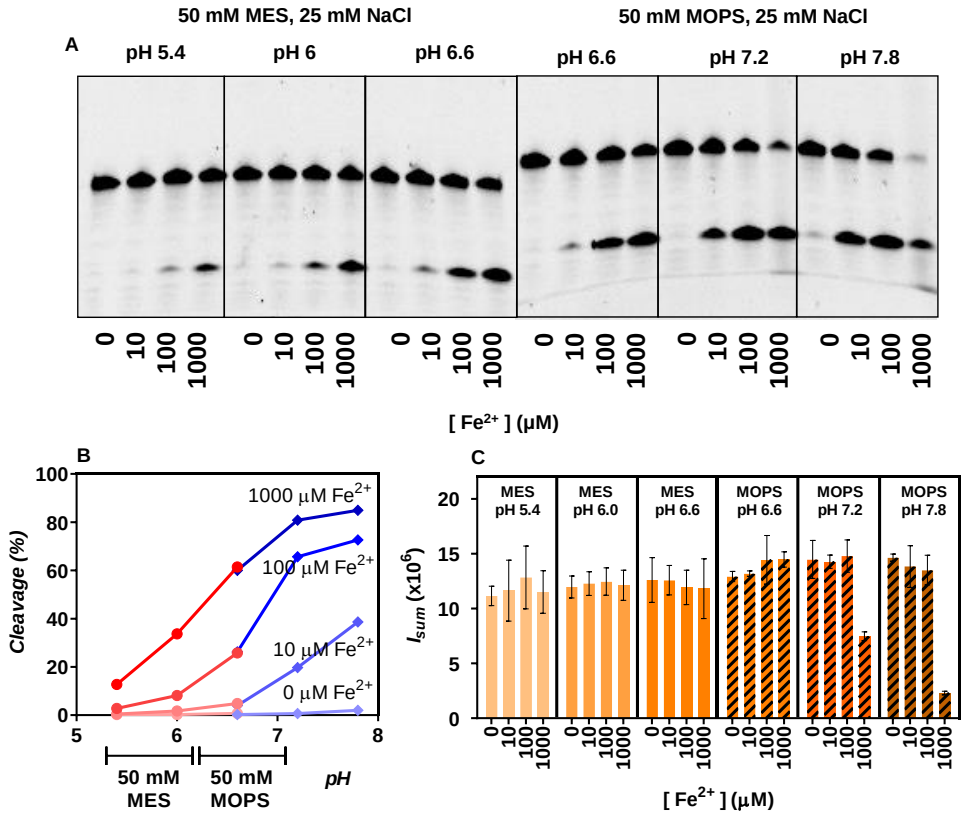

Figure 3.7. A) The gel micrograph image showing the smeared bands at high pH and high Fe^{2+} concentrations with 17E DNAzyme in ambient air. **B)** Comparison of the corresponding cleavage yields with Fe^{2+} in increasing pH for 10 min reaction with 0, 10, 100, and 1000 μM Fe^{2+}, respectively. Connecting lines indicate general increasing trend. **C)** The corresponding I_{sum} calculating the sum of the uncleaved substrate and the specific cleavage product intensity of each condition. A detailed explanation of data analysis is described in the Methods section. Experiments were run in duplicate.

Comparing Fe^{2+} and Fe^{3+}.

Since the oxidation product of Fe^{2+} is Fe^{3+}, we also compared the cleavage activities with these two metal ions in ambient air. **Figure 3.8A** shows the gel micrograph of the two iron species at 0, 10, 100, 1000 μM. It is visually observed that 1 mM concentration results in smeared bands of low molecular weight with Fe^{2+}, but high molecular weight bands with Fe^{3+}. In addition, the I_{sum} analysis also indicates a decrease in the sum of the two bands intensity with 1 mM of both

Fe^{2+} and Fe^{3+} (**Figure 3.8C**). We also noticed a thin brown precipitate layer left stuck in the 1 mM Fe^{3+} sample wells. These observations with the Fe^{3+} can be attributed to the insoluble hydrolyzed precipitate such as $Fe(OH)_3$, as well as its complex with the DNA, leading to a lower electrophoretic rate. As for the cleavage, Fe^{3+} did not specifically cleave the substrate at all and non-specific degradation products were also much less (**Figure 3.8B)**. On the other hand, Fe^{2+} increased cleavage and degradation with higher concentration. Based on these observations, it can be suggested that specifically Fe^{2+} instead of Fe^{3+} is assisting with the RNA-cleavage with 17E. Fe^{3+} alone cannot produce ROS for the degradation.

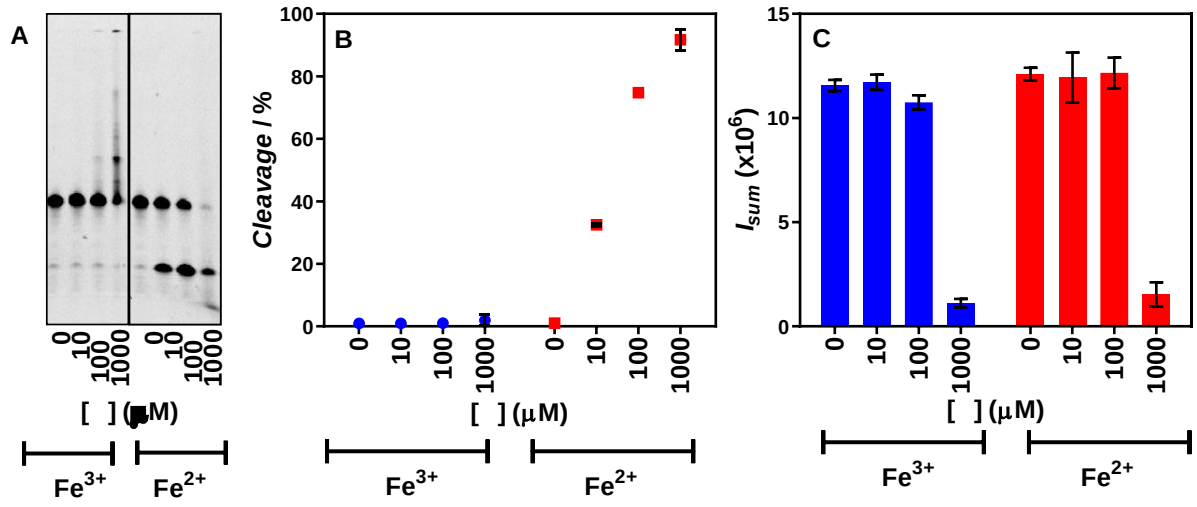

Figure 3.8. Comparison of different concentrations of Fe^{2+} and Fe^{3+} with 17E in 50 mM MOPS pH 7.5, 25mM NaCl for 10 min with **A)** the high contrast gel micrographs, and the corresponding **B)** quantified cleavage percentage, **C)** the total band intensity of the uncleaved substrate and specific cleavage product, $\boldsymbol{I_{sum}}$. This set of experiments were run in duplicate.

Effect of reducing agents.

An interesting question we asked was whether we can inhibit the nonspecific degradation reactions by adding a reducing agent (e.g. antioxidant), which may prevent oxidation of Fe^{2+}. A

few representative antioxidants were selected to examine their effects on the Fe^{2+} reaction. For example, ascorbate is commonly used to reduce Fe^{3+} to Fe^{2+} in the total iron colorimetric assay based on the o-phenanthroline complex with Fe^{2+}.[165] The selected reducing agents here are commonly used in biological systems. Tyrosine was also included as a weak antioxidant.[133, 166]

Figure 3.10A shows a high contrast gel micrograph of 1 mM Fe^{2+} in the presence of 2 mM and 10 mM of ascorbate, tyrosine, glutathione, or citrate. These antioxidants were pre-incubated with Fe^{2+} for 5 min and then incubated with 17E DNAzyme for 10 min. In general, the bands were cleaner with a high concentration of the reducing agents. However, the cleavage activity was significantly reduced in the presence of 10 mM glutathione and citrate (**Figure 3.10B**), likely due to their strong binding to Fe^{2+}. Also, even though the activity was unaffected, 2 mM tyrosine did not improve with the smearing of the bands (**Figure 3.10C**), likely due to its weak antioxidant property. Only the ascorbate was able to lower the degradation, as well as maintain the cleavage activity at both concentrations tested. Therefore, the ascorbate was the best candidate to examine further to optimize for DNAzyme activity.

The DNAzyme activities with 1 mM Fe^{2+} in air, N_2, and ascorbate in air were compared to indicate that the % cleavage was unaffected (**Figure 3.10D**). Therefore, ascorbate did not affect the reaction kinetics and is a weak ligand for Fe^{2+}. In addition, N_2 and ascorbate conditions clearly prevented non-specific degradation of the substrate since the green bars in **Figure 3.10E** maintained a similar height in 1 h.

While ascorbate with Fe^{2+} worked well for the 17E DNAzyme, which showed a fast kinetic rate with Fe^{2+}, it failed in slower DNAzymes. For example, when the 8-17 and E5 DNAzymes were examined with the Fe^{2+}, the cleavage yield was much lower compared to that in N_2. After a few minutes, the added ascorbate was oxidized and it lost its protection effect (**Figure 3.9**). For

Cu^{2+}, ascorbate can promote cleavage in some DNAzymes,[167] and care needs to be taken when working with such metals and DNA.[168, 169]

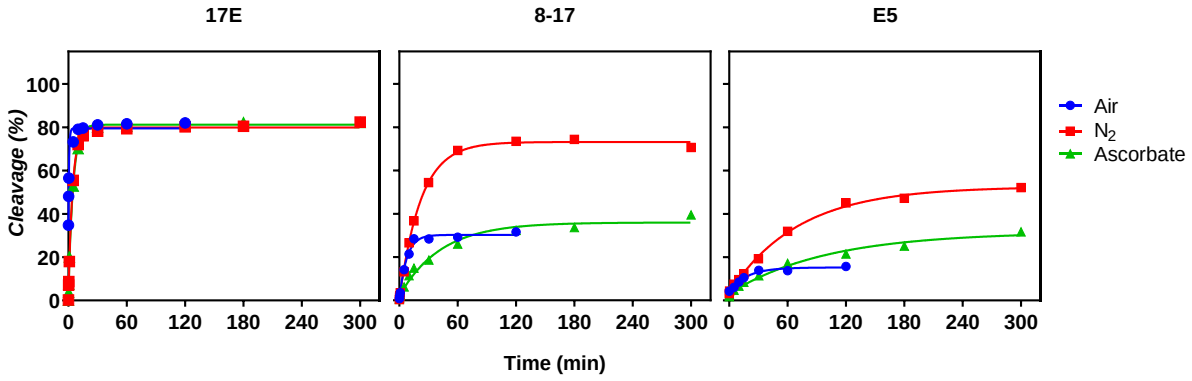

Figure 3.9. Kinetic comparison of 100 μM Fe^{2+} in air, N_2, and ascorbate conditions of 17E, 8-17, and E5. 17E activity is fast enough to allow maximum cleavage within 10 min. However, for slower DNAzymes, oxidation interfered after about 15 min in the air. Presence of ascorbate slowed down the oxidation but cannot eliminate it.

The findings from **Figure 3.10** can provide insights for potential future studies for the sensor development for Fe^{2+} detection. Since both N_2 and ascorbate methods did not change the percentage of activity for fast DNAzymes, both methods can be used for decreasing the non-specific degradation. Ascorbate presents convenience in sample handling compared to the N_2 condition where a glove bag setup is required. Even though N_2 requires more careful sample handling, it can be beneficial for slower DNAzymes, such as 8-17 and E5. Therefore, we suggest using the N_2 environment as a more reliable and general method for experiments with Fe^{2+}.

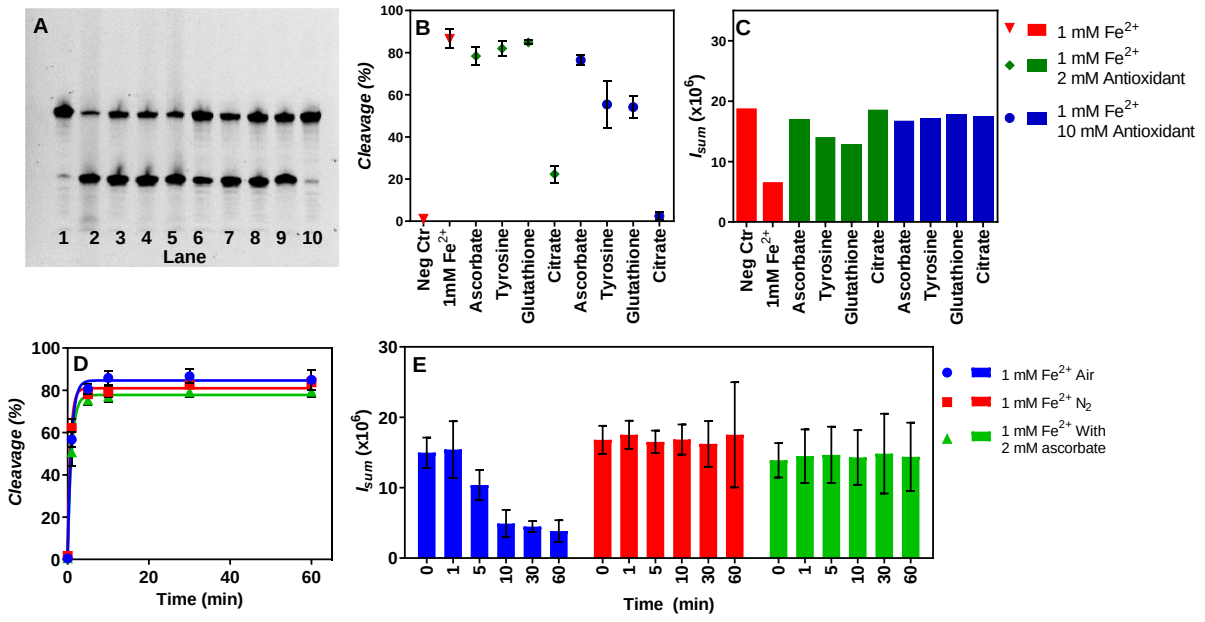

Figure 3.10. A) A high contrast gel micrograph to show the effect of antioxidants using Fe^{2+} as a metal cofactor without the use of N_2. The lanes are (1) negative control (no metal, no antioxidant) (2) positive control of 1 mM Fe^{2+} only; (3) 2 mM ascorbate, (4) 2 mM tyrosine, (5) 2 mM glutathione, (6) 2 mM citrate, (7) 10 mM ascorbate, (8) 10 mM tyrosine, (9) 10 mM glutathione, and (10) 10 mM citrate in the presence of 1 mM Fe^{2+}. The corresponding **B)** cleavage activity and **C)** I_{sum} based on the data in (A). **D)** Cleavage activity comparison of 1 mM Fe^{2+} with 17E DNAzyme in air, N_2, and 2 mM ascorbate in air. See (E) for the meaning of the color symbols. **E)** I_{sum} comparison of 1 mM Fe^{2+} with 17E DNAzyme in air, N_2, or 2 mM ascorbate in air. Error bars are the standard deviations from 2 to 9 replicates.

Summary

Like ribozymes, activities of the Mg^{2+}-dependent DNAzymes can be enhanced by substituting Mg^{2+} with Fe^{2+}, even though the relative increase was different for each DNAzyme tested. On the other hand, for the DNAzymes that are inactive with Mg^{2+}, they are also inactive with Fe^{2+}. In an oxidation-limited environment, DNAzyme 17E can cleave up to 90% of the substrate with 1 mM Fe^{2+} within 10 min. Interestingly, only the oxidation state of Fe^{2+} instead of Fe^{3+} was able to help the cleavage. This probably has to do with the coordination mechanism of the metal with the cleavage site phosphate. However, at basic pH and higher concentrations of

Fe^{2+}, the iron species was prone to oxidation and production of ROS, resulting in non-specific degradation of the DNA. Also, high concentrations of Fe^{3+} were found to hydrolyze easily and bind with DNA to cause larger molecular weight artifacts in gel electrophoresis. The effect of the anoxic and the reducing environments were systematically investigated to eliminate the degradation. Preventing Fe^{2+} oxidation to Fe^{3+} by performing reactions in N_2 allowed high cleavage activity. Ascorbate can also be used to provide a reducing environment to maintain the iron species as Fe^{2+}, but this method failed for DNAzymes with slower cleavage rates, such as 8-17 and E5. Observations from this study can provide insights into potential DNAzyme catalysis in the chemical environment of the early earth. Also, the study can guide with the experimental handling of easily oxidizable metal ion species for the development of the DNAzyme sensors.

Chapter 4 The activity of DNAzymes in biological fluids and the effect of externally added metal ions

Introduction

Sequence-specific cleavage of intracellular RNA is often used for therapeutic applications, such as anti-virus and anti-cancer. Various strategies have been developed to achieve this goal including anti-sense DNA, siRNA, and ribozymes/DNAzymes. Among these, DNAzymes are very attractive since they are highly stable and cost-effective. A few general-purpose RNA-cleaving DNAzymes were reported for this purpose, such as the 8-17 and 10-23 DNAzymes.[139] They can cleave most dinucleotide junctions in full-RNA substrates and they can use Mg^{2+} for cleavage. For a long time, they showed great promise in intracellular RNA cleavage.[170, 171]

However, it was later pointed out that these DNAzymes require very high concentrations of Mg^{2+} for activity, which can hardly be reached for intracellular conditions. A few ways have been developed to overcome this. One is to develop Na^{+}-specific DNAzymes, which is also very abundant in cells.[40, 89, 143, 144, 172] For example, the NaA43 DNAzyme demonstrated its feasibility for intracellular RNA cleavage and detection of metal ions.[40] In addition, metal-free DNAzymes were also selected containing modified nucleotides to better mimic the RNase A.[173] An interesting idea demonstrated recently was to use metal-containing nanomaterials such as ZnO[174, 175] and MnO_2 nanoparticles[176, 177] that are expected to be dissolved inside cells to release Zn^{2+} and Mn^{2+} ions to promote the cleavage reaction. In such a small volume of the intracellular environment, these dissolved ions may reach a high concentration to support catalysis. For example, the 17E DNAzyme is known to be much more active with a low concentration of these particular transition metal ions. This method has been shown to be effective in many reports. Some interesting fundamental questions need to be addressed to better study the reaction. What concentration of

metal ions is needed inside the cells? The intracellular environment is full of crowded proteins. Compared to Mg^{2+}, transition metals such as Zn^{2+} and Mn^{2+} are more likely to be affected by proteins.

Aside from biomedical applications, DNAzymes are more often used for detecting metal ions in environmental samples, where proteins may also exist. Therefore, understanding the effect of proteins in samples is of fundamental and practical importance.

Proteins can affect reactions in at least two aspects. First, they may bind metal ions to decrease the effective concentration of the metal ions available for DNAzymes. Proteins contain more strong metal ligands such as thiol and primary amine groups, while the metal binding affinity of nucleotides is in general much lower. Second, proteins may non-specifically bind DNAzymes to inhibit their activity by impeding folding or other mechanisms. Since the intracellular condition is very complex, most previous studies only relied on fluorescence microscopy or flow cytometry for analysis. However, many important biochemical parameters such as reaction kinetics and inhibition effect cannot be directly measured.

To address this important gap, in this study, we used two model DNAzymes to understand the effect of proteins on DNAzyme reaction in the presence of a few representative metal ions.

Materials and Methods

Chemicals. Sodium chloride, 10x Tris Buffer EDTA (TBE), urea, ammonium persulfate (APS), tetramethylethylenediamine (TEMED), 3-(N-morpholino) propanesulfonic acid (MOPS), and 2-(N-morpholino)ethanesulfonic acid (MES) were purchased from Bio Basic Inc. Gel loading dyes for gel electrophoresis were purchased from New England Biolabs. Magnesium chloride was from Amresco. Zinc chloride, lead nitrate, manganese chloride, bovine serum albumin (BSA),

hemoglobin, and alpha-macroglobulin, sodium hydroxide, lithium hydroxide, and lithium chloride were from Sigma Aldrich. A BioRad ChemiDoc MP Imaging System was used for gel imaging. Tecan plate reader and SpectraMax plate readers were used for sensor optimization and studies.

DNAzyme activity assay with protein. 17E and NaH1 DNAzymes were used in the studies throughout this paper. Their sequences are shown in **Table 4.1**. To measure the DNAzyme activity, the DNAzyme and the FAM-labeled substrate strands are annealed in a 1.5:1 molar ratio, respectively, to ensure that all FAM-labeled substrate strands form the DNAzyme complex. The optimized condition for 17E was to use 50 mM MES pH 6, 25 mM NaCl as the Annealing Buffer. Similarly, NaH1 utilized 50 mM MOPS pH 7.5, 25 mM LiCl as the Annealing Buffer. Using LiCl in the place of NaCl maintained similar ionic strength while eliminating Na^+ for the DNAzyme reaction with Na^+ ions. So, 5 μM FAM-Sub and 7.5 μM DNAzyme (17E or NaH1) strands are hybridized together in the Annealing buffer with a short heat shock of 95°C for 1 min, followed by slow cooling in 4°C for 30 min. The concentration of the DNAzyme complex is expressed as the concentration of the FAM-Substrate.

Table 4.1. DNA sequences, modifications, and the supplier (IDT: Integrated DNA Technologies; Eurofin: Eurofin Genomics). FAM: carboxyfluorescein.

Name	Supplier	Sequence
Sub-FAM	IDT	5′– GTCACGAGTCACTATrAGGAAGATGGCGAAA /36-FAM/ -3′
17E	IDT	5′-TTTCGCCATCTTCTCCGAGCCGGTCGAAATAGTGACTCGTGAC-3′
NaH1	Eurofin	5′-TTTCGCCATAGGTCAAAGGTGGGTGGGAGTTT TTACTCCCCATTAGTGACTCGTGAC -3′

Once the DNAzyme complex is prepared, 1 μL of 5 μM DNAzyme complex is diluted with 4 μL of the Reaction Buffer. For 17E, the optimal Reaction Buffer is 50 mM MOPS pH 7.5, 25

mM NaCl For NaH1, the optimal Reaction Buffer is 50 mM MES pH 6, 25 mM LiCl. Then, 1 μL of concentrated protein (i.e. 70 mg/mL BSA for final condition of 10 mg/mL BSA) is added to the diluted DNAzyme complex mixture and incubated for 5 min before the addition of 1 μL metal stock solution. The metal stock solution was prepared in Milli-Q water. Upon the addition of the metal stock solution, the reaction mixture is incubated for 10 min before it is quenched with 7 μL of quenching solution (8 M Urea and 1X loading dye. The quenched reaction mixture is then loaded into 15% denaturing polyacrylamide gel (dPAGE) for electrophoretic separation to examine the band. After 80 min at 200 V, the obtained gel is imaged on the BioRad ChemiDoc MP Imaging System using the fluorescent channel for FAM dye. The gel image is then quantitatively analyzed using the fluorescence intensities of each band.

During the optimization process, a few technical key points were determined for an optimal procedure. For 17E and NaH1, the annealing pH was different than the reaction pH, to maintain a low background signal. For example, 17E DNAzyme and the substrate strands were annealed in pH 6 and then reacted with the cofactor metal in pH 7.5. For NaH1, the DNAzyme and substrate strands were annealed in pH 7.5 and reacted in pH 6. This was due to the observation of a slightly higher background upon annealing. Even though the annealing buffer is prepared using Milli-Q grade water, any remaining sodium or calcium metal ions would have cleaved the substrate strand more in its optimum pH. So, a slightly different pH was used during the annealing process to keep the background low (

Figure 4.1). This is likely because at its basic optimum pH, the single RNA cleavage site can be hydrolyzed upon non-specific deprotonation of the 2`-OH over a long time. Because during the annealing process, the components of the DNAzyme complex are heated to 95°C briefly, and this can accelerate the non-specific cleavage. To prevent any background cleavage in the sample preparation process, using a slightly different annealing buffer pH simply solved the problem. In addition, when protein solutions were prepared, the stock solutions were desalted using MW cutoff spin filters (slightly smaller than the protein MW) to clear any remaining Na^+ ions. The proteins were washed with Li^+ containing buffers to maintain similar ionic strength.

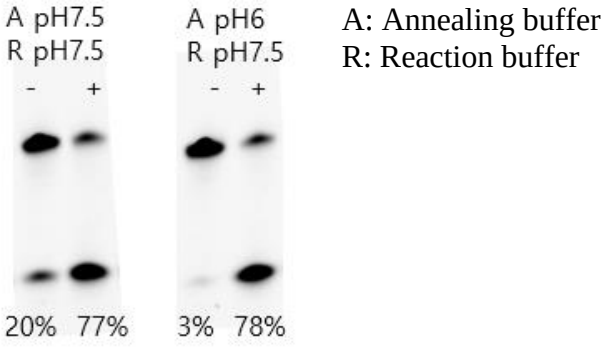

Figure 4.1. Comparison of annealing buffer pH to minimize background cleavage with the 17E. – indicates no metal addition and + indicates 10 µM Pb^{2+}.

Data analysis. Image Lab software (Bio-Rad Laboratories Inc.) was used to quantitate the fluorescence intensities from the obtained gel micrograph. The software can be used to define each lanes and select the area for each bands. "Band %" calculates the fractions of the cleaved band intensity to the total intensity. Kinetic data were fitted to obtain the apparent rate constant, k_{obs}, using the binding model shown in **Equation 4.1**.[45] In this equation, $\%P_0$ is the initial activity

percentage of cleaved product at t=0 and $\%P_\infty$ is at the endpoint of the reaction. Concentration dependence data were fitted to obtain the apparent dissociation constant, K_d, using **Equation 4.2**.[45]

$$\%P_t = \%P_0 + \%P_\infty\left(1 - e^{-(K_{obs})t}\right) \quad \textbf{Eqn. 4.1}$$

$$k_{obs} = \frac{k_{max}[M]}{(K_d+[M])} \quad \textbf{Eqn. 4.2}$$

Fluorescence polarization assay. Fluorescence polarization assay was performed to examine the changes in molecular weight upon the incubation of the FAM-labeled substrate strands with proteins. The total volume of 100 µL was prepared using 1 µL of 5 µM FAM-labeled substrate or the annealed DNAzyme complex and 3 µL of varying BSA concentrations to make the final concentrations of 1.5, 7.5, 15 µM BSA. As a positive control, 3 µL of cetyl trimethylammonium bromide (CTAB) was incubated with the DNA for 30 min and then diluted into the respective buffer to make 15 µM final concentration. The anisotropy of the assay samples was measured in the black 96-well plate. Any increase in molecular weight upon possible binding interaction increases the anisotropy value calculated by **Equation 4.3**, where $I_{parallel}$ and $I_{perpendicular}$ mean the intensities of the parallel and perpendicularly polarized light through the sample solution.[178, 179].

$$r = \frac{I_{parallel} - I_{perpendicular}}{I_{parallel}+2I_{perpendicular}} \quad \textbf{Eqn. 4.3}$$

Results and Discussion

Two DNAzymes to be studied

In this work, we studied two DNAzymes: 17E and NaH1 (**Figure 4.2**). They have the same substrate sequence containing a single RNA linkage (the rAG junction) serving as the cleavage site, although the enzyme strand of 17E is shorter. The 17E DNAzyme is active with most divalent metal ions. For example, as extensively examined in Chapter 2, different metals like Mg^{2+}, Mn^{2+},

Zn^{2+}, and Pb^{2+} are all active with 17E at different rates. Thus, different metal concentrations are required for each metal ion to reach saturation.

17E is frequently used in various application studies as a good representative divalent metal-dependent DNAzyme. For example, the almost identical DNAzyme 8-17 and 17E have been used for the detection of intracellular metal ions and imaging applications.[67, 180] In addition, researchers have designed 17E-based biosensors for the detection of nucleic acids (e.g. miRNA) and proteins (e.g. thrombin).[181, 182] As such, 17E DNAzyme has a great potential for intracellular detection.

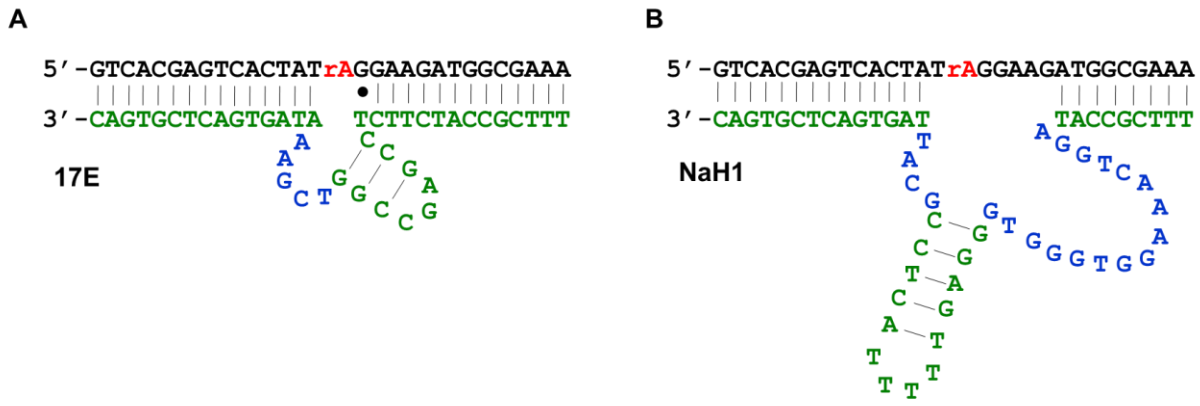

Figure 4.2. The secondary structures of the **A)** 17E and **B)** NaH1 DNAzymes. 17E is active with many divalent metal ions and Mg^{2+}, Mn^{2+}, Zn^{2+}, and Pb^{2+} were used throughout this study. Na^{+} was used with the NaH1 DNAzyme.

In comparison, NaH1 is independent of divalent metal ions and it only requires Na^{+} for activity. Therefore, NaH1 can be a good representative monovalent metal-dependent DNAzyme.[144] NaH1 only has a few bases altered compared to the NaA43T DNAzyme, which also requires Na^{+}. They have different pH optimum. Instead of pH 7.5 of NaA43T, pH 6 was found to be the optimal pH for NaH1. Detection of metal ions in pH 6, which is similar to the intracellular

environment of cancerous cells, can provide useful analytical information. Therefore, NaH1 was examined as the monovalent metal-dependent DNAzyme for this study.

The reaction of 17E and NaH1 with a few model proteins

For the preliminary study, four different proteins were chosen to be examined for their interaction with the 17E DNAzyme. Albumin is the most commonly found protein in vertebrates and their plasma (up to 40 mg/mL that makes up ~60% of the total plasma protein). [183] So, bovine serum albumin (BSA) is often a model protein used in many studies. One of the biological functions of the serum albumin is to transport and regulate metal ions, such as Zn^{2+}.[184] α2-macroglobulin (aM) was chosen because globulin is the second most common protein in blood serum.[185] It is also a representative glycoprotein, containing a carbohydrate chain. Hemoglobin is a representative metalloprotein and is commonly known for its oxygen carriage.[186] This protein contains a heme group, which is centered around an iron metal ion.

As mentioned before, 17E requires different metal concentrations to reach the saturation activity at a fixed incubation time and pH for different metal ions. Therefore, 10 mM Mg^{2+}, 100 μM Mn^{2+}, 100 μM Zn^{2+}, and 10 μM Pb^{2+} were chosen as the metal concentrations to test the effects of the four model proteins on the DNAzyme activities because these concentrations ensures activity saturation. The first three metal ions have been used for intracellular cleavage of this DNAzyme, while Pb^{2+} was used as a target for detection and was the most active metal.

Different metal ions and the chosen model proteins were incubated for 5 min before the reaction with the DNAzyme for 10 min. To follow the DNAzyme cleavage reaction, the substrate strand was labeled with a carboxyfluorescein (FAM) fluorophore, and the gel-based assay was carried out. **Figure 4.3C-F** shows the result of the screening experiment. In the presence of

proteins (such as BSA and aM), the cleavage yield decreased for most metal ions, except for Mg^{2+}. While aM has the strongest inhibition effect for Pb^{2+} and Mn^{2+}, its effect on Zn^{2+} was the weakest. Hb, on the other hand, inhibited Zn^{2+} the most. This was likely a reflection of different metals with different binding affinities to different proteins.

When the proteins were incubated with the Na^{+} and NaH1 in a similar fashion, the two proteins did not decrease activities as the transition metals did (**Figure 4.3B**). This was also consistent with that Na^{+} does not have a high affinity with proteins. Also, since Na^{+} was added at a much higher concentration (100 mM), the concentration of the proteins was relatively much lower, this can also explain the insignificant inhibition.

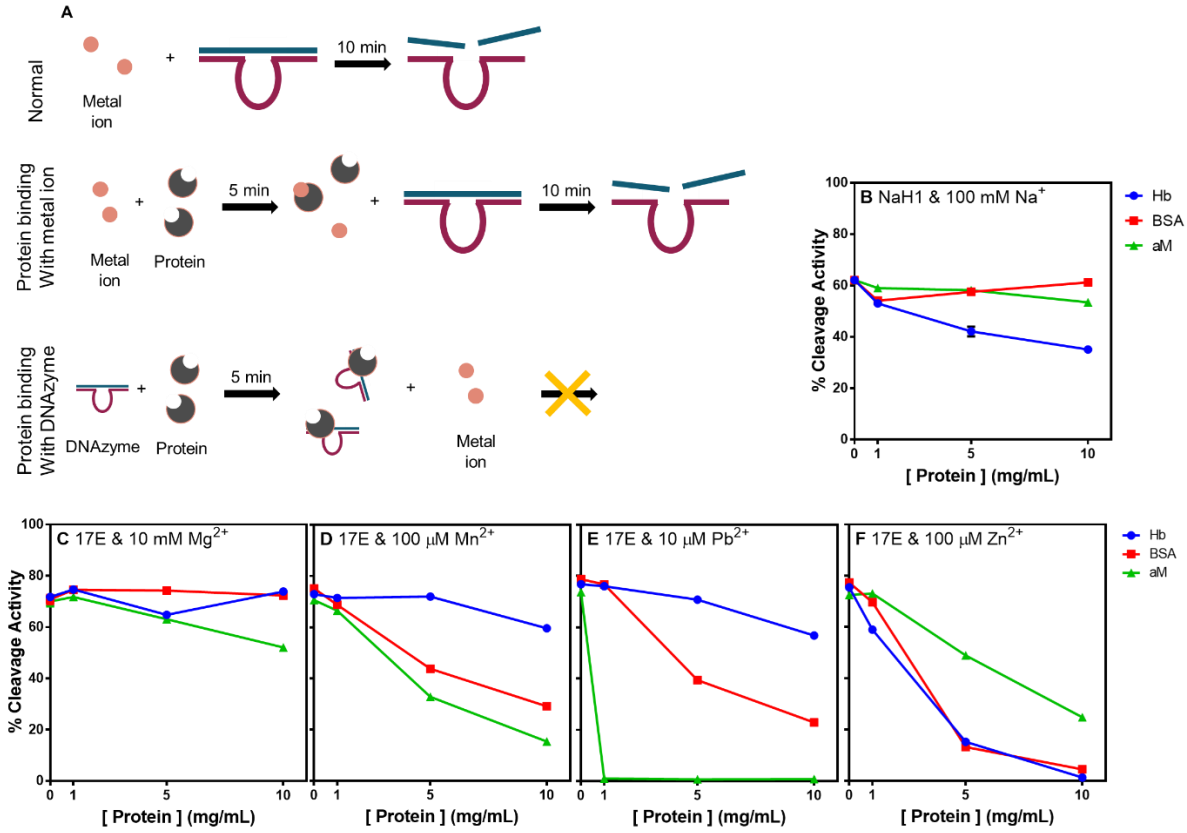

Figure 4.3. A) General scheme of the DNAzyme reaction with metal ions and the proposed scheme of how protein may affect the reaction. **B)** The effect of increasing amounts of different proteins on the DNAzyme NaH1 and 100mM Na^{+}, **C)** 17E with 10 mM Mg^{2+}, **D)** 17E with 100 µM Mn^{2+},

E) 17E with 10 μM Pb^{2+}, and **F)** 17E with 100 μM Zn^{2+}. Blue circle: Hemoglobin (Hb); Red square: Bovine serum albumin (BSA); Green triangle: alpha-2-macroglobulin (aM).

Based on these observations, it was hypothesized that the metal ions could be binding to certain proteins, decreasing the effective free metal, and thus decreasing the DNAzyme activity (**Figure 4.3A**). We also questioned whether the DNAzyme and the protein had any non-specific interactions that could inhibit the DNAzyme activity. In the following sections, more detailed study results will be discussed to address this hypothesis.

Probing non-specific interaction of the model proteins to the tested DNAzymes

To assay the potential binding between the proteins and DNAzymes, we used a fluorescence polarization assay. Fluorescence polarization is a method to observe a change in the molecular weight of fluorophore-labeled molecules.[179] Upon binding of the FAM-labeled DNA with another molecule, the overall molecular weight is increased and hence the polarization anisotropy value is expected to increase due to the slower free rotation in solution.

To assay the binding interaction, 1 μL DNA was incubated with 3 μL CTAB as a positive control or 3 μL BSA as the test samples for 30 min before dilution into the respective buffer to make 100 μL volume for plate reader measurement. The denoted concentrations are the final concentrations.

We first tested the free FAM-labeled substrate without an enzyme strand. The substrate alone had an anisotropy value of 17 (**Figure 4.4)**. As a positive control, the final concentration of 15 μM CTAB increased the anisotropy value up to 40 after 30 min incubation. In the presence of 1.5 μM, 7.5 μM, and 15 μM BSA, the anisotropy also increased. However, the annealed 17E

complex was observed to be more stable in the presence of increasing BSA, while the NaH1 complex showed increased binding with the increasing BSA.

Based on the preliminary data, 17E activity with various metal ions decrease in the presence of BSA. Since the anisotropy data shows that 17E does not bind very well with the BSA, it can be hypothesized that the decreasing activity may be due to the metal-protein binding interaction. However, for the NaH1 complex, the anisotropy trend is the opposite. There are a few different possible explanations for this observation. The NaH1 sequence is longer than the 17E by 20 nt. The larger molecule may be providing more binding sites for the BSA to interact with. Therefore, it does not eliminate the possibility of the protein-DNA binding that can affect the activity, but this may depend on the size of the DNAzyme.

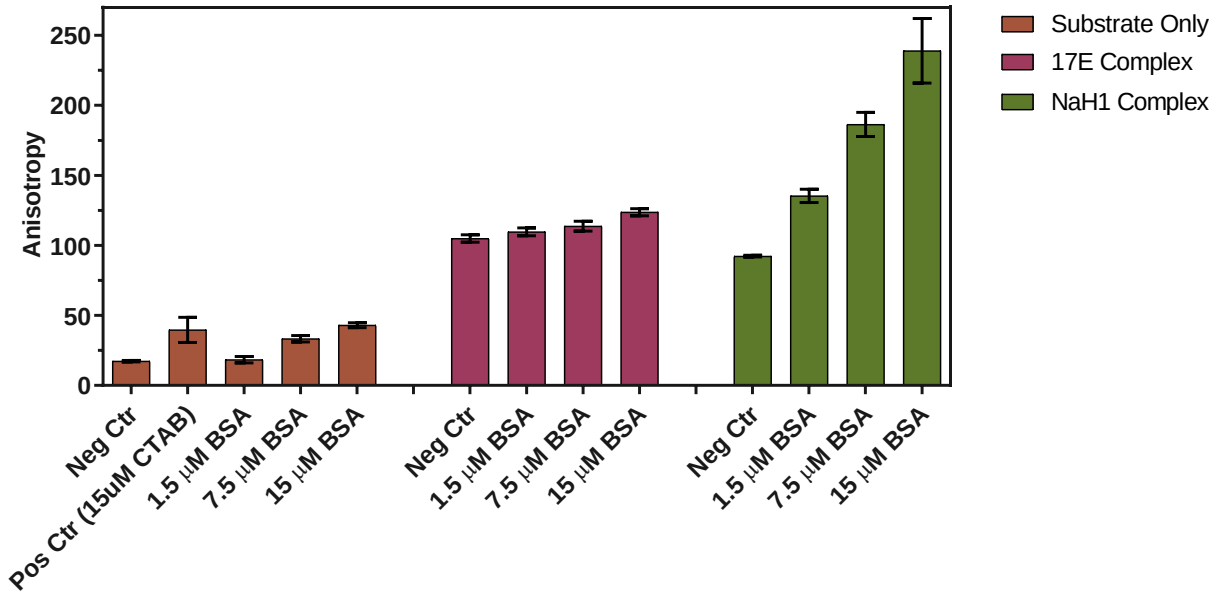

Figure 4.4. Fluorescence polarization anisotropy values of FAM-labeled substrate and the DNAzymes in the presence of BSA. The negative control is only the FAM-labeled substrate or the DNAzyme complex.

The metal-binding affinity of proteins correlates with DNAzyme inhibition.

If there is no significant binding interaction between the 17E DNAzyme complex and the protein, it can be hypothesized that the DNAzyme activity inhibition is caused by the metal-protein binding interaction. If metal ions and protein bind, the effective concentration of the free metal ion for DNAzyme reaction decreases. To quantitate the effect of the presence of protein on the DNAzyme activity, increasing concentration of metal ions with the DNAzymes NaH1 and 17E were examined in the presence of a fixed BSA concentration of 10 mg/mL or 150 μM BSA (**Figure 4.5**). The metal ions-to-DNAzyme apparent dissociation constants (K_d) were determined according to **Equation 4.2** and are presented in **Figure 4.5F**. 5 min pre-incubation with metal ions and the protein was followed by a 10 min DNAzyme reaction. Although each metal ion has a different rate, saturation was reached at a high metal concentration. So, even though different metal concentration ranges were used for different metals, the activity saturation curve could be fitted into the equation.

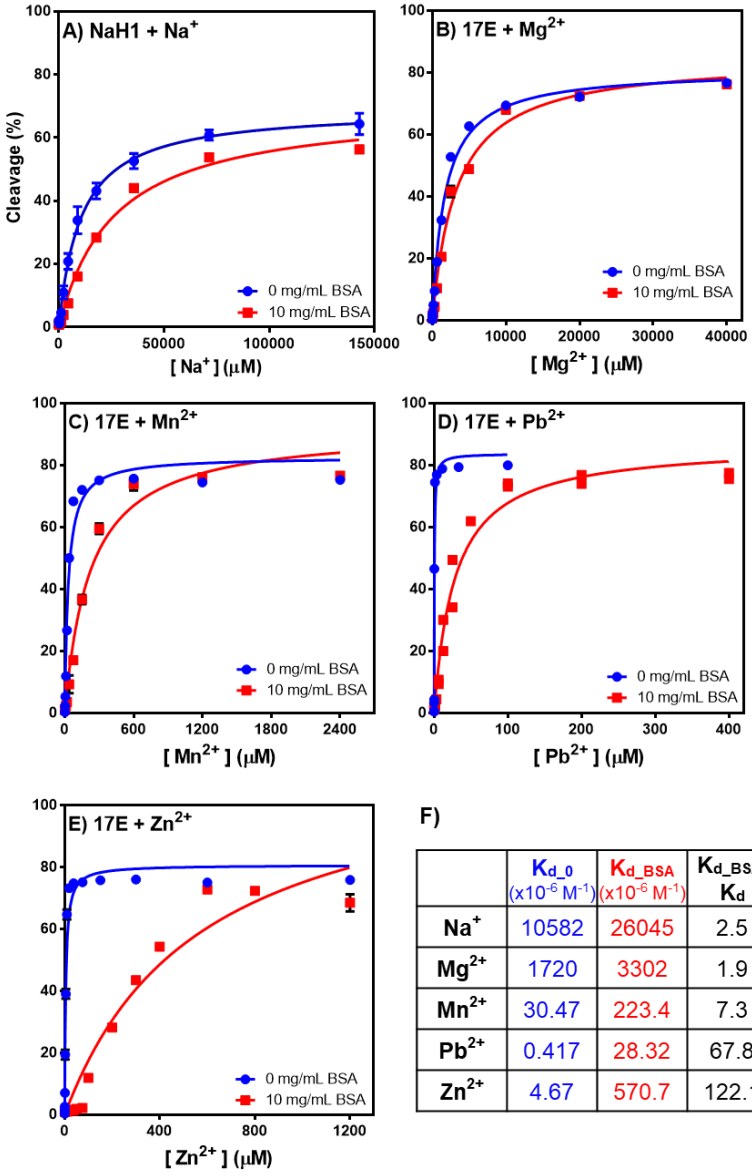

F)

	K_{d_0} ($\times 10^{-6}$ M^{-1})	K_{d_BSA} ($\times 10^{-6}$ M^{-1})	K_{d_BSA}/K_d
Na^+	10582	26045	2.5
Mg^{2+}	1720	3302	1.9
Mn^{2+}	30.47	223.4	7.3
Pb^{2+}	0.417	28.32	67.8
Zn^{2+}	4.67	570.7	122.1

Figure 4.5. A – E) Comparison of DNAzyme activities in the presence of 10 mg/mL BSA (or 150 μM BSA) with different metal ions. Blue circle: no BSA; Red square: with BSA. **F)** Table of K_d with the respective metals and the DNAzyme. The inhibition ratio (K_{d_BSA}/K_d) is also tabulated.

As interpreted from **Figure 4.5**, different metal K_d can be used to obtain the ratio of the decreased activity in the presence of the BSA protein. This ratio was compared to the association constants of the metal ion-to-BSA (K_a) from the literature, presented in Table 4.2. In general, a

positive correlation was observed. It is interesting to note that BSA has the highest affinity for Zn^{2+}, and Zn^{2+} was indeed most inhibited by BSA. Since one of the primary functions of BSA in biological systems is to transport Zn^{2+} ions, the high K_a of Zn^{2+} ion to the protein is understandable. On the other hand, Mg^{2+} barely binds to the BSA protein and it can be illustrated by the low K_a. Based on our results, to supply extra metal ions, Mn^{2+} might be a better choice than Zn^{2+} in serum. For the intracellular environment, the protein content is different and this needs to be further assayed.

Table 4.2. Literature reported values for metal ion – BSA association constants K_a.

Metal	Metal - BSA Association Constants (K_a)	References
Mg^{2+}	100 M^{-1}	*187*
Mn^{2+}	6.3 x 10^3 M^{-1}	*188*
Pb^{2+}	7.5 x 10^4 M^{-1}	*189*
Zn^{2+}	2.2 x 10^6 M^{-1}	*190*

Based on our hypothesis, our observations of activity decrease were correlated to the literature values of the metal-BSA interaction (**Figure 4.6**) with the 17E. As the metal-BSA affinity increases, the higher inhibition occurs in the DNAzyme activity assays. So, the presence of metal-binding proteins and their degree of affinities can affect the detection sensitivities when using the DNAzyme biosensors in the intracellular environment.

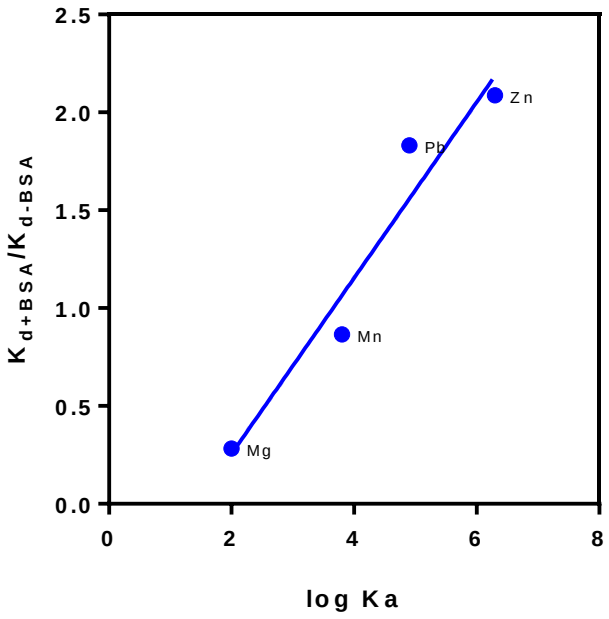

Figure 4.6. Correlation of the inhibition ratios and the reported K_a. As the affinities of the metal-BSA increase, the DNAzyme activity inhibition increases.

Summary

Ranging from metal and nucleic acid sensing to therapeutic agents for anti-virus or anti-cancer treatments, DNAzymes have a great potential for many intracellular applications. Discussions of some RNA-cleaving DNAzymes which only work in the presence of high Mg^{2+} concentration triggered further research into the use of externally added metal ions via nanoparticles or even metal-independent DNAzymes. As one of the efforts to overcome this challenge, the divalent metal-dependent DNAzymes (i.e. 17E) and the Na^{+}-dependent DNAzymes (NaA43 or NaH1) have been suggested as a general-purpose DNAzyme for intracellular detection. In combination with the externally added metal ions, these DNAzymes can provide the benefit of high sensitivities for the target metal ions and the ability to use the high concentration of Mg^{2+} already present within the cells.

To further understand the parameters that affect the effectiveness of these DNAzymes in more complex samples, a fundamental understanding of the DNAzyme behavior was necessary. Since the cellular environments are crowded with proteins, externally added metal ions may interact with the surrounding proteins. In our preliminary screening, different metal ions and different proteins interacted differently. As a model protein, BSA was examined with different metal ions. It was observed that there was an increased degree of inhibition in DNAzyme activities as the binding affinity of the metal ion and the protein increases. The different binding behaviours observed for 17E and NaH1 when incubated with the BSA also hint that DNA-protein binding may be present depending on the size or the sequence of the DNAzymes. This knowledge should provide insights for future DNAzyme designs for intracellular applications.

Chapter 5 Conclusions and Future Work

In vitro selected DNAzymes offer a wide range of potential for biosensor development. Especially, the 17E DNAzyme cleaves RNA in the presence of divalent metal ions and is a great model DNAzyme that can be studied to examine the mechanistic functions of those active divalent metal ions. Such mechanisms not only include the fundamental metal-DNAzyme interaction, but also how the DNAzymes behave in more complex samples, such as the intracellular environment. Throughout the studies discussed in this thesis, the model DNAzyme 17E was examined extensively to deepen our understanding.

By systematically screening the many metal ions from the periodic table, it was observed that only the divalent metal ions were active. Out of those divalent metal ions, the transition metals showed a generally high substrate cleavage activity in a similar metal concentration range. Pb^{2+} showed exceptionally high activity, which explains why Pb^{2+} has been the focus of the studies and applications involving 17E DNAzymes. From the transition metals, Ni^{2+} was identified as an outlier, which was also reported before. Some of those previous studies have cited a correlation with the low pK_a of the metal-bound water, but others have also argued that the stronger acids are less likely to deprotonate the 2′-OH for the nucleophilic attack of the phosphate group for cleavage reaction. Based on the screening of the metal ions from the d-block elements, the cleavage activity appeared to be correlated to the thiophilicity of the metals, which may indicate that metal ions act as a Lewis acid. To probe the idea, the hypothesis of metal ions interaction via inner-sphere coordination mechanism was examined via phosphorothioate substitution and phosphate competition studies. Substitution of the non-bridging oxygen with sulfur indicated that the metal ions interacted with the pro-R_p oxygen. Comparison with the thiophilicity showed a general trend that the more thiophilic metal ions did not affect the cleavage rate with the substituted

stereoisomers, but Ni^{2+} was still an outlier. However, literature reported water ligand exchange rates of the transition metals showed a linear correlation. This observation also further added support for the hypothesis of metal ions acting as a Lewis acid. Inhibition assays in phosphate buffer indirectly probed this idea further by quantifying the inhibition by the phosphate, which also correlated with the cleavage rate constants. Overall, the mechanism of action by the transition metals and the Pb^{2+} appears to be different: as a Lewis acids by the transition metals by coordinating to the non-bridging phosphate to stabilize the leaving group oxygen, and as a general acid by the lead hydrates while the guanine act as the general base for deprotonation.

Although the physical properties cannot be completely isolated to be studied for each metal ion, the thio effect was direct probed via the phosphorothioate substitution studies and the Lewis acid behaviour was indirectly probed via the phosphate inhibition studies. The observed results should benefit future applications using the 17E as a general divalent metal ion sensor by providing some important insights regarding the mechanism of interactions. Further modeling or crystallography studies of other metal ions with the 17E will provide more definitive answers to the question.

Out of those transition metal ions examined, the unexpected finding of high activity with Fe^{2+} lead to a closer examination of the metal. Previous studies have reported that Fe^{2+} could replace the Mg^{2+} in the binding sites in ribozymes. So, it was hypothesized that DNAzymes could be behaving similarly. Indeed, the Fe^{2+} and Mg^{2+} were found to be exchangeable amongst the six DNAzymes screened. The three DNAzymes that were active with Mg^{2+} were also active with the Fe^{2+}, while those that were not active with Mg^{2+} was also not active with Fe^{2+}. It was also found that the presence of air and pH affects the cleavage activity because those factors would affect the oxidation state of the iron. Fe^{3+} exhibited no activity while Fe^{2+} in a reducing environment showed

high cleavage activity. Working in an N_2 environment was important to maintain the oxidation state throughout the reaction. Using reducing agents, such as ascorbate, in the reaction buffer allowed a similar observation without using enclosed equipment for atmosphere control. The observed similarity between the ribozymes and the DNAzymes with Fe^{2+} can provide some insights into the DNAzyme catalysis in the anoxic atmosphere of early earth, as well as provide information for the detection of the most abundant metal ion in biological systems.

Recently, using DNAzymes as an intracellular biosensor or therapeutic agent has been a popular direction of research. The requirement of high metal cofactor concentration has been one of the main challenges and one of the strategies has been using nanomaterial that dissolves into ions upon a trigger to initiate the cleavage activity. To understand the DNAzyme interaction with potentially interfering species in complex samples for intracellular biosensing applications, binding with the model protein BSA has been examined carefully. Based on the observed results, it appears that the 17E DNAzyme did not bind with the BSA but the externally added metal ions could be binding with the present proteins, which can lower the effective metal concentration and thus the overall cleavage activity. Also, the larger-sized DNAzyme NaH1 appeared to bind with the BSA, but the overall DNAzyme activity was not affected much. This finding should help with the designing of the intracellular biosensors using DNAzymes. The remaining work should examine if similar behaviour is observed when using the fluorescent or other nanomaterial-based biosensors within the cells.

References

(1) Velikyan, I., Acharya, S., Trifonova, A., Földesi, A., and Chattopadhyaya, J. (2001) The pKa's of 2′-Hydroxyl Group in Nucleosides and Nucleotides, *J. Am. Chem. Soc. 123*, 2893-2894.

(2) Sigel, R. K. O., and Sigel, H. (2010) A Stability Concept for Metal Ion Coordination to Single-Stranded Nucleic Acids and Affinities of Individual Sites, *Acc. Chem. Res. 43*, 974-984.

(3) Moon, W. J., Huang, P.-J. J., and Liu, J. DNA-Enabled Heavy Metal Detection in Water, In *Encyclopedia of Analytical Chemistry*, pp 1-22.

(4) Ono, A., Torigoe, H., Tanaka, Y., and Okamoto, I. (2011) Binding of Metal Ions by Pyrimidine Base Pairs in DNA Duplexes, *Chem. Soc. Rev. 40*, 5855-5866.

(5) Ono, A., and Togashi, H. (2004) Molecular sensors: Highly selective oligonucleotide-based sensor for mercury(II) in aqueous solutions, *Angewandte Chemie, International Edition 43*, 4300-4302.

(6) Kondo, J., Yamada, T., Hirose, C., Okamoto, I., Tanaka, Y., and Ono, A. (2014) Crystal Structure of Metallo DNA Duplex Containing Consecutive Watson–Crick-like T–HgII–T Base Pairs, *Angew. Chem. Int. Ed. 53*, 2385-2388.

(7) Ono, A., Cao, S., Togashi, H., Tashiro, M., Fujimoto, T., Machinami, T., Oda, S., Miyake, Y., Okamoto, I., and Tanaka, Y. (2008) Specific interactions between silver (I) ions and cytosine-cytosine pairs in DNA duplexes, *Chem. Commun.*, 4825-4827.

(8) Eichhorn, G. L., and Shin, Y. A. (1968) Interaction of Metal Ions with Polynucleotides and Related Compounds. XII. The Relative Effect of Various Metal Ions on DNA Helicity, *J. Am. Chem. Soc. 90*, 7323-7328.

(9) Kosman, J., and Juskowiak, B. (2011) Peroxidase-mimicking DNAzymes for biosensing applications: A review, *Anal. Chim. Acta 707*, 7-17.

(10) Wolski, P., Nieszporek, K., and Panczyk, T. (2019) G-Quadruplex and I-Motif Structures within the Telomeric DNA Duplex. A Molecular Dynamics Analysis of Protonation States as Factors Affecting Their Stability, *J. Phys. Chem. B. 123*, 468-479.

(11) Kennedy, T. A. C., MacLean, J. L., and Liu, J. (2012) Blue emitting gold nanoclusters templated by poly-cytosine DNA at low pH and poly-adenine DNA at neutral pH, *Chem. Commun. 48*, 6845-6847.

(12) Wu, Y., and Lai, R. Y. (2016) Electrochemical Gold(III) Sensor with High Sensitivity and Tunable Dynamic Range, *Anal. Chem. 88*, 2227-2233.

(13) Breaker, R. R., and Joyce, G. F. (1994) A DNA Enzyme that Cleaves RNA, *Chem. Biol. 1*, 223-229.

(14) Zhou, W., Saran, R., and Liu, J. (2017) Metal Sensing by DNA, *Chem. Rev. 117*, 8272-8325.

(15) Hollenstein, M. (2015) DNA Catalysis: The Chemical Repertoire of DNAzymes, *Molecules 20*, 20777-20804.

(16) Hwang, K., Mou, Q., Lake, R. J., Xiong, M., Holland, B., and Lu, Y. (2019) Metal-Dependent DNAzymes for the Quantitative Detection of Metal Ions in Living Cells: Recent Progress, Current Challenges, and Latest Results on FRET Ratiometric Sensors, *Inorg. Chem. 58*, 13696-13708.

(17) Ma, L., and Liu, J. (2020) Catalytic Nucleic Acids: Biochemistry, Chemical Biology, Biosensors, and Nanotechnology, *iScience 23*, 100815.

(18) Silverman, S. K. (2016) Catalytic DNA: Scope, Applications, and Biochemistry of Deoxyribozymes, *Trends in Biochemical Sciences 41*, 595-609.

(19) Zimmermann, A. C., White, I. M., and Kahn, J. D. (2020) Nucleic acid-cleaving catalytic DNA for sensing and therapeutics, *Talanta 211*, 120709.

(20) Dokukin, V., and Silverman, S. K. (2012) Lanthanide ions as required cofactors for DNA catalysts, *Chemical Science 3*, 1707-1714.

(21) Chandra, M., Sachdeva, A., and Silverman, S. K. (2009) DNA-catalyzed sequence-specific hydrolysis of DNA, *Nat Chem Biol 5*, 718-720.

(22) Du, X., Zhong, X., Li, W., Li, H., and Gu, H. (2018) Retraining and Optimizing DNA-Hydrolyzing Deoxyribozymes for Robust Single- and Multiple-Turnover Activities, *ACS Catalysis 8*, 5996-6005.
(23) Gu, H., Furukawa, K., Weinberg, Z., Berenson, D. F., and Breaker, R. R. (2013) Small, Highly Active DNAs That Hydrolyze DNA, *J. Am. Chem. Soc. 135*, 9121-9129.
(24) Travascio, P., Li, Y., and Sen, D. (1998) DNA-enhanced peroxidase activity of a DNA aptamer-hemin complex, *Chem.Biol. 5*, 505-517.
(25) Li, H. Y., Chang, J. F., Hou, T., and Li, F. (2017) HRP-Mimicking DNAzyme-Catalyzed in Situ Generation of Polyaniline To Assist Signal Amplification for Ultrasensitive Surface Plasmon Resonance Biosensing, *Anal. Chem. 89*, 673-680.
(26) Xu, F., Yi, H., Yao, S., Li, W., Li, Y., Liu, Z., Nie, Z., and Lin, B. (2016) Insight into G-quadruplex-hemin DNAzyme/RNAzyme: adjacent adenine as the intramolecular species for remarkable enhancement of enzymatic activity, *Nucleic Acids Res. 44*, 7373-7384.
(27) Li, Y., and Sen, D. (1996) A catalytic DNA for porphyrin metalation, *Nature structural biology 3*, 743-747.
(28) Peng, D., Li, Y., Huang, Z., Liang, R.-P., Qiu, J.-D., and Liu, J. (2019) Efficient DNA-Catalyzed Porphyrin Metalation for Fluorescent Ratiometric Pb2+ Detection, *Anal. Chem. 91*, 11403-11408.
(29) Yang, L., Ding, P., Luo, Y., Wang, J., Lv, H., Li, W., Cao, Y., and Pei, R. (2019) Exploration of Catalytic Nucleic Acids on Porphyrin Metalation and Peroxidase Activity by in Vitro Selection of Aptamers for N-Methyl Mesoporphyrin IX, *Acs Combinatorial Science*.
(30) Silverman, S. K. (2015) Pursuing DNA Catalysts for Protein Modification, *Acc. Chem. Res. 48*, 1369-1379.
(31) Breaker, R. R., and Joyce, G. F. (1994) A DNA enzyme that cleaves RNA, *Chem. Biol. 1*, 223-229.
(32) Lan, T., Furuya, K., and Lu, Y. (2010) A highly selective lead sensor based on a classic lead DNAzyme, *Chem. Commun. 46*, 3896-3898.
(33) Ren, W., Huang, P.-J. J., He, M., Lyu, M., Wang, C., Wang, S., and Liu, J. (2020) Sensitivity of a classic DNAzyme for Pb2+ modulated by cations, anions and buffers, *Analyst 145*, 1384-1388.
(34) Santoro, S. W., and Joyce, G. F. (1997) A general purpose RNA-cleaving DNA enzyme, *Proc. Natl. Acad. Sci. 94*, 4262-4266.
(35) Huo, W., Li, X., Wang, B., Zhang, H., Zhang, J., Yang, X., and Jin, Y. (2020) Recent advances of DNAzyme-based nanotherapeutic platform in cancer gene therapy, *Biophysics Reports 6*, 256-265.
(36) Torabi, S.-F., and Lu, Y. (2015) Identification of the Same Na^+-Specific DNAzyme Motif from Two In Vitro Selections Under Different Conditions, *Journal of Molecular Evolution 81*, 225-234.
(37) Zhou, W., Zhang, Y., Huang, P.-J. J., Ding, J., and Liu, J. (2016) A DNAzyme requiring two different metal ions at two distinct sites, *Nucleic Acids Res. 44*, 354-363.
(38) Zhou, W., Ding, J., and Liu, J. (2016) A highly specific sodium aptamer probed by 2-aminopurine for robust Na+ sensing, *Nucleic Acids Res. 44*, 354-363.
(39) He, Y., Chen, D., Huang, P.-J. J., Zhou, Y., Ma, L., Xu, K., Yang, R., and Liu, J. (2018) Misfolding of a DNAzyme for ultrahigh sodium selectivity over potassium, *Nucleic Acids Res. DOI: 10.1093/nar/gky807*.
(40) Torabi, S.-F., Wu, P., McGhee, C. E., Chen, L., Hwang, K., Zheng, N., Cheng, J., and Lu, Y. (2015) In Vitro Selection of a Sodium-specific DNAzyme and its Application in Intracellular Sensing, *Proc. Natl. Acad. Sci. 112*, 5903-5908.
(41) Ma, L., Kartik, S., Liu, B., and Liu, J. (2019) From general base to general acid catalysis in a sodium-specific DNAzyme by a guanine-to-adenine mutation, *Nucleic Acids Res. 47*, 8154-8162.
(42) Huang, P.-J. J., Lin, J., Cao, J., Vazin, M., and Liu, J. (2014) Ultrasensitive DNAzyme Beacon for Lanthanides and Metal Speciation, *Anal. Chem. 86*, 1816-1821.

(43) Faulhammer, D., and Famulok, M. (1996) The Ca^{2+} Ion as a Cofactor for a Novel RNA-cleaving Deoxyribozyme, *Angew. Chem. Int. Ed. Engl. 35*, 2837-2841.
(44) Li, J., Zheng, W., Kwon, A. H., and Lu, Y. (2000) In Vitro Selection and Characterization of a Highly Efficient Zn(II)-dependent RNA-cleaving Deoxyribozyme, *Nucleic Acids Res. 28*, 481-488.
(45) Brown, A. K., Li, J., Pavot, C. M., and Lu, Y. (2003) A Lead-Dependent DNAzyme with a Two-Step Mechanism, *Biochemistry 42*, 7152-7161.
(46) Ward, W. L., Plakos, K., and DeRose, V. J. (2014) Nucleic Acid Catalysis: Metals, Nucleobases, and Other Cofactors, *Chem. Rev. 114*, 4318-4342.
(47) Bonaccio, M., Credali, A., and Peracchi, A. (2004) Kinetic and Thermodynamic Characterization of the RNA-Cleaving 8-17 Deoxyribozyme, *Nucleic Acids Res. 32*, 916-925.
(48) Mazumdar, D., Nagraj, N., Kim, H.-K., Meng, X., Brown, A. K., Sun, Q., Li, W., and Lu, Y. (2009) Activity, Folding and Z-DNA Formation of the 8-17 DNAzyme in the Presence of Monovalent Ions, *J. Am. Chem. Soc. 131*, 5506-5515.
(49) Athavale, S. S., Petrov, A. S., Hsiao, C., Watkins, D., Prickett, C. D., Gossett, J. J., Lie, L., Bowman, J. C., O'Neill, E., Bernier, C. R., Hud, N. V., Wartell, R. M., Harvey, S. C., and Williams, L. D. (2012) RNA Folding and Catalysis Mediated by Iron (II), *PLoS One 7*, e38024.
(50) Emilsson, G. M., Nakamura, S., Roth, A., and Breaker, R. R. (2003) Ribozyme Speed Limits, *RNA 9*, 907-918.
(51) Peracchi, A., Bonaccio, M., and Credali, A. (2017) Local Conformational Changes in the 8–17 Deoxyribozyme Core Induced by Activating and Inactivating Divalent Metal Ions, *Organic & Biomolecular Chemistry 15*, 8802-8809.
(52) Peracchi, A., Bonaccio, M., and Clerici, M. (2005) A Mutational Analysis of the 8-17 Deoxyribozyme Core, *J. Mol. Biol. 352*, 783-794.
(53) Saran, R., and Liu, J. (2016) A Comparison of Two Classic Pb^{2+}-Dependent RNA-Cleaving DNAzymes, *Inorg. Chem. Front. 3*, 494-501.
(54) Liu, H., Yu, X., Chen, Y., Zhang, J., Wu, B., Zheng, L., Haruehanroengra, P., Wang, R., Li, S., Lin, J., Li, J., Sheng, J., Huang, Z., Ma, J., and Gan, J. (2017) Crystal Structure of an RNA-Cleaving DNAzyme, *Nat. Commun. 8*, 2006.
(55) Li, J. (2000) In Vitro Selection of Highly Efficient DNA Enzymes as RNA Nucleases and Metal Biosensors, University of Illinois at Urbana-Champaign, Ann Arbor.
(56) Bischof, H., Burgstaller, S., Waldeck-Weiermair, M., Rauter, T., Schinagl, M., Ramadani-Muja, J., Graier, W. F., and Malli, R. (2019) Live-Cell Imaging of Physiologically Relevant Metal Ions Using Genetically Encoded FRET-Based Probes, *Cells 8*, 492.
(57) Leeman, M., Choi, J., Hansson, S., Storm, M. U., and Nilsson, L. (2018) Proteins and antibodies in serum, plasma, and whole blood-size characterization using asymmetrical flow field-flow fractionation (AF4), *Anal. Bioanal. Chem. 410*, 4867-4873.
(58) Liu, J., and Lu, Y. (2003) A Colorimetric Lead Biosensor Using DNAzyme-Directed Assembly of Gold Nanoparticles, *J. Am. Chem. Soc. 125*, 6642-6643.
(59) Lee, J. H., Wang, Z., Liu, J., and Lu, Y. (2008) Highly Sensitive and Selective Colorimetric Sensors for Uranyl (UO22+): Development and Comparison of Labeled and Label-Free DNAzyme-Gold Nanoparticle Systems, *J. Am. Chem. Soc. 130*, 14217-14226.
(60) Liu, J., and Lu, Y. (2007) Colorimetric Cu2+ detection with a ligation DNAzyme and nanoparticles, *Chem. Commun.*, 4872-4874.
(61) Memon, A. G., Zhou, X., Xing, Y., Wang, R., Liu, L., Khan, M., and He, M. (2019) Label-free colorimetric nanosensor with improved sensitivity for Pb2 + in water by using a truncated 8–17 DNAzyme, *Frontiers of Environmental Science & Engineering 13*, 12.

(62) Xiao, Y., Rowe, A. A., and Plaxco, K. W. (2007) Electrochemical Detection of Parts-Per-Billion Lead via an Electrode-Bound DNAzyme Assembly, *J. Am. Chem. Soc. 129*, 262-263.
(63) Yang, X., Xu, J., Tang, X., Liu, H., and Tian, D. (2010) A novel electrochemical DNAzyme sensor for the amplified detection of Pb2+ ions, *Chem. Commun. 46*, 3107-3109.
(64) Tian, A., Liu, Y., and Gao, J. (2017) Sensitive SERS detection of lead ions via DNAzyme based quadratic signal amplification, *Talanta 171*, 185-189.
(65) Wang, Y., and Irudayaraj, J. (2011) A SERS DNAzyme biosensor for lead ion detection, *Chem. Commun. 47*, 4394-4396.
(66) Li, J., and Lu, Y. (2000) A Highly Sensitive and Selective Catalytic DNA Biosensor for Lead Ions, *J. Am. Chem. Soc. 122*, 10466-10467.
(67) Hwang, K., Wu, P., Kim, T., Lei, L., Tian, S., Wang, Y., and Lu, Y. (2014) Photocaged DNAzymes as a General Method for Sensing Metal Ions in Living Cells, *Angew. Chem. Int. Ed. 53*, 13798–13802.
(68) Moon, W. J., Yang, Y., and Liu, J. (2020) Zn2+-Dependent DNAzymes: From Solution Chemistry to Analytical, Materials and Therapeutic Applications, *ChemBioChem n/a*.
(69) Cepeda-Plaza, M., and Peracchi, A. (2020) Insights into DNA Catalysis From Structural and Functional Studies of the 8-17 DNAzyme, *Organic & Biomolecular Chemistry 18*, 1697-1709.
(70) Kim, H.-K., Liu, J., Li, J., Nagraj, N., Li, M., Pavot, C. M. B., and Lu, Y. (2007) Metal-Dependent Global Folding and Activity of the 8-17 DNAzyme Studied by Fluorescence Resonance Energy Transfer, *J. Am. Chem. Soc. 129*, 6896-6902.
(71) Kim, H. K., Rasnik, I., Liu, J. W., Ha, T. J., and Lu, Y. (2007) Dissecting Metal Ion-Dependent Folding and Catalysis of a Single DNAzyme, *Nature Chemical Biology 3*, 762-768.
(72) Lam, J. C. F., and Li, Y. (2010) Influence of Cleavage Site on Global Folding of an RNA-Cleaving DNAzyme, *ChemBioChem 11*, 1710-1719.
(73) Lee, N. K., Koh, H. R., Han, K. Y., and Kim, S. K. (2007) Folding of 8-17 deoxyribozyme studied by three-color alternating-laser excitation of single molecules, *J. Am. Chem. Soc. 129*, 15526-15534.
(74) Kratschmer, C., and Levy, M. (2017) Effect of Chemical Modifications on Aptamer Stability in Serum, *Nucleic acid therapeutics 27*, 335-344.
(75) Li, J., Zheng, W., Kwon, A. H., and Lu, Y. (2000) In vitro selection and characterization of a highly efficient Zn(II)-dependent RNA-cleaving deoxyribozyme, *Nucleic acids research 28*, 481-488.
(76) Huang, P.-J. J., Vazin, M., and Liu, J. (2015) Desulfurization Activated Phosphorothioate DNAzyme for the Detection of Thallium, *Anal. Chem. 87*, 10443-10449
(77) Saran, R., and Liu, J. (2016) A Silver DNAzyme, *Anal. Chem. 88*, 4014-4020.
(78) Liu, J. (2015) Lanthanide-Dependent RNA-Cleaving DNAzymes as Metal Biosensors, *Can. J. Chem. 93*, 273-278.
(79) Zhou, W., Vazin, M., Yu, T., Ding, J., and Liu, J. (2016) In Vitro Selection of Chromium-Dependent DNAzymes for Sensing Chromium(III) and Chromium(VI), *Chemistry – A European Journal 22*, 9835-9840.
(80) Huang, P.-J. J., and Liu, J. (2015) Rational Evolution of Cd^{2+}-Specific DNAzymes with Phosphorothioate Modified Cleavage Junction and Cd^{2+} Sensing, *Nucleic Acids Res. 43*, 6125-6133.
(81) Zhang, J., and Lu, Y. (2018) Biocomputing for Portable, Resettable, and Quantitative Point-of-Care Diagnostics: Making the Glucose Meter a Logic-Gate Responsive Device for Measuring Many Clinically Relevant Targets, *Angew. Chem. Int. Ed. Engl. 57*, 9702-9706.
(82) Ma, L., and Liu, J. (2019) An in Vitro–Selected DNAzyme Mutant Highly Specific for Na^{+} under Slightly Acidic Conditions, *ChemBioChem 20*, 537-542.
(83) Huang, P.-J. J., Vazin, M., and Liu, J. (2014) In Vitro Selection of a New Lanthanide-Dependent DNAzyme for Ratiometric Sensing Lanthanides, *Anal. Chem. 86*, 9993-9999.

(84) Liu, J., Brown, A. K., Meng, X., Cropek, D. M., Istok, J. D., Watson, D. B., and Lu, Y. (2007) A Catalytic Beacon Sensor for Uranium with Parts-Per-Trillion Sensitivity and Millionfold Selectivity, *Proc. Natl. Acad. Sci. 104*, 2056-2061.
(85) Liu, J., Cao, Z., and Lu, Y. (2009) Functional Nucleic Acid Sensors, *Chem. Rev. 109*, 1948–1998.
(86) Zhang, X.-B., Kong, R.-M., and Lu, Y. (2011) Metal Ion Sensors Based on DNAzymes and Related DNA Molecules, *Annu. Rev. Anal. Chem. 4*, 105-128.
(87) Hwang, K., Hosseinzadeh, P., and Lu, Y. (2016) Biochemical and Biophysical Understanding of Metal Ion Selectivity of DNAzymes, *Inorganica chimica acta 452*, 12-24.
(88) Roth, A., and Breaker, R. R. (1998) An Amino Acid as a Cofactor for a Catalytic Polynucleotide, *Proc.Natl.Acad.Sci.U.S.A. 95*, 6027-6031.
(89) Geyer, C. R., and Sen, D. (1997) Evidence for the metal-cofactor independence of an RNA phosphodiester-cleaving DNA enzyme, *Chem.Biol. 4*, 579-593.
(90) Santoro, S. W., Joyce, G. F., Sakthivel, K., Gramatikova, S., and Barbas, C. F. (2000) RNA Cleavage by a DNA Enzyme with Extended Chemical Functionality, *J. Am. Chem. Soc. 122*, 2433-2439.
(91) Huang, P.-J. J., and Liu, J. (2016) An Ultrasensitive Light-up Cu^{2+} Biosensor Using a New DNAzyme Cleaving a Phosphorothioate-Modified Substrate, *Anal. Chem. 88*, 3341-3347.
(92) Hollenstein, M., Hipolito, C., Lam, C., Dietrich, D., and Perrin, D. M. (2008) A Highly Selective DNAzyme Sensor for Mercuric Ions, *Angew. Chem. Int. Ed. 47*, 4346-4350.
(93) Huang, P.-J. J., Vazin, M., Matuszek, Ż., and Liu, J. (2015) A New Heavy Lanthanide-Dependent DNAzyme Displaying Strong Metal Cooperativity and Unrescuable Phosphorothioate Effect, *Nucleic Acids Res. 43*, 461-469.
(94) Ren, W., Huang, P.-J. J., He, M., Lyu, M., Wang, S., Wang, C., and Liu, J. (2020) The Two Classic Pb2+-Selective DNAzymes Are Related: Rational Evolution for Understanding Metal Selectivity, *ChemBioChem 21*, 1293 – 1297.
(95) Wang, B., Cao, L., Chiuman, W., Li, Y., and Xi, Z. (2010) Probing the Function of Nucleotides in the Catalytic Cores of the 8-17 and 10-23 DNAzymes by Abasic Nucleotide and C3 Spacer Substitutions, *Biochemistry 49*, 7553-7562.
(96) Schlosser, K., Gu, J., Sule, L., and Li, Y. F. (2008) Sequence-Function Relationships Provide New Insight into the Cleavage Site Selectivity of the 8-17 RNA-Cleaving Deoxyribozyme, *Nucleic Acids Res. 36*, 1472-1481.
(97) Peracchi, A. (2000) Preferential Activation of the 8-17 Deoxyribozyme by Ca^{2+} Ions: Evidence for the Identity of 8-17 with the Catalytic Domain of the Mg5 Deoxyribozyme, *J. Biol. Chem. 275*, 11693-11697.
(98) Cruz, R. P. G., Withers, J. B., and Li, Y. (2004) Dinucleotide Junction Cleavage Versatility of 8-17 Deoxyribozyme, *Chem. Biol. 11*, 57-67.
(99) Schlosser, K., and Li, Y. (2010) A Versatile Endoribonuclease Mimic Made of DNA: Characteristics and Applications of the 8-17 RNA-Cleaving DNAzyme, *ChemBioChem 11*, 866-879.
(100) Kasprowicz, A., Stokowa-Soltys, K., Wrzesinski, J., Jezowska-Bojczuk, M., and Ciesiolka, J. (2015) In Vtro Selection of Deoxyribozymes Active with Cd2+ Ions Resulting in Variants of DNAzyme 8-17, *Dalton Transactions 44*, 8138-8149.
(101) Zhou, W., Zhang, Y., Ding, J., and Liu, J. (2016) In Vitro Selection in Serum: RNA-Cleaving DNAzymes for Measuring Ca2+ and Mg2+, *ACS Sens. 1*, 600-606.
(102) Cepeda-Plaza, M., McGhee, C. E., and Lu, Y. (2018) Evidence of a General Acid–Base Catalysis Mechanism in the 8–17 DNAzyme, *Biochemistry 57*, 1517-1522.
(103) Zhou, W., and Liu, J. (2018) Multi-Metal-Dependent Nucleic Acid Enzymes, *Metallomics 10*, 30-48.
(104) Sigel, R. K. O., and Pyle, A. M. (2007) Alternative Roles for Metal Ions in Enzyme Catalysis and the Implications for Ribozyme Chemistry, *Chem. Rev. 107*, 97-113.

(105) Liebe, D. C., and Stuehr, J. E. (1972) Copper(II)–DNA denaturation. I. Concentration Dependence of Melting Temperature and Terminal Relaxation Time, *Biopolymers 11*, 145-166.
(106) Sigel, A., Operschall, B. P., Sigel, R. K. O., and Sigel, H. (2018) Metal Ion Complexes of Nucleoside Phosphorothioates Reflecting the Ambivalent Properties of Lead(II), *New Journal of Chemistry 42*, 7551-7559.
(107) Wang, F., Saran, R., and Liu, J. (2015) Tandem DNAzymes for mRNA Cleavage: Choice of Enzyme, Metal Ions and the Antisense Effect, *Bioorg. Med. Chem. Lett. 25*, 1460-1463.
(108) Breaker, R. R., and Joyce, G. F. (1995) A DNA Enzyme with Mg^{2+}-Dependent RNA Phosphoesterase Activity, *Chem. Biol. 2*, 655-660.
(109) Lan, T., and Lu, Y. (2012) Metal Ion-Dependent DNAzymes and Their Applications as Biosensors, In *Interplay between Metal Ions and Nucleic Acids* (Sigel, A., Sigel, H., and Sigel, R. K. O., Eds.), pp 217-248, Springer Netherlands, Dordrecht.
(110) Breaker, R. R., Emilsson, G. M., Lazarev, D., Nakamura, S., Puskarz, I. J., Roth, A., and Sudarsan, N. (2003) A Common Speed Limit for RNA-Cleaving Ribozymes and Deoxyribozymes, *RNA 9*, 949-957.
(111) Lott, W. B., Pontius, B. W., and von Hippel, P. H. (1998) A Two-Metal Ion Mechanism Operates in the Hammerhead Ribozyme-Mediated Cleavage of an RNA Substrate, *Proceedings of the National Academy of Sciences of the United States of America 95*, 542-547.
(112) Pontius, B. W., Lott, W. B., and Von Hippel, P. H. (1997) Observations on Catalysis by Hammerhead Ribozymes are Consistent with a Two-Divalent-Metal-Ion Mechanism, *Proc.Natl.Acad.Sci.U.S.A. 94*, 2290-2294.
(113) Hud, N. V. *Nucleic Aicd-Metal Ion Interactions*, Royal Society of Chemistry, Cambridge, UK.
(114) Hancock, R. D., and Martell, A. E. (1996) Hard and Soft Acid-Base Behavior in Aqueous Solution: Steric Effects Make Some Metal Ions Hard: A Quantitative Scale of Hardness-Softness for Acids and Bases, *J. Chem. Educ. 73*, 654.
(115) Sekhon, G. S., and Sen, D. (2010) A Stereochemical Glimpse of the Active Site of the 8−17 Deoxyribozyme from Iodine-Mediated Cross-Links Formed with the Substrate's Scissile Site, *Biochemistry 49*, 9072-9077.
(116) Nawrot, B., Widera, K., Sobczak, M., Wojcik, M., and Stec, W. J. (2008) Effect of R(P) and S(P)Phosphorothioate Substitution at the Scissile Site on the Cleavage Activity of Deoxyribozyme 10-23, *Curr. Org. Chem. 12*, 1004-1009.
(117) Vazin, M., Huang, P.-J. J., Matuszek, Ż., and Liu, J. (2015) Biochemical Characterization of a Lanthanide-Dependent DNAzyme with Normal and Phosphorothioate-Modified Substrates, *Biochemistry 54*, 6132-6138.
(118) Moon, W. J., and Liu, J. (2020) Replacing Mg2+ by Fe2+ for RNA-Cleaving DNAzymes, *ChemBioChem 21*, 401-407.
(119) Kovacheva, Y. S., Tzokov, S. B., Murray, I. A., and Grasby, J. A. (2004) The Role of Phosphate Groups in the VS Ribozyme–Substrate Interaction, *Nucleic Acids Res. 32*, 6240-6250.
(120) Hougland, J. L., Kravchuk, A. V., Herschlag, D., and Piccirilli, J. A. (2005) Functional Identification of Catalytic Metal Ion Binding Sites within RNA, *PLOS Biology 3*, e277.
(121) Liu, X., Chen, Y., and Fierke, C. A. (2017) Inner-Sphere Coordination of Divalent Metal Ion with Nucleobase in Catalytic RNA, *J. Am. Chem. Soc. 139*, 17457-17463.
(122) Kepp, K. P. (2016) A Quantitative Scale of Oxophilicity and Thiophilicity, *Inorg. Chem. 55*, 9461-9470.
(123) Helm, L., and Merbach, A. E. (2005) Inorganic and Bioinorganic Solvent Exchange Mechanisms, *Chem. Rev. 105*, 1923-1960.
(124) Mohammed, A. M. (2010) HYDRATION STRUCTURE AND WATER EXCHANGE DYNAMICS OF Fe(II) ION IN AQUEOUS SOLUTION, *Bulletin of the Chemical Society of Ethiopia 24*, 239-250.

(125) Inada, Y., Mohammed, A. M., Loeffler, H. H., and Funahashi, S. (2005) Water-Exchange Mechanism for Zinc(II), Cadmium(II), and Mercury(II) Ions in Water as Studied by Umbrella-Sampling Molecular-Dynamics Simulations, *Helv. Chim. Acta 88*, 461-469.
(126) Jaffe, E. K., and Cohn, M. (1979) Diastereomers of the Nucleoside Phosphorothioates as Probes of the Structure of the Metal Nucleotide Substrates and of the Nucleotide Binding Site of Yeast Hexokinase, *J. Biol. Chem. 254*, 10839-10845.
(127) Ekesan, Ş., and York, D. M. (2019) Dynamical Ensemble of the Active State and Transition State Mimic for the RNA-Cleaving 8–17 DNAzyme in Solution, *Nucleic Acids Res. 47*, 10282-10295.
(128) Ganguly, A., Weissman, B. P., Piccirilli, J. A., and York, D. M. (2019) Evidence for a Catalytic Strategy to Promote Nucleophile Activation in Metal-Dependent RNA-Cleaving Ribozymes and 8-17 DNAzyme, *ACS Catalysis 9*, 10612-10617.
(129) Zhou, W., Saran, R., and Liu, J. (2017) Metal Sensing by DNA, *Chem. Rev. 117*, 8272–8325.
(130) Gong, B., Chen, J.-H., Bevilacqua, P. C., Golden, B. L., and Carey, P. R. (2009) Competition between Co(NH3)63+ and Inner Sphere Mg2+ Ions in the HDV Ribozyme, *Biochemistry 48*, 11961-11970.
(131) Feig, A. L., Scott, W. G., and Uhlenbeck, O. C. (1998) Inhibition of the hammerhead ribozyme cleavage reaction by site-specific binding of Tb(III), *Science 279*, 81-84.
(132) Tang, J., and Breaker, R. R. (2000) Structural diversity of self-cleaving ribozymes, *Proceedings of the National Academy of Sciences of the United States of America 97*, 5784-5789.
(133) Valko, M., Morris, H., and Cronin, M. T. D. (2005) Metals, Toxicity and Oxidative Stress, *Curr. Med. Chem. 12*, 1161-1208.
(134) Popović, M., Ditzler, M. A., and Fliss, P. S. (2015) In vitro evolution of distinct self-cleaving ribozymes in diverse environments, *Nucleic Acids Res. 43*, 7070-7082.
(135) Petrov, A. S., Okafor, C. D., Bowman, J. C., Lanier, K. A., Hud, N. V., Athavale, S. S., and Williams, L. D. (2017) Iron mediates catalysis of nucleic acid processing enzymes: support for Fe(II) as a cofactor before the great oxidation event, *Nucleic Acids Res. 45*, 3634-3642.
(136) Bray, M. S., Lenz, T. K., Haynes, J. W., Bowman, J. C., Petrov, A. S., Reddi, A. R., Hud, N. V., Williams, L. D., and Glass, J. B. (2018) Multiple prebiotic metals mediate translation, *Proc. Natl. Acad. Sci. 115*, 12164-12169.
(137) Joyce, G. F. (2004) Directed evolution of nucleic acid enzymes, *Annual Review of Biochemistry 73*, 791-836.
(138) Fan, H., Zhang, X., and Lu, Y. (2017) Recent advances in DNAzyme-based gene silencing, *Science China Chemistry 60*, 591-601.
(139) Santoro, S. W., and Joyce, G. F. (1997) A general purpose RNA-cleaving DNA enzyme, *Proc. Natl. Acad. Sci. U.S.A. 94*, 4262-4266.
(140) Breaker, R. R., and Joyce, G. F. (1995) A DNA enzyme with Mg2+-dependent RNA phosphoesterase activity, *Chem. Biol. 2*, 655-660.
(141) Xiang, Y., and Lu, Y. (2014) DNA as Sensors and Imaging Agents for Metal Ions, *Inorg. Chem. 53*, 1925-1942.
(142) Gong, L., Zhao, Z., Lv, Y.-F., Huan, S.-Y., Fu, T., Zhang, X.-B., Shen, G.-L., and Yu, R.-Q. (2015) DNAzyme-based biosensors and nanodevices, *Chem. Commun. 51*, 979-995.
(143) Zhou, W., Saran, R., Chen, Q., Ding, J., and Liu, J. (2016) A New Na+-Dependent RNA-Cleaving DNAzyme with over 1000-fold Rate Acceleration by Ethanol, *ChemBioChem 17*, 159-163.
(144) Ma, L., and Liu, J. (2019) An In Vitro Selected DNAzyme Mutant Highly Specific for Na+ in Slightly Acidic Conditions, *ChemBioChem 20*, 537-542.
(145) Gao, G., Cao, Y., Liu, W., Li, D., Zhou, W., and Liu, J. (2017) Fluorescent sensors for sodium ions, *Analytical Methods 9*, 5570-5579.

(146) He, Y., Chen, D., Huang, P.-J. J., Zhou, Y., Ma, L., Xu, K., Yang, R., and Liu, J. (2018) Misfolding of a DNAzyme for ultrahigh sodium selectivity over potassium, *Nucleic Acids Res. 46*, 10262-10271.
(147) Saran, R., and Liu, J. (2016) A Silver DNAzyme, *Anal. Chem. 88*, 4014–4020.
(148) Zhou, W., Saran, R., Huang, P.-J. J., Ding, J., and Liu, J. (2017) An Exceptionally Selective DNA Cooperatively Binding Two Ca2+ Ions, *ChemBioChem 18*, 518–522.
(149) Liu, J., Brown, A. K., Meng, X., Cropek, D. M., Istok, J. D., Watson, D. B., and Lu, Y. (2007) A catalytic beacon sensor for uranium with parts-per-trillion sensitivity and millionfold selectivity, *Proc. Natl. Acad. Sci. U.S.A. 104*, 2056-2061.
(150) Huang, P.-J. J., and Liu, J. (2016) An Ultrasensitive Light-up Cu2+ Biosensor Using a New DNAzyme Cleaving a Phosphorothioate-Modified Substrate, *Anal. Chem. 88*, 3341–3347.
(151) Huang, P.-J. J., Vazin, M., Lin, J. J., Pautler, R., and Liu, J. (2016) Distinction of Individual Lanthanide Ions with a DNAzyme Beacon Array, *ACS Sens. 1*, 732-738.
(152) Brown, A. K., Li, J., Pavot, C. M. B., and Lu, Y. (2003) A Lead-Dependent DNAzyme with a Two-Step Mechanism, *Biochemistry 42*, 7152-7161.
(153) Saran, R., and Liu, J. (2016) A comparison of two classic Pb2+-dependent RNA-cleaving DNAzymes, *Inorg. Chem. Front. 3*, 494-501.
(154) Liu, H. H., Yu, X., Chen, Y. Q., Zhang, J., Wu, B. X., Zheng, L. N., Haruehanroengra, P., Wang, R., Li, S. H., Lin, J. Z., Li, J. X., Sheng, J., Huang, Z., Ma, J. B., and Gan, J. H. (2017) Crystal structure of an RNA-cleaving DNAzyme, *Nat. Commun. 8*.
(155) Cepeda-Plaza, M., McGhee, C. E., and Lu, Y. (2018) Evidence of a General Acid-Base Catalysis Mechanism in the 8-17 DNAzyme, *Biochemistry 57*, 1517-1522.
(156) Li, J., Zheng, W., Kwon, A. H., and Lu, Y. (2000) In vitro selection and characterization of a highly efficient Zn(II)-dependent RNA-cleaving deoxyribozyme, *Nucleic Acids Res. 28*, 481-488.
(157) Faulhammer, D., and Famulok, M. (1996) The Ca2+ ion as a cofactor for a novel RNA-cleaving deoxyribozyme, *Angew. Chem., Int. Ed. 35*, 2837-2841.
(158) Huang, P.-J. J., and Liu, J. (2014) Sensing Parts-per-Trillion Cd^{2+}, Hg^{2+}, and Pb^{2+} Collectively and Individually Using Phosphorothioate DNAzymes, *Anal. Chem. 86*, 5999-6005.
(159) Li, Y., and Breaker, R. R. (1999) Kinetics of RNA Degradation by Specific Base Catalysis of Transesterification Involving the 2'-Hydroxyl Group, *J. Am. Chem. Soc. 121*, 5364-5372.
(160) Celander, D. W., and Cech, T. R. (1990) Iron(II)-ethylenediaminetetraacetic acid catalyzed cleavage of RNA and DNA oligonucleotides: similar reactivity toward single- and double-stranded forms, *Biochemistry 29*, 1355-1361.
(161) Balasubramanian, B., Pogozelski, W. K., and Tullius, T. D. (1998) DNA strand breaking by the hydroxyl radical is governed by the accessible surface areas of the hydrogen atoms of the DNA backbone, *Proc. Natl. Acad. Sci. U.S.A. 95*, 9738.
(162) Graf, E., Mahoney, J. R., Bryant, R. G., and Eaton, J. W. (1984) Iron-catalyzed hydroxyl radical formation. Stringent requirement for free iron coordination site, *J. Biol. Chem. 259*, 3620-3624.
(163) Kanzaki, Y., and Murakami, T. (2013) Rate law of Fe(II) oxidation under low O2 conditions, *Geochim. Cosmochim. Acta 123*, 338-350.
(164) Stumm, W., and Lee, G. F. (1961) Oxygenation of Ferrous Iron, *Ind. Eng. Chem. 53*, 143-146.
(165) Saywell, L. G., and Cunningham, B. B. (1937) Determination of Iron: Colorimetric o-Phenanthroline Method, *Industrial & Engineering Chemistry Analytical Edition 9*, 67-69.
(166) Yen, G.-C., and Hsieh, C.-L. (1997) Antioxidant Effects of Dopamine and Related Compounds, *Bioscience, Biotechnology, and Biochemistry 61*, 1646-1649.
(167) Carmi, N., Balkhi, H. R., and Breaker, R. R. (1998) Cleaving DNA with DNA, *Proc.Natl.Acad.Sci.U.S.A. 95*, 2233-2237.

(168) Ma, J.-L., Yin, B.-C., Wu, X., and Ye, B.-C. (2016) Copper-Mediated DNA-Scaffolded Silver Nanocluster On–Off Switch for Detection of Pyrophosphate and Alkaline Phosphatase, *Anal. Chem. 88*, 9219-9225.
(169) Liu, J., and Lu, Y. (2007) A DNAzyme Catalytic Beacon Sensor for Paramagnetic Cu2+ Ions in Aqueous Solution with High Sensitivity and Selectivity, *J. Am. Chem. Soc. 129*, 9838-9839.
(170) Zhou, W. H., Ding, J. S., and Liu, J. W. (2017) Theranostic DNAzymes, *Theranostics 7*, 1010-1025.
(171) Huanhuan, F., Xiaobing, Z., and Yi, L. (2017) Recent advances in DNAzyme-based gene silencing, *SCIENCE CHINA Chemistry null*.
(172) Ma, L., Kartik, S., Liu, B., and Liu, J. (2019) From general base to general acid catalysis in a sodium-specific DNAzyme by a guanine-to-adenine mutation, *Nucleic Acids Res.*
(173) Wang, Y. J., Liu, E. K., Lam, C. H., and Perrin, D. M. (2018) A densely modified M2+-independent DNAzyme that cleaves RNA efficiently with multiple catalytic turnover, *Chem. Sci. 9*, 1813-1821.
(174) Wang, J., Wang, H., Wang, H., He, S., Li, R., Deng, Z., Liu, X., and Wang, F. (2019) Nonviolent Self-Catabolic DNAzyme Nanosponges for Smart Anticancer Drug Delivery, *ACS Nano 13*, 5852-5863.
(175) Wang, H., Chen, Y., Wang, H., Liu, X., Zhou, X., and Wang, F. (2019) DNAzyme-Loaded Metal–Organic Frameworks (MOFs) for Self-Sufficient Gene Therapy, *Angew. Chem. Int. Ed. 58*, 7380-7384.
(176) Fan, H., Zhao, Z., Yan, G., Zhang, X., Yang, C., Meng, H., Chen, Z., Liu, H., and Tan, W. (2015) A Smart DNAzyme–MnO2 Nanosystem for Efficient Gene Silencing, *Angew. Chem. Int. Ed.*, 4883-4887.
(177) Liu, F., Li, X.-L., and Zhou, H. (2020) Biodegradable MnO2 nanosheet based DNAzyme-recycling amplification towards: Sensitive detection of intracellular MicroRNAs, *Talanta 206*, 120199.
(178) Checovich, W. J., Bolger, R. E., and Burke, T. (1995) Fluorescence polarization — a new tool for cell and molecular biology, *Nature 375*, 254-256.
(179) Mann, T. L., and Krull, U. J. (2003) Fluorescence polarization spectroscopy in protein analysis, *Analyst 128*, 313-317.
(180) Xiao, L., Gu, C., and Xiang, Y. (2019) Orthogonal Activation of RNA-Cleaving DNAzymes in Live Cells by Reactive Oxygen Species, *Angewandte Chemie 131*, 14305-14310.
(181) Peng, H., Li, X.-F., Zhang, H., and Le, X. C. (2017) A microRNA-initiated DNAzyme motor operating in living cells, *Nat. Commun. 8*, 14378.
(182) Chen, J., Zuehlke, A., Deng, B., Peng, H., Hou, X., and Zhang, H. (2017) A Target-Triggered DNAzyme Motor Enabling Homogeneous, Amplified Detection of Proteins, *Anal. Chem. 89*, 12888-12895.
(183) Topală, T., Bodoki, A., Oprean, L., and Oprean, R. (2014) Bovine Serum Albumin Interactions with Metal Complexes, *Clujul medical 87*, 215-219.
(184) Bal, W., Sokołowska, M., Kurowska, E., and Faller, P. (2013) Binding of transition metal ions to albumin: Sites, affinities and rates, *Biochimica et Biophysica Acta (BBA) - General Subjects 1830*, 5444-5455.
(185) Rehman, A. A., Ahsan, H., and Khan, F. H. (2013) Alpha-2-macroglobulin: A physiological guardian, *J. Cell. Physiol. 228*, 1665-1675.
(186) Wilson, C. J., Apiyo, D., and Wittung-Stafshede, P. (2005) Role of cofactors in metalloprotein folding, *Quarterly Reviews of Biophysics 37*, 285-314.
(187) Majorek, K. A., Porebski, P. J., Dayal, A., Zimmerman, M. D., Jablonska, K., Stewart, A. J., Chruszcz, M., and Minor, W. (2012) Structural and immunologic characterization of bovine, horse, and rabbit serum albumins, *Molecular Immunology 52*, 174-182.
(188) Maret, W., and Wedd, A. (2014) *Binding, Transport and Storage of Metal Ions in Biological Cells*, The Royal Society of Chemistry, Cambridge, UK.
(189) Belatik, A., Hotchandani, S., Carpentier, R., and Tajmir-Riahi, H.-A. (2012) Locating the Binding Sites of Pb(II) Ion with Human and Bovine Serum Albumins, *PLoS One 7*, e36723.

(190) Ohyoshi, E., Hamada, Y., Nakata, K., and Kohata, S. (1999) The interaction between human and bovine serum albumin and zinc studied by a competitive spectrophotometry, *J. Inorg. Biochem. 75*, 213-218.